boundary layer thicknesses d_h and d_v of Eq. (6.4.31), the effects can be approximated by adding to the surface admittance β_m of Eq. (8.2.7) the additional term

$$\beta_{sm} = \tfrac{1}{2}(1 - i)\left[(\gamma - 1)kd_h + \frac{m(m+1)}{a^2}kd_v\right]$$

for each value of m, with the sums $\beta_m + \beta_{sm}$ to be used instead of β_m in Eqs. (8.2.14) and elsewhere. According to the discussion following Eq. (6.4.36), as well as Eq. (6.4.41), this additional admittance will account for the effects of thermal and viscous losses whenever a is large compared with d_h and d_v. Since the β_{sm}'s are small, they can be neglected whenever the β_m's are larger.

When a is small, however, the effects cannot be expressed in terms of effective admittances; the shear and thermal waves must be calculated, and the boundary conditions must be worked out in detail. Fortunately, when a is small, we usually need only to consider the $m = 0$ and $m = 1$ terms in the series, since a will then usually be small compared with the wavelength. As an example of this situation we consider the material inside the sphere to have much greater viscosity and thermal conduction than does air; so we can neglect the thermal and shear waves inside the sphere (this would be the case for a water droplet suspended in air, for instance). The fluid inside the sphere has effective density ρ_e, compressibility κ_e, and wave velocity $c_e = 1/\sqrt{\rho_e\kappa_e}$. Thus the wave inside the sphere will be [Eq. (8.2.7)]

$$p_e = A\sum_m B_m{}^e P_m(\cos\vartheta) j_m(k_e r) \qquad r \leqslant a; \qquad k_e = \frac{\omega}{c_e}$$

When $k_e a$ is small we can neglect all but the first two terms of this series and can use the first terms in the series for the Bessel functions.

$$j_0(z) \simeq 1 - \tfrac{1}{6}z^2 \qquad j_1(z) \simeq \tfrac{1}{3}z \qquad h_0(z) \simeq 1 - \frac{i}{z} \qquad h_1(z) \simeq -\frac{i}{2} - \frac{i}{z^2}$$

The temperature fluctuation accompanying these incident and scattered waves is $\tau_p = [(\gamma - 1)/\gamma\alpha](p_i + p_s)$ for $r \geqslant a$ and is zero for $r \leqslant a$.

The thermal scattered wave, just outside the sphere, is obtained by using the k of Eq. (6.4.25) in the spherical Hankel functions

$$\tau_h = A\sum_m E_m P_m(\cos\vartheta) h_m \frac{(1+i)r}{d_h}$$

For frequencies around a kilocycle, in air at standard conditions, d_h is roughly equal to 10^{-4} cm. Thus, even for spheres as small as 0.01 cm in radius, the argument of this Hankel function is large enough so that its asymptotic form, $h_m(z) \to (i^{-m-1}/z)e^{iz}$, can be used, at least for $m = 0$ and 1. Therefore we write the first two terms of the series, with the corresponding pressure and

radial velocity, as

$$\tau_h \simeq -(1-i)\frac{Ad_h}{2r}(iE_0 + E_1\cos\vartheta)e^{(i-1)r/d_h}$$

$$p_h \simeq i\gamma\alpha k^2(d_h^2 - d_v'^2)\frac{\tau_h}{2}$$

$$u_{hr} \simeq \frac{\gamma\alpha A}{2i\rho c}\frac{kd_h^2}{r}(iE_0 + E_1\cos\vartheta)e^{(i-1)r/d_h}$$

Because d_h^2 can be neglected compared with d_h, we can neglect p_h and $u_{h\vartheta}$ at $r = a$; but τ_h and u_{hr} cannot be neglected.

There can be no shear wave which is spherically symmetric; the $m = 0$ terms have no tangential velocity components, and no shear wave is needed to fit boundary conditions. Thus the $m = 0$ terms satisfy the following conditions at $r = a$:

p continuous:

$$B_0^e j_0(k_e a) = j_0(ka) + B_0 h_0(ka)$$

or

$$B_0^e \simeq 1 - \frac{iB_0}{ka}$$

u_r continuous:

$$\frac{1}{i\rho_e c_e}B_0^e j_0'(k_e a) = \frac{1}{i\rho c}\left[j_0'(ka) + B_0 h_0'(ka) + \frac{i\alpha\gamma k d_h^2 C_0}{2a}\right]$$

or

$$-\frac{\rho c}{3\rho_e c_e}B_0^e k_e a \simeq -\tfrac{1}{3}ka + \frac{iB_0}{k^2a^2} + \frac{i\alpha\gamma k d_h^2 C_0}{2a}$$

τ zero:

$$\frac{\gamma-1}{\gamma\alpha}\left[j_0(ka) + B_0 h_0(ka)\right] - (1+i)\frac{d_h C_0}{2a} = 0$$

or

$$\frac{\gamma-1}{\gamma\alpha}\left(1 - \frac{iB_0}{ka}\right) - (1+i)\frac{d_h C_0}{2a} \simeq 0$$

where $C_0 = E_0 e^{(i-1)r/d_h}$.

The approximate solution of this trio of equations, valid for ka and d_h/a small, is

$$B_0 \simeq \tfrac{1}{3}(ka)^3\left[i\gamma_\kappa - 3(1+i)(\gamma-1)\frac{d_h}{a}\right]$$

$$B_0^e \simeq 1 + \tfrac{1}{3}(ka)^3 \qquad C_0 \simeq (1-i)\left[(\gamma-1)\frac{a}{\alpha\gamma d_h}\right]$$

where $\gamma_\kappa = (\kappa_e - \kappa)/\kappa$ from Eq. (8.1.11), and $d_h = \sqrt{2K/\rho\omega C_p}$ from Eq.

(6.4.31). We note that the reflection coefficient

$$R_0 \simeq -\left[1 - (1+i)(ka)^3(\gamma-1)\frac{d_h}{a} - \tfrac{2}{3}i(ka)^3\gamma_\kappa\right]$$

has a magnitude squared (to the first order in kd_h and γ_κ),

$$|R_0|^2 \simeq 1 - 2(\gamma-1)(ka)^2 kd_h$$

which is smaller than unity, representing energy absorption.

To satisfy boundary conditions for the $m = 1$ terms, we must include a shear wave in the boundary layer just outside the sphere, a solution of Eqs. (6.4.17) and (6.4.29) with $k_v^2 = 2i/d_v^2$, d_v as defined in Eqs. (6.4.31). The r and ϑ components of the shear wave required to fit the boundary conditions are

$$u_{tr} = \frac{2AV}{k_v r}\cos\vartheta\, h_1(k_v r) \to 2iAV\cos\vartheta\,\frac{kd_h^2}{2k_v r^2}\,e^{(i-1)r/d_v}$$

$$u_{t\vartheta} = \frac{-AV}{k_v r}\frac{d}{dr}[rh_1(k_v r)]\sin\vartheta \to (1+i)AV\sin\vartheta\,\frac{d_v}{2r}\,e^{(i-1)r/d_v}$$

where u_ϑ is the velocity component tangential to the sphere in the rz plane. Again we can use the asymptotic form for $h_1(k_v r)$ because d_v is so small. That this wave is purely transverse can be demonstrated by showing that

$$\operatorname{div}\mathbf{u} \equiv \frac{1}{r^2}\frac{\partial}{\partial r}(r^2 u_r) + \frac{1}{r\sin\vartheta}\frac{\partial}{\partial\vartheta}(\sin\vartheta\, u_\vartheta) = 0$$

It also can be shown that curl (curl $\mathbf{u}$) $= k_v^2\mathbf{u}$.

The boundary conditions at $r = a$ for these waves are p continuous:

$$B_1^e j_1(k_e a) = 3ij_1(ka) + B_1 h_1(ka)$$

or

$$\tfrac{1}{3}k_e a B_1^e \simeq ika - \frac{i}{k^2a^2}B_1$$

τ zero:

$$\frac{\gamma-1}{\gamma\alpha}\left[3ij_1(ka) + B_1 h_1(ka)\right] - (1-i)\frac{C_1 d_h}{2a} = 0$$

or

$$ika\,\frac{\gamma-1}{\gamma\alpha}\left(1 - \frac{B_1}{k^3a^3}\right) \simeq (1-i)\frac{C_1 d_h}{2a}$$

u_r continuous:

$$\frac{1}{i\rho_e c_e}B_1^e j_1'(k_e a) = \frac{1}{i\rho c}\left[3ij_1'(ka) + B_1 h_1'(ka) + \alpha\gamma\frac{kd_h^2}{2a}C_1 - \frac{d_v^2}{a^2}D_1\right]$$

or

$$\frac{1}{3}\frac{\rho c}{\rho_e c_e}B_1^e \simeq i + \frac{2iB_1}{k^3a^3} + \alpha\gamma\frac{kd_h^2}{2a}C_1 - \frac{d_v^2}{a^2}D_1$$

where

$$C_1 = E_1 e^{(i-1)a/d_h} \qquad \text{and} \qquad D_1 = \rho c V e^{(i-1)a/d_v}$$

u_ϑ continuous:

$$\frac{-B_1{}^e}{i\rho_e c_e k_e a} j_1(k_e a) = \frac{-1}{i\rho c k a} [3ij_1(ka) + B_1 h_1(ka) - \tfrac{1}{2}(1-i)kd_v D_1]$$

or

$$\frac{1}{3}\frac{\rho c}{\rho_e c_e} B_1{}^e \simeq i - i\frac{B_1}{k^2a^2} - \tfrac{1}{2}(1-i)\frac{d_v}{a} D_1$$

These suffice to calculate the various coefficients; the approximate formulas for ka small are

$$B_1 \simeq -\tfrac{1}{3}(ka)^3 \gamma'_\rho \left[1 - (1+i)\frac{3\rho_e}{2\rho_e + \rho}\frac{d_v}{a}\right]$$

$$B_1{}^e \simeq \frac{9i\rho_e}{2\rho_e + \rho}\frac{c_e}{c}\left[1 - \tfrac{1}{3}(1+i)\gamma'_\rho \frac{d_v}{a}\right]$$

$$D_1 \simeq -(1-i)\frac{\delta'_\rho a}{d_v}\left[1 - \tfrac{1}{3}(1+i)\frac{d_v}{a}\gamma'_\rho\right]$$

$$C_1 \simeq (1+i)\frac{\gamma - 1}{\gamma\alpha}\frac{3i\rho_e}{2\rho_e + \rho}\frac{ka^2}{d_h}\left[1 - \tfrac{1}{3}(1+i)\gamma'_\rho \frac{d_v}{a}\right]$$

where

$$\gamma'_\rho = \frac{3\rho_e - 3\rho}{2\rho_e + \rho}$$

We note that the thermal wave for $m = 1$ can be neglected; its magnitude C_1 and its contribution to the scattered wave are another order of magnitude smaller than the viscous effects for $m = 1$. This is in contrast to the $m = 0$ wave, for which the viscous wave is nonexistent and the only energy loss comes from thermal diffusion. The $m = 0$ wave is primarily a compressive mode, to which thermal diffusion responds; the $m = 1$ wave is primarily one of motion of the sphere back and forth along the z axis, which produces viscous energy loss. Next we note that the viscous loss cannot be computed by using Eq. (8.2.17) to determine the absorption cross section, as can be done for the thermal loss; the viscous loss is caused by shear motion, and it must be computed by using Eq. (6.4.38). Using the expressions for u_t and D_1, we see that the viscosity contribution to the absorption cross section $\Sigma_a = \rho c/|A|^2$ (power lost) is

$$\frac{1}{2}\frac{\rho c}{|A|^2}\rho\omega d_v \iint |u_{t\vartheta}|^2\, dA \simeq \tfrac{9}{2}kd_v\gamma'^2_\rho\, 2\pi a^2 \int \sin^3\vartheta\, d\vartheta = 12\pi k a^2 d_v \gamma'^2_\rho$$

Therefore the expressions for pressure and velocity at the surface of the sphere, the scattered wave, and the cross sections, appropriate for long

wavelengths, are

$$p_s(r,\vartheta) \to A\frac{e^{ikr}}{r}\Phi(\vartheta) \qquad \gamma_\kappa = \frac{\kappa_e - \kappa}{\kappa} \qquad \gamma'_\rho = \frac{3\rho_e - 3\rho}{2\rho_e + \rho}$$

$$\Phi(\vartheta) \simeq \tfrac{1}{3}k^2a^3\left\{\gamma_\kappa - 3(1-i)(\gamma-1)\frac{d_h}{a} + \gamma'_\rho\cos\vartheta\left[1 - (1+i)\frac{3\rho_e}{2\rho_e+\rho}\frac{d_v}{a}\right]\right\}$$

$$\Sigma_s \simeq \tfrac{4}{9}\pi a^2(ka)^4\left\{(\gamma_\kappa)^2 - 6(\gamma-1)\gamma_\kappa\frac{d_h}{a} + \tfrac{1}{3}(\gamma'_\rho)^2\left[1 - \frac{6\rho_e}{2\rho_e+\rho}\frac{d_v}{a}\right]\right\}$$

$$\Sigma_a \simeq 2\pi a^2(\gamma-1)kd_h + \tfrac{4}{3}\pi a^2(\gamma'_\rho)^2 kd_v \tag{8.2.22}$$

$$p_\omega(a,\vartheta) \simeq A + ikaA\frac{3\rho_e}{2\rho_e+\rho}\left[1 - \tfrac{1}{3}(1+i)\gamma'_\rho\frac{d_v}{a}\right]\cos\vartheta$$

$$u_r \simeq \frac{A}{\rho c}\left[\tfrac{1}{3}ika\frac{\kappa_e}{\kappa} - (\gamma-1)kd_h\begin{Bmatrix}1+i\\-(1+3i)\end{Bmatrix}\right] + \frac{A\cos\vartheta}{\rho c}\left[\frac{3\rho}{2\rho_e+\rho} + (1+i)\frac{\gamma'_\rho}{2\rho_e+\rho}\frac{d_v}{a}\begin{Bmatrix}(2\rho_e)\\(-\rho)\end{Bmatrix}\right]$$

$$u_\vartheta \simeq \frac{A\sin\vartheta}{\rho c}\left[\frac{-3}{2\rho_e+\rho} + (1+i)\frac{\gamma'_\rho}{2\rho_e+\rho}\frac{d_v}{a}\right]\begin{Bmatrix}\rho_e\\\rho\end{Bmatrix}$$

where $d_v = \sqrt{2\mu/\rho\omega}$ and $d_h = \sqrt{2K/\rho\omega C_p}$, μ being the viscosity of the air, K its thermal conductivity, and C_p its specific heat at constant pressure. For the two velocity components, the upper factors in the braces are the values just outside the boundary layer, and the lower factors are to be used in computing the velocity at the surface $r = a$.

We see that the $m = 0$ quantities are modified by the thermal conduction, and the $m = 1$ terms, by the viscosity of the medium outside the sphere. The angle distribution of the scattered wave is only slightly modified from that given in Eqs. (8.2.19), which neglects these losses, but the absorption cross section is of course entirely dependent on their presence [unless ρ_e or κ_e is complex, in which case these terms must be added, as in Eqs. (8.2.19)]. The sphere expands and contracts with an amplitude proportional to κ_e/κ. It also moves back and forth along the z axis with a velocity amplitude

$$U \simeq \frac{3A}{(2\rho_e+\rho)c}\left[1 - \tfrac{1}{3}(1+i)\gamma'_\rho\frac{d_v}{a}\right]$$

this amplitude being slightly diminished because of the viscosity. The air clings to it as it moves. The part of the pressure there which is proportional to $\cos\vartheta$ is in phase with the part of the radial velocity which is proportional to $\cos\vartheta$, but the spherically symmetric parts of the surface pressure and radial

velocity at the surface are not in phase, so that energy is lost, both in the thermal boundary layer and inside the sphere itself (by thermal conduction into the sphere). The tangential motion of the air increases through the viscous boundary layer, corresponding to the shear action there. Just outside the layer the amplitude of the tangential velocity, relative to the moving sphere, is proportional to $\rho_e - \rho$: the air outside moves faster than the sphere if $\rho_e > \rho$; slower than the sphere if the medium's density is greater than that of the sphere. The viscous-loss term in the absorption cross section is therefore proportional to $(\gamma'_\rho)^2$, that is, to $(\rho_e - \rho)^2$.

Cloud of scatterers

When sound traverses a cloud of small objects, such as air bubbles in water or fog droplets in air, each object produces a scattered wave, and these wavelets reinforce in some directions and interfere in some others. The wave incident on each scatterer is affected because of the presence of the others, which in turn affects the shape of the scattered wave. This gives rise to coherent, incoherent, and multiple scattering and, in cases where the scatterers are regularly spaced, to diffraction.

Suppose the dimensions of the scattering objects are all quite small compared with the wavelength λ; furthermore, that the mean distance between scatterers is not larger than λ. Next, suppose that the dimensions of the region R, inhabited by the scatterers, are considerably larger than λ and, finally, that the distance from R to the point of measurement is much larger than the dimensions of R (and thus is very much larger than λ). All this is usually the case with mists or with bubble clouds. Also suppose that the scatterers are all spheres; that there are, on the average, N of them per unit volume inside R; that the nth sphere has radius a_n, compressibility κ_n, density ρ_n; and that its center is at the point represented by vector $\mathbf{r}_n$. The fluid outside R and in the space between scatterers inside R has compressibility κ_0 and density ρ_0. The incident wave will be the plane wave $Ae^{ikz} = Ae^{i\mathbf{k}_i\cdot\mathbf{r}}$, where k_i points along the z axis.

In the integral of Eqs. (8.1.19) the quantities $(\kappa_n/\kappa_0) - 1$ and $1 - (\rho_0/\rho_n)$ (we are not considering turbulence here; so $\Re = 0$) differ from zero inside each of the scattering spheres inside R. The scattered wave at r will thus be a sum of waves arising from the various small spheres, each having a relative phase and amplitude determined by the particular sphere's size and position. If the spheres are regularly placed, these phases will all add up, in certain directions, to produce diffracted beams, as with the Bragg diffraction of x-rays from crystals. However, the objects scattering sound waves are usually distributed at random, in which case no reinforcement occurs except in the direction of the incident wave.

In this forward direction the reinforced scattering modifies the incident wave as though it were traveling through a region R of different index of refraction. To see this, let us separate the compressibility and density

factors γ_κ and γ_ρ in the integrand of Eqs. (8.1.19) into their mean values, throughout the region R, plus the variation of these factors from their mean values. The mean values are equal to the sums $\sum [(\kappa_n/\kappa_0) - 1] \cdot \frac{4}{3}\pi a_n{}^3$ and $\sum [1 - (\rho_0/\rho_n)] \cdot \frac{4}{3}\pi a_n{}^3$ over each of the N spheres per unit volume in R.

These sums are responsible for the coherent scattering. Considering only the average terms for γ_κ and γ_ρ for the moment, Eq. (8.1.13), inside region R, has the form

$$p_\omega(\mathbf{r}) = p_i(\mathbf{r}) + \left[\sum_n \tfrac{4}{3}\pi a_n{}^3\left(\frac{\kappa_n}{\kappa_0} - 1\right)\right]\iiint k^2 p_\omega(\mathbf{r}_0) g_\omega(\mathbf{r} \mid \mathbf{r}_0)\, dv_0$$
$$- \left[\sum_n \tfrac{4}{3}\pi a_n{}^3\left(1 - \frac{\rho_0}{\rho_n}\right)\right]\iiint g_\omega(\mathbf{r} \mid \mathbf{r}_0)\, \nabla_0{}^2 p_\omega(\mathbf{r}_0)\, dv_0$$

where $k^2 = \rho_0\kappa_0\omega^2$. This is the equation for a wave, induced by the incident wave p_i, which has an equation of motion $\nabla^2 p_\omega + k^2 p_\omega = 0$ in the region outside R and an equation of motion

$$\nabla^2 p_\omega + k^2 p_\omega = \left[\sum_n \left(\frac{\rho_0}{\rho_n} - 1\right)\tfrac{4}{3}\pi a_n{}^3\right]\nabla^2 p_\omega + \left[\sum_n \left(\frac{\kappa_n}{\kappa_0} - 1\right)\tfrac{4}{3}\pi a_n{}^3\right]k^2 p_\omega$$

inside R. This last equation is that for sound waves in a medium of density and compressibility given by

$$\rho_R = \left[\frac{1}{\rho_0} + \sum_{n=1}^{N} \tfrac{4}{3}\pi a_n{}^3\left(\frac{1}{\rho_n} - \frac{1}{\rho_0}\right)\right]^{-1} \qquad \kappa_R = \kappa_0 + \sum_{n=1}^{N} \tfrac{4}{3}\pi a_n{}^3(\kappa_n - \kappa_0) \tag{8.2.23}$$

The effective compressibility is the average of the compressibility over each unit volume of R; the effective density is the reciprocal of the average value of $1/\rho$ over each unit volume.

Thus, as far as the average terms in the integrand are concerned, region R behaves as though it had a uniform density and compressibility which differ from that of the medium outside R. This difference will produce scattering (or reflection or refraction, whichever term seems more appropriate) of sound incident on R. For example, if R is a spherical region of radius a_R, Eq. (8.2.15) can be used, with Eq. (8.2.9) used to calculate the effective admittances β_m in terms of a_R, ρ_R, and κ_R. In the very long wavelength limit of Eqs. (8.2.19), the scattered intensity is proportional to the squares of the summations for ρ_R and κ_R in Eqs. (8.2.23), in other words, to the square of the number N of scattering particles per unit volume in R. This cooperative portion of the scattered wave, in which each scatterer adds its contribution to the wave amplitude (and thus the intensity is proportional to N^2), is called the *coherent* scattered wave. The rest of the scattering, the intensity of which we shall see is proportional to N rather than to N^2, is called the *incoherent* scattered wave.

Incoherent scattering

The incoherent scattering is, of course, generated by the variable parts of the functions κ and ρ, after the constant average values have been taken into account by the change of index of refraction just worked out and given in Eqs. (8.2.23). The nth little sphere will produce its scattered wave as though it were a sphere of radius a_n, with density and compressibility ρ_n and κ_n, in a medium of density ρ_R and κ_R throughout R. The incident wave will have been refracted by the change of index of refraction as it enters R, but if R is large and the interface is a plane, it will have the form $A_R e^{ik_R z}$ inside R, where $k_R{}^2 = \rho_R \kappa_R \omega^2$. The wave scattered from the nth sphere will have the form $A_R(e^{ik_R r}/r)\Phi_n(\vartheta)$ inside R, but by the time it has emerged from R and reached the measurement point, its wavenumber will have changed back from k_R to $k = \omega\sqrt{\rho_0\kappa_0}$, with corresponding (but very small, if k_R does not differ much from k) change in amplitude A.

The easiest way to compute the incoherent scattering, if the N scatterers are distributed at random throughout R, is to use the correlation function of the variable parts of the compressibility and density factors γ_κ and γ_ρ. If all scatterers are spheres, we can use Eqs. (8.2.19) to ensure accuracy even when κ_n and ρ_n differ greatly from κ_0 and ρ_0 (as long as $a_n \ll \lambda$) and obtain an expression for the pressure at very large distances from R.

$$p(\mathbf{r}) \to A_i e^{ikz} + \sum_n \tfrac{4}{3}\pi a_n{}^3(\gamma_{\kappa n} + \gamma_{\rho n}\cos\vartheta)k_R{}^2 p(\mathbf{r}_n)(e^{ik_R R_n}/4\pi R_n)$$

where

$$\gamma_{\kappa n} = \frac{\kappa_n - \kappa_R}{\kappa_R} \qquad \gamma_{\rho n} = \frac{3\rho_n - 3\rho_R}{2\rho_n + \rho_R}$$

$\mathbf{r}_n$ is the radius vector to the center of the nth sphere from the center of R, and $R_n = |\mathbf{r} - \mathbf{r}_n|$. This expresses the incoherent scattering as the sum of wavelets scattered from each sphere. But it would be more convenient, for our present purposes, to express the scattered wave as an integral of the form of Eq. (8.1.14).

We have already included the average values of the factors γ_κ and γ_ρ in the index of refraction of region R, which gives rise to the coherent scattering. The variable parts of the γ's may be expressed in terms of the function

$$\delta(\mathbf{r}) = \begin{cases} \dfrac{\kappa_n - \kappa_R}{\kappa_R} + \dfrac{3\rho_n - 3\rho_R}{2\rho_n + \rho_R}\cos\vartheta & (\mathbf{r} \text{ inside the } n\text{th sphere}) \\ \dfrac{\kappa_0 - \kappa_R}{\kappa_R} + \dfrac{3\rho_0 - 3\rho_R}{2\rho_0 + \rho_R}\cos\vartheta & (\text{inside } R, \text{ outside a sphere}) \end{cases} \tag{8.2.24}$$

which has average value zero over R, by definition, since we have subtracted the average values of the γ's. This function can be defined in terms of its correlation function

$$\Upsilon(\mathbf{d}) = \frac{1}{V}\iiint_R \delta(\mathbf{r})\delta(\mathbf{r} + \mathbf{d})\, dv$$

where V is the volume of region R. As usual, the value of $\Upsilon(0)$ is the mean-square value of function $\delta(\mathbf{r})$,

$$\langle \delta^2 \rangle \simeq N(\tfrac{4}{3}\pi a^3)\,|\gamma_\kappa + \gamma_\rho \cos\vartheta|^2 \tag{8.2.25}$$

where N is the mean number of spheres per unit volume in R, a is their mean radius, and γ_κ and γ_ρ are the mean values of their factors $(\kappa_n - \kappa_0)/\kappa_0$ and $(3\rho_n - 3\rho_0)/(2\rho_n + \rho_0)$, respectively. However, since the mean value of $\delta(\mathbf{r})$ is zero, it must be that the integral of $\Upsilon(\mathbf{d})$ over R is zero. Thus $\Upsilon(\mathbf{d})$ cannot simply fall off exponentially to zero as d increases; it must go negative to a sufficient extent so that its average value is zero. The simplest form satisfying these requirements is

$$\Upsilon(\mathbf{d}) = \langle \delta^2 \rangle \left(1 - \frac{d^2}{3a^2}\right) \exp\left[-\frac{1}{2}\left(\frac{d}{a}\right)^2\right] \tag{8.2.26}$$

where a is a scale factor proportional to, perhaps nearly equal to, the mean radius of the scattering spheres.

If the density of scattering particles is sufficiently small so that the chance of multiple scattering is negligible, we can use the Born approximation, as with Eq. (8.1.18). The incoherently scattered wave at the observation point is

$$p_{is}(\mathbf{r}) \to \frac{A_i e^{ikr}}{4\pi r} k_R{}^2 \iiint_R \delta(\mathbf{r}_0) e^{-i\boldsymbol{\mu}\cdot\mathbf{r}_0}\, dv_0 \qquad \mu = 2k_R \sin\frac{\vartheta}{2}$$

and thus the incoherently scattered intensity at $\mathbf{r}$, divided by the incident intensity $|A_i|^2/\rho c$, is $(4\pi^4 k_R{}^4/r^2)\,|\Delta(\boldsymbol{\mu})|^2$, where $\Delta(\mathbf{K})$ is the Fourier transform

$$\Delta(\mathbf{K}) = \frac{1}{8\pi^3} \iiint_R \delta(\mathbf{r}) e^{-i\mathbf{K}\cdot\mathbf{r}}\, dv \tag{8.2.27}$$

Note that $\Delta(0) = 0$. We know, from Eq. (8.1.26), that $|\Delta(\mathbf{K})|^2$ is proportional to the Fourier transform of the correlation function of $\delta(\mathbf{r})$.

$$\begin{aligned} |\Delta(\mathbf{K})|^2 &= \frac{V}{64\pi^6} \iiint \delta(\mathbf{d}) e^{-i\mathbf{K}\cdot\mathbf{d}}\, dv_d \\ &= \langle \delta^2 \rangle \frac{VK^2a^5}{3(2\pi)^{\frac{9}{2}}} e^{-\frac{1}{2}K^2a^2} \end{aligned} \tag{8.2.28}$$

Therefore the incoherently scattered intensity, per unit incident intensity, at angle ϑ to the incident wave, for frequency $\omega/2\pi$, is (for $K = \mu$)

$$\frac{I_{is}}{I_i} \simeq NV \frac{\sqrt{2\pi}}{9} \frac{k_R{}^4 a^6}{r^2} |\gamma_\kappa + \gamma_\rho \cos\vartheta|^2 \left(\tfrac{1}{8} k_R{}^2 a^2 \sin^2 \tfrac{1}{2}\vartheta\right) \exp\left(-2k_R{}^2 a^2 \sin^2 \tfrac{1}{2}\vartheta\right) \tag{8.2.29}$$

to the approximation which neglects multiple scattering. If thermal and viscous losses are included, we use the quantity in braces in the Φ of Eqs. (8.2.22) instead of $(\gamma_\kappa + \gamma_\rho \cos\vartheta)$.

If we had just used Eqs. (8.2.19), assuming that each of the NV scatterers in R scattered sound independently of the others and that each wavelet did not interfere with any other, so that we could add intensities, the ratio of scattered

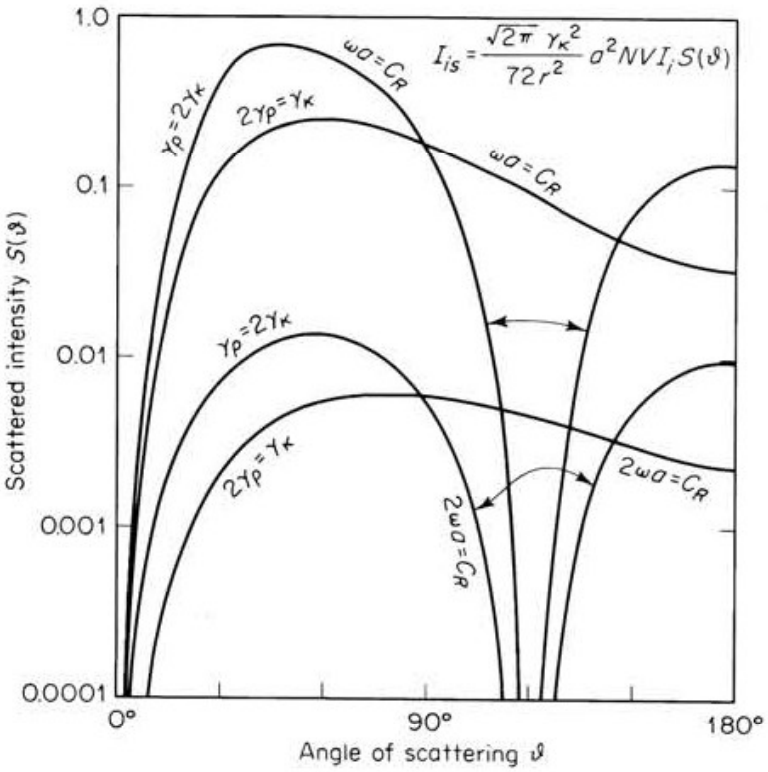


FIGURE 8.6
Incoherent scattering from a cloud of particles of radius a, with compressibility factors γ_κ and density factors γ_ρ.

to incident power at r would have the value

$$\left(\frac{I_{is}}{I_i}\right)_0 \simeq \tfrac{1}{9} NV \frac{k_0^4 a^6}{r^2} |\gamma_\kappa + \gamma_\rho \cos\vartheta|^2$$

Equations (8.2.29) show that the interference between the wavelets modifies the distribution-in-angle of the scattered wave, reducing it in the forward direction and augmenting it to the side and backward, so that the power fraction scattered is

$$\left(\frac{I_{is}}{I_i}\right)_0 \cdot \tfrac{1}{8}\sqrt{2\pi}\left(\frac{k_R}{k_0}\right)^4 (k_R\, a \sin\tfrac{1}{2}\vartheta)^2 \exp\left(-2k_R{}^2 a^2 \sin^2\tfrac{1}{2}\vartheta\right)$$

Plots of the incoherent scattering are shown in Fig. 8.6 ($k_R = \omega/c_R$).

This formula holds only if region R is small enough, or is so sparsely populated with scatterers that the total power scattered out of the incident

beam is a small fraction of the power incident on R. According to the discussion on page 407, the power scattered away from the incident beam in traversing a distance dz of R is I_i times $N\Sigma_s\,dz$, and the power absorbed by the scatterers is $I_i N\Sigma_a\,dz$. Thus the incident intensity a distance z inside R is not I_{i0}, the intensity at the start of penetration, but $I_{i0}\exp[-Nz(\Sigma_s+\Sigma_a)]$. But Eq. (8.2.29) was derived assuming that I_i is constant throughout R, which means that we have assumed that $Nl(\Sigma_s+\Sigma_a)$, where l is the distance along the beam from one side of R to the other, is small compared with unity. If this is not the case, much of the scattered wave will be rescattered before it emerges from R; multiple scattering will be important. Considerations of space persuade us to omit this complex subject.

Whether multiple scattering is important or not, the attenuation of the *incident* wave in traversing a distance z of region R is given by the factor $\exp[-Nz(\Sigma_s+\Sigma_a)]$, with Σ_s and Σ_a given by Eqs. (8.2.19), (8.2.20), or (8.2.22) for small scatterers, by Eq. (8.2.18) for larger ones, and with N the mean number of scatterers per unit volume of R. In a distance dz the fraction of *incident* energy absorbed by the scatterers is $N\Sigma_a\,dz$, and the fraction which is scattered in directions other than the incident direction is $N\Sigma_s\,dz$. When multiple scattering is important, some energy is absorbed by the scattered wave before it emerges from R, and some of the scattered wave is rescattered, but these formulas still tell what happens to the incident wave, the part of the wave which has not yet been affected by a scatterer.

8.3 SCATTERING FROM SURFACE IRREGULARITIES

When a plane wave of sound impinges on a surface, large in extent with respect to a wavelength but irregular either in shape or in regard to its reaction to sound, the wave returning from the surface will be distorted because of the irregularities. The simplest example of these effects occurs for a plane reflecting surface, as shown in Fig. 8.7. We saw in Sec. 6.3 that a plane wave of amplitude P_i, incident at angle ϑ_i on a smooth boundary plane of uniform point impedance $\rho c/\beta$, is reflected as a plane wave at angle

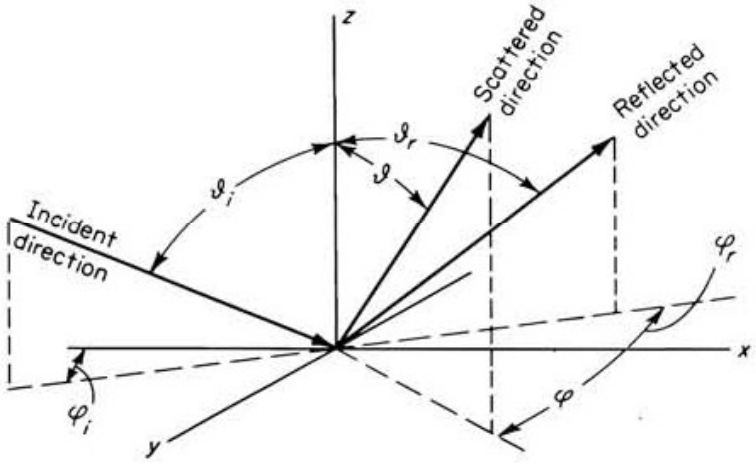


FIGURE 8.7
Directions and angles for reflection and scattering of a plane wave incident on the xy plane.

$\vartheta_r = \vartheta_i$ to the z axis, with amplitude $P_i C_r$, where

$$C_r = \frac{\cos\vartheta - \beta}{\cos\vartheta_i + \beta}$$

If either the specific admittance β changes from point to point along the plane or if the boundary itself is not a perfect plane, the reflected wave will not be plane. If the surface deviation is not large, the wave reflected may be represented as a reflected plane wave plus a scattered wave, which measures the degree of distortion.

Irregularities in surface admittance

Suppose the xy plane has point impedance $\rho c/\beta_0$ everywhere except over an area A, which can be circumscribed by a circle of radius a, with center at the origin. Within A the surface admittance is $\beta(x,y)$, different from β_0. As before, we carry out the analysis by means of the Green's function of Fig. 7.6 and Eqs. (7.4.10) and (7.4.11), corresponding to a source point at (x_0,y_0,z_0) (with $z_0 \geqslant 0$) plus an image point at $(x_0, y_0, -z_0)$, producing a reflected wave of amplitude modified by the factor $(\cos\vartheta' - \beta_0)/(\cos\vartheta' + \beta_0)$, corresponding to the uniform admittance β_0 over the whole xy plane. This Green's function satisfies the boundary condition

$$(\partial G/\partial z)_{z=0} = -ik\beta_0 G(x,y,0 \mid x_0,y_0,z_0)$$

The acoustic pressure wave, on the other hand, must satisfy the boundary conditions $(\partial p/\partial z)_{z=0} = -ik\beta p_{z=0}$ within area A; $(\partial p/\partial z)_{z=0} = -ik\beta_0 p_{z=0}$ over the rest of the boundary plane.

If there were no irregularity in surface admittance, β being β_0 everywhere, the complete solution, for the case of a plane incident wave at angle ϑ_i, in a plane at angle φ_i to the xz plane, would be the combination of incident and reflected waves,

$$p_i(r) = P_i \exp\left[ik \sin\vartheta_i(x\cos\varphi_i + y\sin\varphi_i) - ikz\cos\vartheta_i\right]$$
$$+ P_i \frac{\cos\vartheta_i - \beta_0}{\cos\vartheta_i + \beta_0} \exp\left[ik\sin\vartheta_i(x\cos\varphi_i + y\sin\varphi_i) + ikz\cos\vartheta_i\right] \quad (8.3.1)$$

times the factor $e^{-i\omega t}$. This is an obvious generalization of Eq. (6.3.7). When $\beta \neq \beta_0$ inside A, the complete solution may be obtained from Eq. (7.1.17) as p_i plus a surface integral over area A.

$$p(\mathbf{r}) = p_i(\mathbf{r}) + ik\iint_A (\beta - \beta_0)p(x_0,y_0,0)G(x,y,z \mid x_0,y_0,0)\,dx_0\,dy_0 \quad (8.3.2)$$

This is an inhomogeneous integral equation for p, which must usually be solved by approximation techniques.

The far field

In order to measure the scattered wave, represented by the integral, separately from the incident-reflected wave, the measurement point r, ϑ, φ must be far from the area A, usually far enough so that the approximation

$$G \simeq \frac{e^{ikr}}{4\pi r}\left[e^{-ikz_0\cos\vartheta} + \frac{\cos\vartheta - \beta_0}{\cos\vartheta + \beta_0}\, e^{ikz_0\cos\vartheta}\right] \times \exp\left[-ik\sin\vartheta\,(x_0\cos\varphi + y_0\sin\varphi)\right] \quad (8.3.3)$$

is valid. To compute the asymptotic form for the scattered wave, we need only insert this form for G, times a good approximation for the pressure $p(x_0,y_0,0)$ on the area A, into the integral.

Well outside A this surface pressure will be approximately equal to $p_i(x_0,y_0,0)$, having amplitude $2P_i\cos\vartheta_i/(\cos\vartheta_i + \beta_0)$ and phase factor $\exp[ik\sin\vartheta_i(x\cos\varphi_i + y\sin\varphi_i)]$, whereas, if A is very large, the surface pressure well inside A will be approximately $2P_i\cos\vartheta_i/(\cos\vartheta_i + \beta_a)$ times the same phase factor, if β inside A does not differ much from its mean value β_a inside A. Probably a good approximation is to use this last expression for $p(x_0,y_0,0)$ everywhere inside A.

Thus an approximate formula for the scattered wave, at large distances from the scattering area, is

$$p_s(\mathbf{r}) \to P_i\Phi(\vartheta_i,\varphi_i \mid \vartheta,\varphi)\frac{e^{ikr}}{r} \qquad r \gg a$$

$$\Phi \simeq \frac{ik\cos\vartheta\cos\vartheta_i}{2\pi(\cos\vartheta + \beta_0)(\cos\vartheta_i + \beta_a)}\iint_A (\beta - \beta_0)e^{i\mu_x x_0 + \mu_y y_0}\,dx_0\,dy_0 \quad (8.3.4)$$

where

$$\mu_x = k(\sin\vartheta_i\cos\varphi_i - \sin\vartheta\cos\varphi)$$
$$\mu_y = k(\sin\vartheta_i\sin\varphi_i - \sin\vartheta\sin\varphi)$$
$$k^2\gamma^2 = \mu_x^2 + \mu_y^2 = k^2[\sin^2\vartheta_i + \sin^2\vartheta - 2\sin\vartheta_i\sin\vartheta\cos(\varphi - \varphi_i)]$$

Thus the scattered amplitude is approximately proportional to the two-dimensional Fourier transform of the admittance difference $\beta - \beta_0$ for area A. If we define vector $\mathbf{k}_r = (k\sin\vartheta_i\cos\varphi_i, k\sin\vartheta_i\sin\varphi_i, k\cos\vartheta_i)$ as the wavenumber vector, of magnitude k, in the direction of propagation of the reflected wave, and $\mathbf{k}_s = (k\sin\vartheta\cos\varphi,\ k\sin\vartheta\sin\varphi,\ k\cos\vartheta)$ as the wavenumber vector in the direction of the point of observation, then the quantity in the exponent in the integral is $i\boldsymbol{\mu}\cdot\mathbf{r}_0$, where $\mathbf{r}_0 = (x_0,y_0,0)$ is the radius vector to a point on the scattering area A, and $\boldsymbol{\mu} = \mathbf{k}_r - \mathbf{k}_s$ is the recoil vector of Eq. (8.1.20). Thus $k\gamma$ is the length of the projection of vector $\boldsymbol{\mu}$ on the xy plane.

In general (but not always), the integral, and thus the amplitude of the scattered wave, is largest when $\boldsymbol{\mu} = 0$, that is, in the direction of the reflected

wave. When the dimensions of A are small compared with the wavelength, the scattered wave is nearly isotropic; when A is large compared with λ, the scattered wave is (usually) concentrated in the direction of the reflected wave.

To illustrate these generalities we compute the angle-distribution factor $\Phi(\vartheta_i,\varphi_i \mid \vartheta,\varphi)$ for a few simple distributions of admittance. The first is a rectangular patch of length l in the x direction and width w in the y direction, with β constant (and different from β_0) over the whole area lw. The angle-distribution factor is

$$\Phi_\beta \simeq \frac{iklw(\beta - \beta_0)\cos\vartheta_i \cos\vartheta}{2\pi(\cos\vartheta_i + \beta)(\cos\vartheta + \beta_0)} \left[\frac{\sin(\mu_x l/2)}{(\mu_x l/2)} \frac{\sin(\mu_y w/2)}{\mu_y w/2}\right] \tag{8.3.5}$$

Referring to the definition of $\boldsymbol{\mu}$ and of γ, we see that if both kl and kw are less than $\frac{1}{2}\pi$, the quantity in brackets changes very little with ϑ or φ, so the scattered wave is nearly independent of ϑ and φ. On the other hand, if $kl \gg \frac{1}{2}\pi$ and $kw < \frac{1}{2}\pi$, then the scattered amplitude is only large when $\gamma_x = \sin\vartheta_i \cos\varphi_i - \sin\vartheta\cos\varphi$ is much smaller than unity, i.e., when the vector $\boldsymbol{\mu} = \mathbf{k}_r - \mathbf{k}_s$ is nearly perpendicular to the x axis (the long axis of the rectangle); in other words, the scattered wave is confined mainly to the plane defined by the reflection vector k_r and the y axis. If both l and w are large compared with a wavelength, the scattered wave is concentrated mostly in the direction of reflection.

If the patch of admittance β is a circular area of radius a, the angle factor is

$$\Phi_\beta \simeq \frac{ik\pi a^2(\beta - \beta_0)\cos\vartheta_i \cos\vartheta}{2\pi(\cos\vartheta_i + \beta)(\cos\vartheta + \beta_0)} \left[\frac{2J_1(k\gamma a)}{k\gamma a}\right] \tag{8.3.6}$$

the only difference from Eq. (8.3.5) being in the factor in brackets, which is more symmetric, depending on $\varphi - \varphi_i$ instead of on φ and φ_i separately. Figure 8.8 shows plots of $|\Phi_\beta|$ for the incident wave at 45° on a circular "soft spot" of radius a. Contours of constant amplitude of Φ_β are plotted on the ϑ, φ surface, for two different values of $ka = 2\pi a/\lambda$, to show the variation of scattered pressure amplitude with angle of scattering. For the longer wavelength, the scattered wave is not much dependent on ϑ or φ; for $ka = 4$, the scattered wave is concentrated in a peak around the direction of the reflected wave, at $\varphi = 0°$, $\vartheta = 45°$, indicated by the small circle on both plots. In the latter case the scattered wave has a node ($|\Phi_\beta| = 0$) and one diffraction band (where Φ_β changes sign).

An example where the scattered wave is not most intense in the direction of the reflected wave is that where β is periodic, forming a "diffraction grating,"

$$\beta - \beta_0 = B\cos\frac{2\pi x}{d} \qquad \text{for } -\tfrac{1}{2}l < x < \tfrac{1}{2}l,\ -\tfrac{1}{2}w < y < \tfrac{1}{2}w$$

In this case, integration of Eq. (8.3.4) produces

$$\Phi_\beta \simeq \frac{iklwB\cos\vartheta_i\cos\vartheta}{2\pi(\cos\vartheta_i+\beta_0)(\cos\nu+\beta_0)}\left\{\frac{\sin\left[\frac{1}{2}\mu_x l-(\pi l/d)\right]}{\frac{1}{2}\mu_x l-(\pi l/d)}+\frac{\sin\left[\frac{1}{2}\mu_x l+(\pi l/d)\right]}{\frac{1}{2}\mu_x l+(\pi l/d)}\right\}\frac{\sin(\mu_y w/2)}{\mu_y w/2} \quad (8.3.7)$$

Here the strongest scattered wave is not in the direction of reflection, but rather in the directions of the diffracted beams, for which $\mu_x/2\pi \equiv (1/\lambda)\times(\sin\vartheta_i\cos\varphi_i-\sin\vartheta\cos\varphi)=\pm(1/d)$.

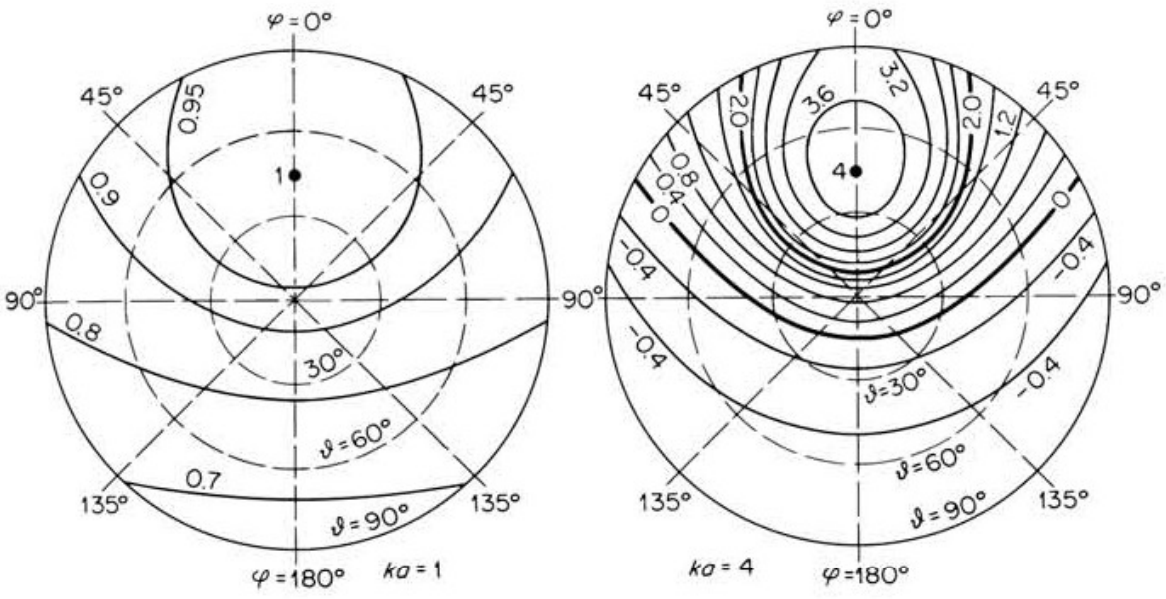


FIGURE 8.8
Contours of equal scattered pressure amplitude, plotted against angles of scattering ϑ, φ for plane wave incident at angles $\vartheta_i = 45°$, $\varphi_i = 0°$, on an absorbing disk of radius a, set in an otherwise rigid plane. See Eq. (8.3.6).

Surface roughness

If the irregularity in area A is in actual shape rather than in admittance, the scattering effect will come from the fact that the boundary condition is now applied for a surface which differs from the xy plane. Suppose the reflecting surface is not $z = 0$ for all values of x and y, but is $z = \xi(x,y)$ within A; suppose also that this surface, at x, y, has admittance $\beta(x,y)$, which may differ from the constant admittance β_0 of the flat surface outside A. The integral equation for the pressure wave is then

$$p(x,y,z) = p_i(x,y,z) + \iint\left[G(x,y,z\mid x_0,y_0,\xi)\frac{\partial}{\partial n_0}p(x_0,y_0,\xi) - p(x_0,y_0,\xi)\frac{\partial}{\partial n_0}G(x,y,z\mid x_0,y_0,\xi)\right]dx_0\,dy_0 \quad (8.3.8)$$

where p_i is the incident-reflected wave of Eq. (8.3.1), G is as given in Eq. (8.3.3), and the normal gradient $\partial/\partial n_0$ is normal to the surface $\xi(x_0,y_0)$.

$$\frac{\partial}{\partial n_0} = -\frac{\partial}{\partial z_0} + \frac{\partial \xi}{\partial x_0}\frac{\partial}{\partial x_0} + \frac{\partial \xi}{\partial y_0}\frac{\partial}{\partial y_0} \qquad \text{if } \operatorname{grad}_0 \xi \ll 1$$

If the displacement ξ of the surface from the xy plane is everywhere less than a wavelength, we can expect the Born approximation to be valid. In this case we can use the approximations

$$p \simeq P_i \frac{2\cos\vartheta_i}{\cos\vartheta_i + \beta}(1 - ik\beta z_0)\exp\left[ik\sin\vartheta_i(x_0\cos\varphi_i + y_0\sin\varphi_i)\right]$$

$$G \simeq \frac{e^{ikr}}{4\pi r}\frac{2\cos\vartheta}{\cos\vartheta + \beta_0}(1 - ik\beta_0 z_0)\exp\left[-ik\sin\vartheta\,(x_0\cos\varphi + y_0\sin\varphi)\right]$$

inside the integral; the approximate expression for the incident plus reflected plus scattered wave becomes $p = p_i(\mathbf{r}) + p_s(\mathbf{r})$, where p_i is given in Eq. (8.3.1), and $p_s(\mathbf{r}) = P_i(e^{ikr}/r)\Phi(\vartheta,\varphi)$, with

$$\Phi(\vartheta,\varphi) \simeq \frac{i}{\pi}\frac{\cos\vartheta_i\cos\vartheta}{(\cos\vartheta_i + \beta)(\cos\vartheta + \beta_0)}\iint\left[k(\beta - \beta_0) + \mu_x\frac{\partial\xi}{\partial x_0} + \mu_y\frac{\partial\xi}{\partial y_0}\right]e^{i(\mu_x x_0 + \mu_y y_0)}\,dx_0\,dy_0 \qquad (8.3.9)$$

The components of vector $\boldsymbol{\mu}$ are given in Eq. (8.3.4). This equation for the angle distribution of the scattered wave is a generalization of Eq. (8.3.4) when the area A is rough, as well as uneven in admittance.

Since this integral can be manipulated just as that of Eq. (8.3.4) was, we shall content ourselves with a single example, that of a rectangular, raised area of length l, width w, and height h. In this case the expressions for the components of the gradient of ξ are given in terms of delta functions at the edges.

$$\frac{\partial\xi}{\partial x_0} \simeq h[\delta(x_0 + \tfrac{1}{2}l) - \delta(x_0 - \tfrac{1}{2}l)] \qquad \text{for } -\tfrac{1}{2}w < y_0 < \tfrac{1}{2}w$$

$$\frac{\partial\xi}{\partial y_0} \simeq h[\delta(y_0 + \tfrac{1}{2}w) - \delta(y_0 - \tfrac{1}{2}w)] \qquad \text{for } -\tfrac{1}{2}l < x_0 < \tfrac{1}{2}l$$

The scattering arising from the difference in admittance has already been computed. The additional scattering coming from the change in shape of the boundary is

$$\Phi_\xi(\vartheta_i,\varphi_i \mid \vartheta,\varphi) \simeq \frac{ikwkh\cos\vartheta_i\cos\vartheta}{\pi(\cos\vartheta_i + \beta)(\cos\vartheta + \beta_0)}\left[\gamma^2\frac{\sin(\mu_x l/2)}{\mu_x l/2}\frac{\sin(\mu_y w/2)}{\mu_y w/2}\right] \qquad (8.3.10)$$

which does not differ much from the expression of Eq. (8.3.5). Aside from

the dimensionless factor kh, measuring the change in shape, which replaces the dimensionless factor $\beta - \beta_0$, there is an additional directional factor,

$$\gamma^2 = \sin^2 \vartheta_i + \sin^2 \vartheta - 2 \sin \vartheta_i \sin \vartheta \cos (\varphi_i - \varphi) \qquad (8.3.11)$$

proportional to the square of the length of the projection of vector $\boldsymbol{\mu}$ on the xy plane. This is small when $\boldsymbol{\mu}$ is small, i.e., for scattering in a direction close to the direction of the reflected wave, and large only when $\boldsymbol{\mu}$ is large and nearly horizontal, i.e., in a direction near that of the negative of the incident wave. Thus the factor γ^2 is small when the rest of the factors in brackets are large, and vice versa, so that this part of the scattering is small for all directions. This is not surprising, for the "roughness" in the example we have chosen is only at the edges of the raised panel; the rest of area A is flat and contributes nothing to this part of the scattering.

The effect of random roughness

A situation of some practical interest involves the scattering of sound incident on a patch of rough surface which also has random variations in surface admittance. In area A the quantities $\beta - \beta_0$ and ξ exhibit random fluctuations, with correlation lengths w_β and w_ξ, respectively. Area A may be the only area of the surface in which $\beta - \beta_0$ and ξ differ from zero, or it may be that area A is the only part of the surface which is "illuminated" by the beam of sound sent out by a distant source. If the beam covers a solid angle Ω, if the axis of the beam is at an angle ϑ_i to the z axis, and if the distance r_s to the source is great, then the area $A = \Omega r_s^2/\cos \vartheta_i$ and the scattered sound will arise from this area. Figure 8.9 shows the quantities involved.

An obvious modification of Eq. (8.3.9) gives, for the scattered pressure reaching point $\mathbf{r}$ at angle ϑ, φ, if the source is producing a steady wave of

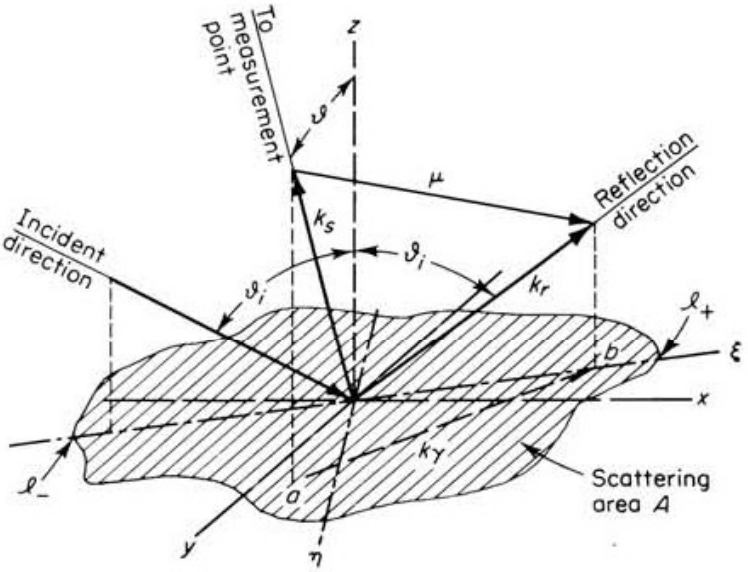


FIGURE 8.9
Directions and axes involved in calculating the scattering from a rough surface..

frequency $\omega/2\pi$, having a pressure amplitude P_i by the time it reaches A,

$$p_s(\mathbf{r},\omega) = P_i \frac{e^{ikr}}{\pi r} \frac{\cos\vartheta_i \cos\vartheta}{(\cos\vartheta_i + \beta_0)(\cos\vartheta + \beta_0)} \iint [ikb(\mathbf{r}_0) + k^2\gamma^2\xi(\mathbf{r}_0)] e^{i\mu_x x_0 + i\mu_y y_0}\, dx_0\, dy_0$$

By now the rest of the procedure is familiar. The function $b = \beta - \beta_0$ is the deviation of the admittance at point $\mathbf{r}_0$ on the surface from the mean value β_0, and ξ is the normal displacement of the boundary surface from its mean shape, the xy plane. Their correlation functions will be, approximately,

$$\Upsilon_\beta(\mathbf{d}) = \langle b^2\rangle e^{-\frac{1}{2}(d^2/w_\beta{}^2)} \qquad \Upsilon_\xi(\mathbf{d}) = \langle \xi^2\rangle e^{-\frac{1}{2}(d^2/w_\xi{}^2)}$$

if their fluctuations are random and isotropic. Quantities $\langle b^2\rangle$ and $\langle \xi^2\rangle$ are the mean-square values of b and of ξ over the illuminated area A. If, in addition, the two variations are statistically independent, the intensity of the scattered sound turns out to be

$$I_s \simeq 4\pi^2 I_i \frac{A}{r^2} \left| \frac{\cos\vartheta_i \cos\vartheta}{(\cos\vartheta_i + \beta_0)(\cos\vartheta + \beta_0)} \right|^2 \{k^2 |B(k\gamma)|^2 + k^4\gamma^4 |Z(k\gamma)|^2\}$$

$$= I_i \frac{A}{2\pi r^2} \left| \frac{\cos\vartheta_i \cos\vartheta}{(\cos\vartheta_i + \beta_0)(\cos\vartheta + \beta_0)} \right|^2 \{k^2 w_\beta{}^2 \langle b^2\rangle e^{-\frac{1}{2}k^2\gamma^2 w_\beta{}^2} + k^4\gamma^4 w_\xi{}^2 \langle \xi^2\rangle e^{-\frac{1}{2}k^2\gamma^2 w_\xi{}^2}\} \quad (8.3.12)$$

where $B(\mathbf{K})$ is the two-dimensional spatial Fourier transform of $b(\mathbf{r})$, and $Z(\mathbf{K})$ is the corresponding transform of $\xi(\mathbf{r})$. The angles and quantities involved are shown in Fig. 8.9. $I_i = |P_i|^2/\rho c$ is the intensity incident on A; the dependence of γ^2 on the angles of incidence and of scattering is given in Eq. (8.3.11). For scattering in the direction of reflection, $\gamma = 0$; for scattering back to the source, $\gamma = 2 \sin\vartheta_i$.

The first term in braces, the scattering caused by the admittance variation, has its maximum in the direction of the reflected wave, as mentioned earlier. When the incident wavelength is large compared with the admittance correlation length w_β, this scattering is nearly isotropic. The second term in braces, the scattering caused by roughness, avoids the direction of reflection and, for very long wavelengths, produces little scattering. For shorter wavelengths the scattered intensity concentrates in a cone around the reflection direction; this term is zero when $\gamma = 0$ and has its maximum value for $k\gamma w_\zeta = 2$, that is, at an angle roughly $\lambda/\pi w_\zeta$ radians from the reflection direction. Figure 8.10 shows a typical example, with the admittance scattering given in one plot, the roughness scattering in the other. Note that the roughness scattering avoids the reflection direction. Compare with Fig. 8.8.

If we work out the scattering of a pulse-wave from this area, we should obtain a result quite similar to that of Prob. 11. The scattered wave would not be a pulse (except in the reflection direction), but would be a rumble, reproducing in time the spatial irregularities of admittance and shape. The spectrum density of this scattered sound would equal the I_s of Eq. (8.3.12).

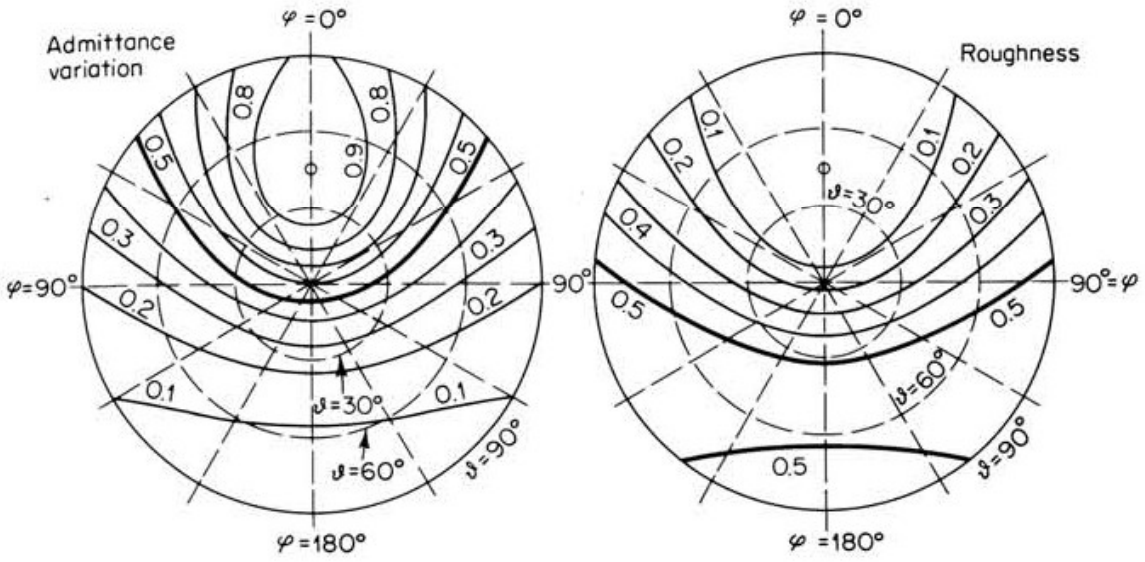


FIGURE 8.10
Contours of equal amplitude of wave scattered from a patch of random variation in admittance or from a rough patch, as function of angles ϑ, φ of scattering for $kw = 2\pi w/\lambda = 0.707$, w being the correlation length for admittance or for roughness. Reflection direction is $\vartheta = 45°$, $\varphi = 0°$, position of maximum for admittance scattering, of zero scattering for roughness. Compare with Fig. 8.8.

8.4 DIFFRACTION

When the scattering object is large compared with the wavelength of the scattered sound, we usually say the sound is reflected and diffracted, rather than scattered. The effects are really the same, but the relative magnitudes differ enough so that there seems to be a qualitative difference. Behind the object there is a shadow, where the pressure amplitude is vanishingly small; in front or to the side, in the "illuminated" region, there is a combination of the incident wave and the wave reflected from the surface of the scattering object. At the edge of the shadow the wave amplitude does not drop discontinuously from its value in the illuminated region to zero; the amplitude oscillates about its illuminated value, with increasing amplitude, reaching its maximum just before the edge of the shadow, and then dropping monotonically, approaching zero well inside the shadow.

These fluctuations of amplitude, near the shadow edge, are called *diffraction bands*. Their angular spacing depends on the ratio between the

wavelength of the incident sound and the distance from the observation point to the line on the scattering object separating "light" from "shadow." This behavior was touched on in connection with the scattering from a cylinder [see discussion of Eq. (8.1.4)] and from a sphere. To study it in detail we shall compute the diffraction of an incident plane wave from a rigid half-plane. Diffraction patterns also arise in the reflection of a plane wave from a plane surface, one large area of which differs in impedance from the rest of the plane.

Diffraction from a knife-edge

The simplest diffraction problem is that of a plane wave traveling in the negative x direction, striking a rigid half-plane extending from the line $x = y = 0$, $-\infty < z < \infty$, to infinity in the direction $\frac{3}{2}\pi - \Psi$, as shown in Fig. 8.11. The "shadow line" is the negative x axis; the region III, $\pi < \phi < \frac{3}{2}\pi - \Psi$, is in shadow. In region I, $-2\Psi < \phi < \pi$, the incident wave $Ae^{-ikx} = Ae^{-ikr\cos\phi}$ predominates, and in region II, $-\frac{1}{2}\pi - \Psi < \phi < -2\Psi$, there is, in addition to the incident wave, a reflected wave $Ae^{ikr\cos(\phi+\Psi)}$. The details of how these solutions join together at the edges of the regions must be obtained from the solution of the boundary-value problem.

This solution is most easily obtained from the function

$$U(r,\phi) = \tfrac{1}{2}\sum_{m=0}^{\infty} \epsilon_m(-i)^{\frac{1}{2}m}\cos(\tfrac{1}{2}m\phi)J_{\frac{1}{2}m}(kr) \qquad (8.4.1)$$

Comparison with Eq. (8.1.1) shows that this is not the expansion of a plane wave in polar coordinates because it includes half-integer orders as well as integral orders of J. In fact, the plane wave is

$$e^{-ikr\cos\phi} = \sum_{n=0}^{\infty} \epsilon_n(-i)^n\cos(n\phi)J_n(kr) = U(r,\phi) + U(r,\phi+2\pi)$$

Reference to Eq. (7.3.1) indicates that $U(r,\phi)$ is a solution of the wave equation; but it is not periodic in ϕ with period 2π; it is periodic with period 4π.

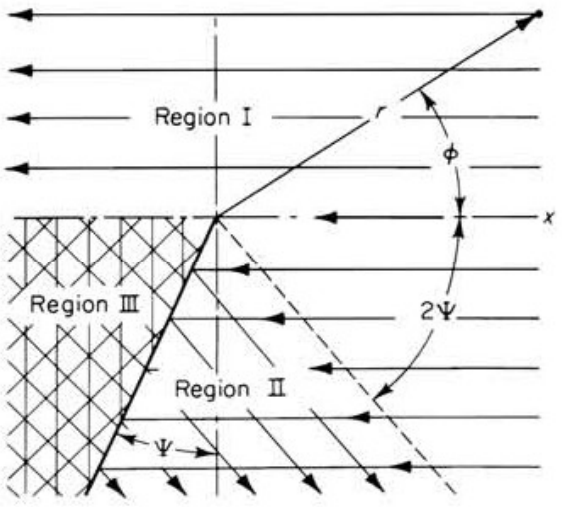


FIGURE 8.11
Diffraction of a plane wave by the edge of a rigid half-plane.

Thus, to use U for a solution in free space would be forbidden, for U is two-valued in ϕ if ϕ is unlimited.

In the problem we are now solving, however, ϕ is limited in range; its greatest positive value is $\frac{3}{2}\pi - \Psi$, and its largest negative value is $-\frac{1}{2}\pi - \Psi$ (Ψ can be negative, of course; its allowed range of values is $-\frac{1}{2}\pi < \Psi < \frac{1}{2}\pi$). Within this range of values of ϕ, we can use a combination of U's to satisfy boundary conditions at the half-plane. If the plane is rigid, the condition is that $\partial p/\partial\phi = 0$ at $\phi = \frac{3}{2}\pi - \Psi$ or $-\frac{1}{2}\pi - \Psi$. This is satisfied if we use the following combination for the pressure:

$$p(r,\phi) = AU(r,\phi) + AU(r, 3\pi - 2\Psi - \phi) \tag{8.4.2}$$

Since U is periodic with period 4π, the two U's do not cancel everywhere; their ϕ gradients do cancel on both sides of the plane barrier, however.

In order to find out the details of this solution, we should find a closed form for the series U. This can be done in several ways. By using the first of Eqs. (5.2.21) and combining the series, we can show that

$$\frac{\partial U}{\partial \phi} - ikr \sin\phi\, U = -\sqrt{\frac{kr}{2\pi i}}\, e^{ikr} \sin\tfrac{1}{2}\phi$$

Solution of this, plus the fact that $U(0,\phi) = \frac{1}{2}$, shows that

$$U(r,\phi) = e^{ikr\cos\phi}\, E(\sqrt{2kr}\cos\tfrac{1}{2}\phi) \tag{8.4.3}$$

where

$$E(z) = \frac{1}{\sqrt{i\pi}} \int_{-\infty}^{z} e^{it^2} dt \to \begin{cases} 1 - \sqrt{\dfrac{i}{4\pi z^2}}\, e^{iz^2} & z \to +\infty \\ \dfrac{1}{2} & z \to 0 \\ -\sqrt{\dfrac{i}{4\pi z^2}}\, e^{iz^2} & z \to -\infty \end{cases}$$

Alternatively, the integral expression for U can be expanded in a Fourier series and shown to be equal to the series of Eq. (8.4.1).

For intermediate values of $z = \sqrt{u}$, we can express $E(z)$ in terms of Fresnel integrals

$$C(u) = \sqrt{\frac{2}{\pi}} \int_0^{\sqrt{u}} \cos t^2\, dt \qquad S(u) = \sqrt{\frac{2}{\pi}} \int_0^{\sqrt{u}} \sin t^2\, dt \tag{8.4.4}$$

as follows:

$$E(\sqrt{u}) = \begin{cases} 1 - \frac{1}{2}[1 - C(u) - S(u)] - \frac{1}{2}i[C(u) - S(u)] & \sqrt{u} \geqslant 0 \\ \frac{1}{2}[1 - C(u) - (u)] + \frac{1}{2}i[C(u) - S(u)] & \sqrt{u} \leqslant 0 \end{cases} \tag{8.4.5}$$

The functions $1 - C(u) - S(u)$ and $C(u) - S(u)$ are plotted in Fig. 8.14. Tables of the functions are not hard to find.

Returning to Eq. (8.4.2) for the solution, we see that

$$p(r,\phi) = Ae^{-ikr\cos\phi}\, E[\sqrt{2kr}\cos\tfrac{1}{2}\phi] + Ae^{ikr\cos(\phi+2\Psi)}\, E[\sqrt{2kr}\cos(\tfrac{3}{2}\pi - \Psi - \tfrac{1}{2}\phi)] \quad (8.4.6)$$

$$p \xrightarrow[kr\to\infty]{} \begin{cases} AD(r,\phi) & \text{(in region III)} \\ Ae^{-ikr\cos\phi} + AD(r,\phi) & \text{(in region I)} \\ Ae^{-ikr\cos\phi} + Ae^{ikr\cos(\phi+2\Psi)} + AD(r,\phi) & \text{(in region II)} \end{cases} \quad (8.4.7)$$

where

$$D(r,\phi) = \frac{e^{ikr}}{\sqrt{8\pi ikr}}\left[\frac{1}{\sin(\Psi + \frac{1}{2}\phi)} - \frac{1}{\cos\frac{1}{2}\phi}\right]$$

The first expression in the asymptotic formula is for the shadow region; in this region the only wave is a cylindrical wave represented by function D, emanating as if from the knife-edge, with amplitude which diminishes as one goes deeper into the shadow as $\phi - \pi$ increases; the asymptotic form is not valid for ϕ very close to π or very close to -2Ψ. In region I the predominant term is the incident wave, but the cylindrical wave is also present. Finally, in region II, the wave reflected from the half-plane is present, as well as the incident wave and the cylindrical "diffraction wave" $D(r,\phi)$.

Looking more closely at the behavior of the wave, let us calculate the mean-square pressure in the region near the shadow line dividing region III from region I. Suppose the pressure is measured along a line $x = -l$, for different values of y: $y = 0$ being the edge of the geometric shadow, y negative being in shadow, and y positive being in region I. We define

$$\begin{aligned} &\alpha = \pi - \phi \qquad y = r\sin\alpha \qquad l = r\cos\alpha \\ &u = kr(1 + \cos\phi) = k(\sqrt{l^2 + y^2} - l) \\ &v = kr[1 + \cos(2\Psi - \alpha)] = u + kl(1 + \cos 2\Psi) + ky\sin 2\Psi \end{aligned} \quad (8.4.8)$$

Then the asymptotic expression for the mean-square pressure as function of y is

$$|p|^2 \to |A|^2 \begin{cases} \dfrac{1}{4\pi}[(v)^{-\frac{1}{2}} - (u)^{-\frac{1}{2}}]^2 & y < -\sqrt{\dfrac{l}{k}} \\ 1 + \dfrac{1}{\sqrt{\pi}}[(v)^{-\frac{1}{2}} - (u)^{-\frac{1}{2}}]\cos(u + \frac{1}{4}\pi) & y > \sqrt{\dfrac{l}{k}} \end{cases} \quad (8.4.9)$$

This formula predicts the monotonic decrease in $|p|^2$ inside the shadow as $-y$ increases. It also indicates that $|p|^2$ oscillates about its mean value $|A|^2$ as y is increased in the illuminated region I. But it is not valid close

to the edge of the shadow, where $|y| < \sqrt{l/k}$, because we have used the asymptotic form of Eq. (8.4.3) in Eq. (8.4.6) for both the functions E. A more accurate formula, using (8.4.5) for $E(\sqrt{2kr}\cos\frac{1}{2}\phi)$ and the asymptotic form for the other E, since it is valid throughout the region near $\phi = \pi$ as long as $kr > 20$, is

$$\left|\frac{p}{A}\right|^2 \simeq \begin{cases} [\frac{1}{2} + \frac{1}{2}C(u) + \frac{1}{2}S(u) + (4\pi v)^{-\frac{1}{2}}\cos(u + \frac{1}{4}\pi)]^2 \\ \quad + [\frac{1}{2}C(u) - \frac{1}{2}S(u) - (4\pi v)^{-\frac{1}{2}}\sin(u + \frac{1}{4}\pi)]^2 & y \geqslant 0 \\ [\frac{1}{2} - \frac{1}{2}C(u) - \frac{1}{2}S(u) + (4\pi v)^{-\frac{1}{2}}\cos(u + \frac{1}{4}\pi)]^2 \\ \quad + [\frac{1}{2}C(u) - \frac{1}{2}S(u) + (4\pi v)^{-\frac{1}{2}}\sin(u + \frac{1}{4}\pi)]^2 & y \leqslant 0 \end{cases} \tag{8.4.10}$$

plotted in Fig. 8.12 for $kl = 50$, as function of y/l. It shows that the transition from illumination to shadow indicates that $|p/A|^2$ is about $\frac{1}{4}$ at $y = 0$, the geometric shadow line, and that its maximum value is about $\frac{4}{3}$ at a point about two wavelengths inside the illuminated region. It also shows that the asymptotic formula (8.4.9) is adequate for $|y|$ greater than about three wavelengths. These results would be somewhat altered for different values of kl or of Ψ. The effect of Ψ on the results is small, however; the curve for $|p/A|^2$ versus y/l for $kl = 50$ and $\Psi = 45°$ would be too close to the curve for $\Psi = 0°$, which is plotted, to be able to distinguish clearly between the two.

The transition from region I to region II is provided with similar diffraction bands, further complicated by the interference between the incident and reflected waves. Equations (8.4.5) and (8.4.6) enable one to compute $|p/A|^2$ here also.

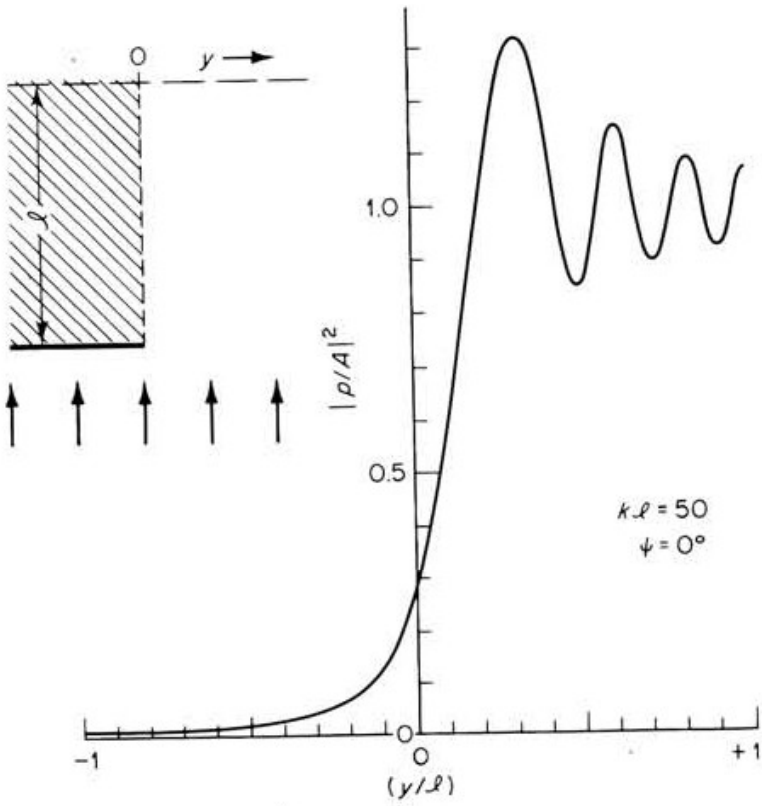


FIGURE 8.12
Mean-square pressure of diffracted plane wave at point l beyond obstructing half-plane and distance y from "shadow line," for $l \simeq 8\lambda$.

Diffraction of a reflected wave

Similar diffraction effects occur when a sound wave reflects from an infinite plane wall, one half of which is rigid, the other half soft. Suppose the wall is the xy plane, the half of the wall for x positive having a uniform, specific acoustic admittance β, and the half for x negative having $\beta = 0$. If the incident-wave direction is given by the angles ϑ_i, φ_i of Fig. 8.7, we can separate off the factor $\exp [i(\omega/c) \sin \vartheta_i \sin \varphi_j]$ from all the equations, leaving a two-dimensional formula for the motion in the xz plane. For example, the wave equation for p can be written

$$e^{iy(\omega/c) \sin \vartheta_i \sin \varphi_i}\left(\frac{\partial^2}{\partial x^2} + \frac{\partial^2}{\partial z^2} + k^2\right)p = 0$$

where

$$k^2 = \left(\frac{\omega}{c}\right)^2(1 - \sin^2 \vartheta_i \sin^2 \varphi_i)$$

and the equation for the Green's function is

$$e^{iy(\omega/c) \sin \vartheta_i \sin \varphi_i}\left(\frac{\partial^2}{\partial x^2} + \frac{\partial^2}{\partial z^2} + k^2\right)G = \delta(x - x_0)\delta(z - z_0)e^{iy(\omega/c) \sin \vartheta_i \sin \phi_i} \tag{8.4.11}$$

In terms of the component wavenumber k in the xz plane, the x and z components are $k_x = k \sin \theta_i$, $k_z = k \cos \theta_i$, where

$$\sin \theta_i = \frac{\sin \vartheta_i \cos \varphi_i}{\sqrt{1 - \sin^2 \vartheta_i \sin^2 \varphi_i}} \qquad \cos \theta_i = \frac{\cos \vartheta_i}{\sqrt{1 - \sin^2 \vartheta_i \sin^2 \varphi_i}} \tag{8.4.12}$$

We can thus neglect the y component of the wave and work out the problem as though the incident wave were pointed in the xz plane, with a wavenumber $k < \omega/c$ and at an angle of incidence θ_i.

Referring to Eqs. (8.3.1) and (8.3.2), we see that the integral equation for the pressure wave in the region $z > 0$ is

$$p(x,z) = 2P_i e^{ikx \sin \theta_i} \cos (kz \cos \theta_i) + ik\beta \int_0^\infty p(x_0,0)G_k(x,z \mid x_0,z_0)\, dx_0 \tag{8.4.13}$$

The Green's function is the two-dimensional one satisfying the boundary condition $\partial G/\partial z = 0$ at $z = 0$. It can be expressed in a number of different forms [see Eqs. (7.3.17) and (7.4.7)],

$$\begin{aligned} G_k(x,z \mid x_0,z_0) &= \frac{i}{4} H_0^{(1)}(kR) + \frac{i}{4} H_0^{(1)}(kR') \\ &= \frac{1}{2\pi^2} \int_{-\infty}^{\infty} dK_x \int_{-\infty}^{\infty} dK_z \frac{\cos (K_z z_0) e^{iK_x(x - x_0) + iK_z z}}{K_x^2 + K_z^2 - k^2} \end{aligned} \tag{8.4.14}$$

where $R^2 = (x - x_0)^2 + (z - z_0)^2$, $R'^2 = (x - x_0)^2 + (z + z_0)^2$, and the function $H_0^{(1)}$ is the Hankel function [see discussion following Eq. (7.3.2)]

$$H_0^{(1)}(z) = J_0(z) + iN_0(z) \to \sqrt{\frac{\pi}{2ikr}} \exp(ikr) \qquad kr \to \infty \quad (8.4.15)$$

The integral equation (8.4.13) uses $\beta_0 = 0$ as the "average" admittance (in the sense of page 445), so the incident-plus-reflected wave is for a completely rigid wall. We could, of course, have chosen the reflected wave and the Green's function for the wall admittance β, in which case the integral in Eq. (8.4.13) changes sign and the integration is from $-\infty$ to 0. We know,

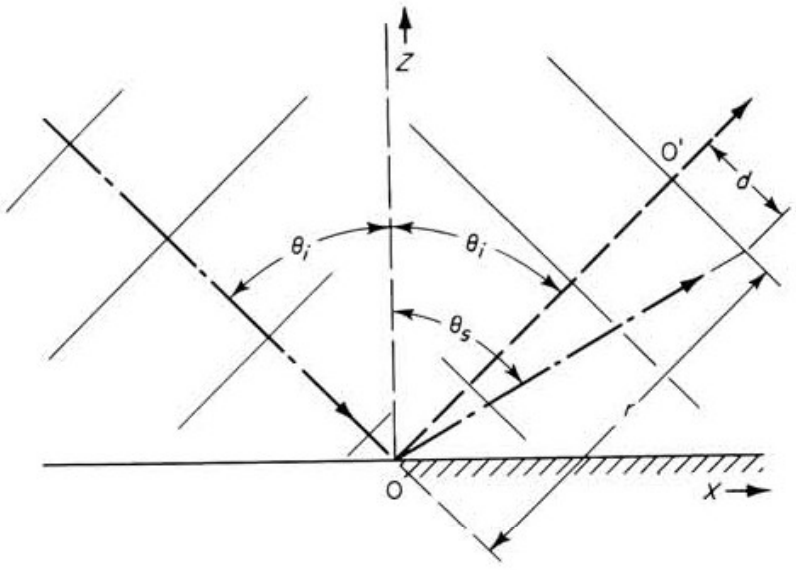


FIGURE 8.13
Incident and reflected plane waves from a half-rigid–half-soft plane at $z = 0$. Diffraction pattern is exhibited in reflected wavefront near point O'.

of course, that well to the left of point 0′ in Fig. 8.13 (i.e., for d large and negative) the amplitude of the reflected wave is P_i, since this part of the wave has been reflected from the rigid part of the wall; whereas well to the right of 0′ (d large and positive) the reflected-wave amplitude is $P_i[(\cos\theta_i - \beta)/(\cos\theta_i + \beta)]$, since this part is reflected from the region of admittance β [see Eq. (6.3.5)]. In between, for $|d|$ small, a diffraction-pattern curve connects the two different values.

Integral equation (8.3.13) can be solved exactly using the Wiener-Hopf technique. The problem is clearly related to that of the diffraction of waves by a straightedge, which has just been discussed. The result, of course, involves the Fresnel functions defined in Eqs. (8.4.4). The exact solution produces the Fourier transform of the pressure distribution on the soft part of the reflecting plane, and this, according to Eq. (8.3.3), is proportional to

the shape of the reflected wave a large distance from the origin. In fact, the exact solution predicts that the reflected amplitude, as a function of d, along the wavefront, when kr is very large, is

$$P_{\text{ref}} \to \begin{cases} P_i - \dfrac{P_i\beta/2}{\cos\theta_i + \beta}\{[1 - C(u) - S(u)] - i[C(u) - S(u)]\} & d < 0 \\ P_i\dfrac{\cos\theta_i - \beta}{\cos\theta_i + \beta} + \dfrac{P_i\beta/2}{\cos\theta_i + \beta}\{[1 - C(u) - S(u)] & \\ \qquad - i[C(u) - S(u)]\} & d > 0 \end{cases} \tag{8.4.16}$$

where $u = (kd/\sqrt{2kr})^2$. The functions $(1 - C - S)$ and $(C - S)$ are plotted at the top of Fig. 8.14; we see that they go asymptotically to zero as $u \to \infty$. Therefore, for d large and negative, the reflected amplitude is P_i, the amplitude of a wave reflected from a rigid plane; for d large and positive, the amplitude is

$$P_i\frac{\cos\theta_i - \beta}{\cos\theta_i + \beta}$$

the amplitude of a wave reflected from a plane of admittance β everywhere. For $|d|$ small, the functions $(1 - C - S)$ and $(C - S)$ produce the changes in amplitude and phase typical of a diffraction pattern.

Although the exact form of the Fourier transform of the surface pressure distribution is obtained, the inverse transform, the pressure itself, cannot be expressed in closed form. Therefore we shall be satisfied with an approximate solution of the integral equation, obtained from Eq. (8.4.13) by setting $z = 0$. We set into the right-hand integral the first approximation to p,

$$p(x_0,0) \simeq \begin{cases} 2P_i e^{ikx_0\sin\theta_i} & x_0 < 0 \\ 2P_i\dfrac{\cos\theta_i}{\cos\theta_i + \beta}e^{ikx_0\sin\theta_i} & x_0 > 0 \end{cases}$$

to obtain, as a second-order approximation,

$$p(x,0) \simeq 2P_i e^{ikx\sin\theta_i} - \frac{P_i\beta\cos\theta_i}{\cos\theta_i + \beta}\int_0^\infty e^{ikx_0\sin\theta_i}H_0(k\,|x - x_0|)\,d(kx_0)$$

$$\simeq 2P_i e^{ikx\sin\theta_i} - \frac{P_i\beta\, e^{ikx\sin\theta_i}}{\cos\theta_i + \beta}\begin{cases}[X(\theta_i,-kx) + iY(\theta_i,-kx)] & x < 0 \\ [2 - X(-\theta_i, kx) - iY(-\theta_i,kx)] & x > 0\end{cases} \tag{8.4.17}$$

where

$$X(\theta,u) + iY(\theta,u) = \cos\theta\int_u^\infty e^{iw\sin\theta}[J_0(w) + iN_0(w)]\,dw$$

$$\to \begin{cases} 1 + \dfrac{2\theta}{\pi} & u \to 0 \\ 0 & u \to \infty \end{cases}$$

These functions, for $\theta = 0$, are plotted in the lower half of Fig. 8.14. They are sufficiently similar to the functions (1-C-S) and (C-S) to lead us to believe that Eq. (8.4.17) is a good approximation, at least for $|\beta| < 1$. And the integrals X and Y are much easier to compute than is the exact solution for $\theta \neq 0$.

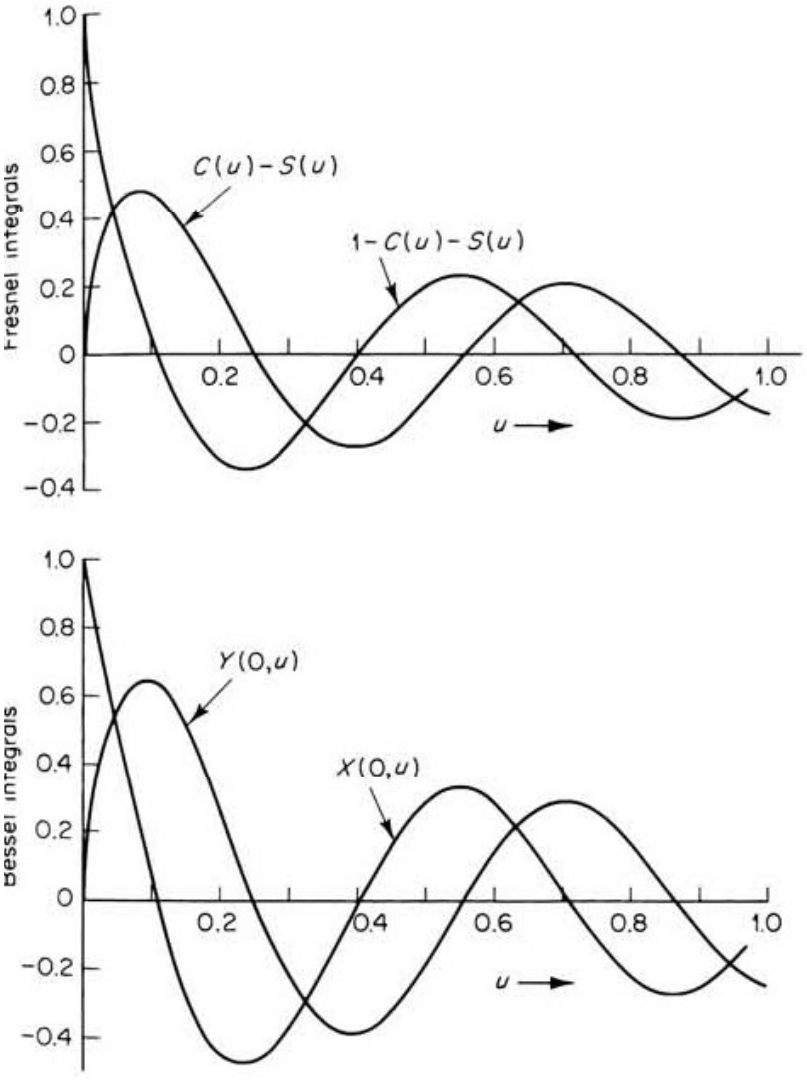


FIGURE 8.14
Comparison of Fresnel integrals, defined in Eqs. (8.4.4), and Bessel integrals, defined in Eq. (8.4.17).

The power absorbed by the wall, per unit area, a distance x from the edge of the soft region, is $\xi\,|p|^2/\rho c$ for $x > 0$ and is zero for $x < 0$ (note that $\beta = \xi - i\sigma$). Therefore the strip of width about $\lambda/2\pi$, next to the edge, absorbs more energy than the average; the next strip, of width about $\lambda/2$, absorbs less than the average; and so on. Since the integral of $X + iY$ from $x = 0$ to $x = \infty$ is zero, the mean rate of energy loss per unit area for a strip much wider than $\lambda = 2\pi/k$ nearly equals $|2P_i \cos\theta_i/(\cos\theta_i + \beta)|^2(\xi/\rho c)$ if the admittance $|\beta| < 1$. Since this would be the loss rate if the whole

wall had admittance β [see Eq. (6.3.6)], we see that no edge correction is necessary in calculating the average energy lost near the edge of an absorbing area of dimensions large compared with λ; to first order in $|\beta|$ the diffraction fluctuations in p near the edge average out, and even the second-order correction is a small fraction times $|\beta|^2$. Under the next heading we shall see that this is not true when two edges are close together, i.e., when the smallest dimension of the absorbing area is not large compared with λ.

Scattering from an absorbing strip

Suppose the wall at $z = 0$ is rigid except for a strip from $x = -\frac{1}{2}a$ to $x = +\frac{1}{2}a$, within which the specific acoustic impedance is β, independent of x and y. In this case the equation for the pressure wave is

$$p(x,z) = 2P_i e^{ikx\sin\theta_i}\cos(kz\cos\theta_i) - \tfrac{1}{2}k\beta\int_{-\frac{1}{2}a}^{\frac{1}{2}a} p(x_0,0)H_0^{(1)}(kR)\,dx_0 \quad (8.4.18)$$

using the same notation as in Eq. (8.4.13). An exact solution, using the Wiener-Hopf technique, is not possible for this case; so we shall use the variational procedure discussed in Sec. 4.5.

First we shall use the asymptotic form for the Hankel function of Eq. (7.3.3) to obtain a formula for the wave at a point designated by the polar coordinates r, θ_s,

$$H_0^{(1)}(kR) \to \sqrt{\frac{2}{i\pi kr}}\exp(ikr - ikx_0\sin\theta_s)$$

when kr is large compared with both unity and kx_0. The first term in Eq. (8.4.18) is the incident-plus-reflected combination of plane waves; the second term is the wave scattered by the strip,

$$p_{\theta i}(x,z) \to 2P_i e^{ikx\sin\theta_i}\cos(kz\cos\theta_i) - \sqrt{\frac{1}{2\pi ikr}}\,e^{ikr}F_{\theta i}(k\sin\theta_s) \quad (8.4.19)$$

The function F describes the distribution-in-angle of the scattered wave; it is the Fourier transform of the function

$$\begin{aligned} f_\theta(x) &= 2\pi k\beta(x)p_\theta(x,0) = \int_{-\infty}^{\infty} F_\theta(\kappa)e^{i\kappa x}\,d\kappa \\ F_\theta(\kappa) &= k\beta\int_{-\frac{1}{2}a}^{\frac{1}{2}a} p_\theta(x_0,0)e^{-i\kappa x_0}\,dx_0 \end{aligned} \quad (8.4.20)$$

where $\beta(x)$ equals the constant β in the range $-\frac{1}{2}a < x < +\frac{1}{2}a$ and equals zero for other values of x.

The integral equation which $p(x,0)$ must satisfy is

$$p_{\theta_i}(x,0) = 2P_i e^{ikx\sin\theta_i} - \tfrac{1}{2}\beta\int_{-\frac{1}{2}a}^{\frac{1}{2}a} p_{\theta_i}(x_0,0)H_0^{(1)}(k\,|x - x_0|)\,d(kx_0) \quad (8.4.21)$$

If this can be solved for p in the range $-\frac{1}{2}a < x < +\frac{1}{2}a$, then p, for any value of θ_i, of x and of z, can be computed from Eq. (8.4.18) or, asymptotically,

from Eq. (8.4.19). We might try to solve this equation on the average by multiplying it by $\beta P(x,0)$, integrating over x from $-\frac{1}{2}a$ to $+\frac{1}{2}a$, and adjusting the average value of p in this range to satisfy the resulting equation. But we can do better than this if we notice that the integral of the first term on the right in Eq. (8.4.21), times βp, is related to the angle-distribution factor F; in fact, it is the F for the angle of incidence changed from θ_s to $-\theta_i$, as though the incident wave originated from the observation point r, θ_s and the scattered wave were being observed at the point r, $-\theta_i$.

Suppose we multiply Eq. (8.4.21) for $\theta_i = \theta$ by $\beta p_\theta{}^a(x,0)$ and integrate from $x = -\frac{1}{2}a$ to $x = +\frac{1}{2}a$, where we shall have to determine the relation between p^a and p later. Simplifying our notation in an obvious manner, we have the equation

$$0 = 2P_i k \int_{-\frac{1}{2}a}^{\frac{1}{2}a} e^{ikx\sin\theta_i}\,\beta p_\theta{}^a\,dx - \tfrac{1}{2}k^2 \int \beta p_\theta{}^a\,dx \int H_0^{(1)}(k\,|x - x_0|)\beta p_\theta\,dx_0 - k\int p_\theta{}^a \beta p_\theta\,dx$$

We also write down the equation for F for $\theta_s = \theta_i = \theta$ in the form

$$2P_i F_\theta(k\sin\theta) = 2P_i k \int e^{-ikx\sin\theta}\beta p_\theta\,dx$$

and add the equations to obtain a symmetric expression.

$$2P_i F_\theta(k\sin\theta) = 2P_i k\left(\int e^{ikx\sin\theta}\beta p_\theta{}^a\,dx + \int e^{-ikx\sin\theta}\,\beta p_\theta\,dx\right) - k\int p_\theta{}^a\beta p_\theta\,dx - \tfrac{1}{2}k^2\int \beta p_\theta{}^a\,dx\int H_0^{(1)}(k\,|x - x_0|)\beta p_\theta\,dx_0 \quad (8.4.22)$$

This equation for F can serve as a basis for our variational procedure.

For example, if we vary the shape of p^a slightly, so that it becomes $p^a + \delta p^a$, the variation of $2P_iF$ is

$$k\int \beta\delta p_\theta{}^a\,dx\left[2P_i e^{ikx\sin\theta} - \tfrac{1}{2}k\int H_0^{(1)}(k\,|x - x_0|)\beta p_\theta\,dx_0 - p_\theta\right]$$

If p_θ is a solution of Eq. (8.4.21), this variation is zero. Likewise, if p is varied, the change in $2P_iF$ proportional to δp is zero if p^a is a solution of the equation resulting when θ is changed to $-\theta$ in Eq. (8.4.21) [i.e., $p_\theta{}^a$ is the surface pressure when source point and observation point are interchanged; this equation and its solution are said to be *adjoint* to Eq. (8.4.21) and its solution].

Generalizing the arguments of page 156, we can say that if the exact solution p_θ and its adjoint $p_\theta{}^a$ are inserted in the right-hand side of Eq. (8.4.22), the result will equal $2P_i$ times the correct angle-distribution function $F_\theta(k\sin\theta)$ for the angle of incidence θ, but if trial functions $\chi(\alpha)$ and $\chi^a(\alpha)$

are used in the integrals, and if these functions differ from p and p^a by small quantities of the order of δ, the resulting expression will differ from $2P_iF$ by a constant of the order of δ^2. Furthermore, if the shape of $\chi(\alpha)$ can be varied by changing the value of the parameter α, then the shape of $\chi(\alpha)$ for which the derivative $\partial/\partial\alpha$ of the variational expression is zero is the shape most closely corresponding to p, and the value of the variational expression for this minimal value of α is most nearly equal to $2P_iF(k \sin\theta)$.

For example, suppose we assume that the pressure over the soft strip is proportional to $e^{ikx\sin\theta}$ (as it would if $\beta = 0$) but that its magnitude is not $2P_i$ but A. We should obtain a Born approximation for F if we inserted $2P_ie^{ikx\sin\theta}$ for p in Eq. (8.4.20) for F; this would be correct to first order in β. We expect a second-order approximation if we insert the trial function $\chi = Ae^{ikx\sin\theta}$ instead of p_θ and its adjoint $Ae^{-ikx\sin\theta}$ for $p_\theta{}^a$ into Eq. (8.4.22) and vary the value of A to obtain a zero slope. The resulting variational expression is

$$4P_ika\beta A - ka\beta A^2 - \tfrac{1}{2}k^2\beta^2A^2\int e^{-ikx\sin\theta}\,dx\int H_0^{(1)}(k\,|x - x_0|)e^{ikx\sin\theta}\,dx_0 \tag{8.4.23}$$

The derivative of this with respect to A vanishes when

$$A = \frac{2P_i}{1 + \dfrac{k\beta}{2a}\displaystyle\int e^{-ikx\sin\theta}\,dx\int H_0^{(1)}(k\,|x - x_0|)e^{ikx_0\sin\theta}\,dx_0}$$

This can be expressed in terms of the functions X and Y of Eq. (8.4.17) for

$$Z(\theta,u) \equiv \cos\theta\int_0^u e^{iw\sin\theta}H_0^{(1)}(w)\,dw$$

$$= \begin{cases} -1 - \dfrac{2\theta}{\pi} + X(\theta,u) + iY(\theta,u) & u < 0 \\ 1 + \dfrac{2\theta}{\pi} - X(\theta,u) - iY(\theta,u) & u > 0 \end{cases} \tag{8.4.24}$$

so that

$$k\cos\theta\int_{-\frac{1}{2}a}^{\frac{1}{2}a} H_0^{(1)}(k\,|x - x_0|)e^{ikx\sin\theta}\,dx_0 = e^{ikx\sin\theta}\,[Z(\theta,\tfrac{1}{2}ka - kx) + Z(-\theta,\tfrac{1}{2}ka + kx)]$$

and

$$\frac{1}{a}\int_{-\frac{1}{2}a}^{\frac{1}{2}a} e^{-ikx\sin\theta}\,dx\int_{-\frac{1}{2}a}^{\frac{1}{2}a} H_0^{(1)}(k\,|x - x_0|)e^{ikx_0\sin\theta}\,dx_0 = \frac{1}{ka}\int_0^{ka}[Z(\theta,-u) + Z(-\theta,u)]\,du \equiv W(\theta,ka) + W(-\theta,ka)$$

The real and imaginary parts of Z and W, for $\theta = 0$, are plotted in Fig. 8.15.

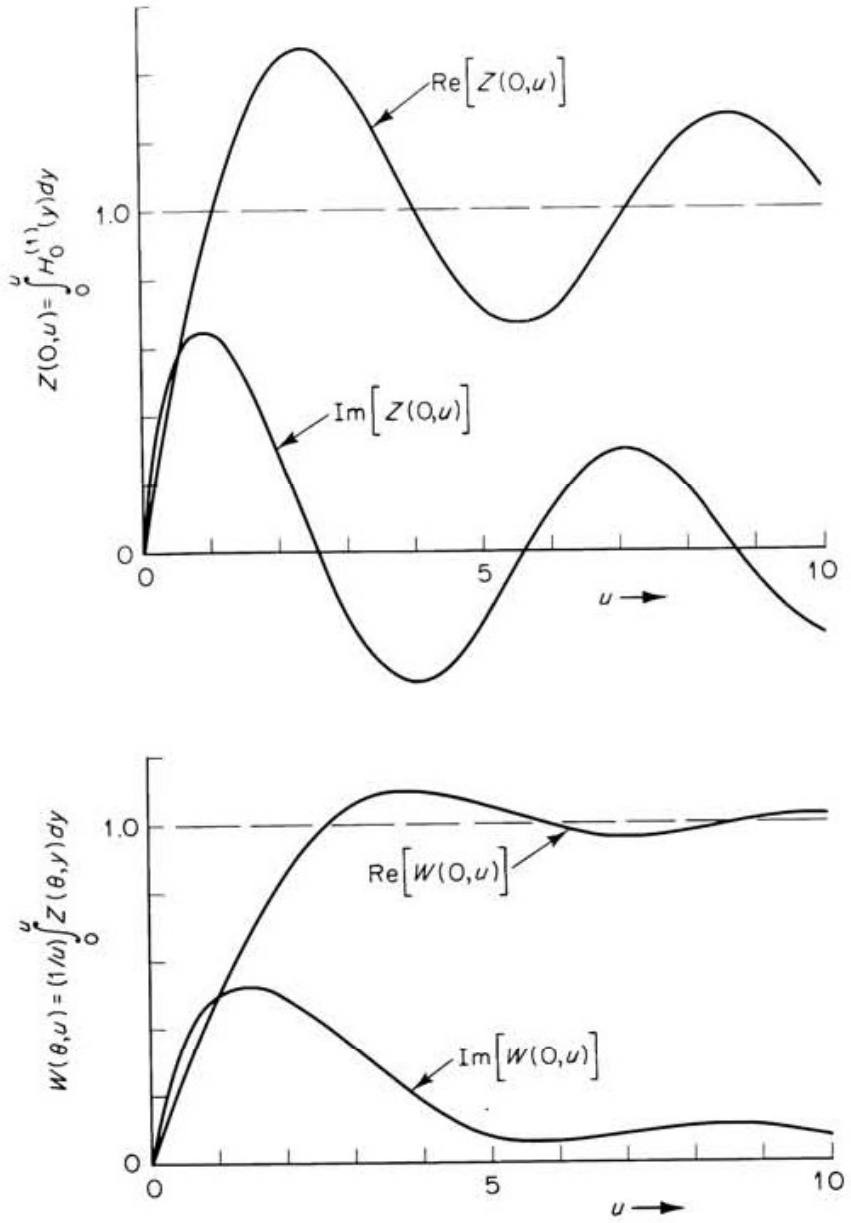


FIGURE 8.15
Functions entering the calculation of pressure distribution across a strip of absorbing material.

In terms of the Z's and the W's, the variational solution is

$$A = \frac{2P_i \cos\theta}{\cos\theta + \frac{1}{2}\beta[W(\theta,ka) + W(-\theta,ka)]}$$

$$p_{\theta_i}(x,0) \simeq 2P_i\left\{1 - \tfrac{1}{2}\beta\frac{Z(\theta_i, \frac{1}{2}ka - kx) + Z(-\theta_i, \frac{1}{2}ka + kx)}{\cos\theta_i + \frac{1}{2}\beta[W(\theta_i,ka) + W(-\theta_i,ka)]}\right\}e^{ikx\sin\theta_i}$$

$$\rightarrow \begin{cases} 2P_i e^{ikx\sin\theta_i} & |x| \gg a \\ 2P_i e^{ikx\sin\theta_i}\dfrac{\cos\theta_i}{\cos\theta_i + \beta} & |kx| \ll ka \gg 1 \end{cases} \tag{8.4.25}$$

$$F_{\theta_i}(k\sin\theta_s) \simeq \frac{2P_i ka\beta\cos\theta_i}{\cos\theta_i + (\beta/2)[W(\theta_i,ka) + W(-\theta_i,ka)]}\frac{\sin[\frac{1}{2}ka(\sin\theta_s - \sin\theta_i)]}{\frac{1}{2}ka(\sin\theta_s - \sin\theta_i)}$$

All these expressions are good to second order in the mean-square departure of the surface pressure on the soft strip from its mean value there (i.e., the mean-square difference between the true p and $Ae^{ikx\sin\theta}$). The formula for $p_{\theta_i}(x,0)$ is obtained by inserting the "best" trial function into the integral on the right of Eq. (8.4.21); that for the angle-distribution function

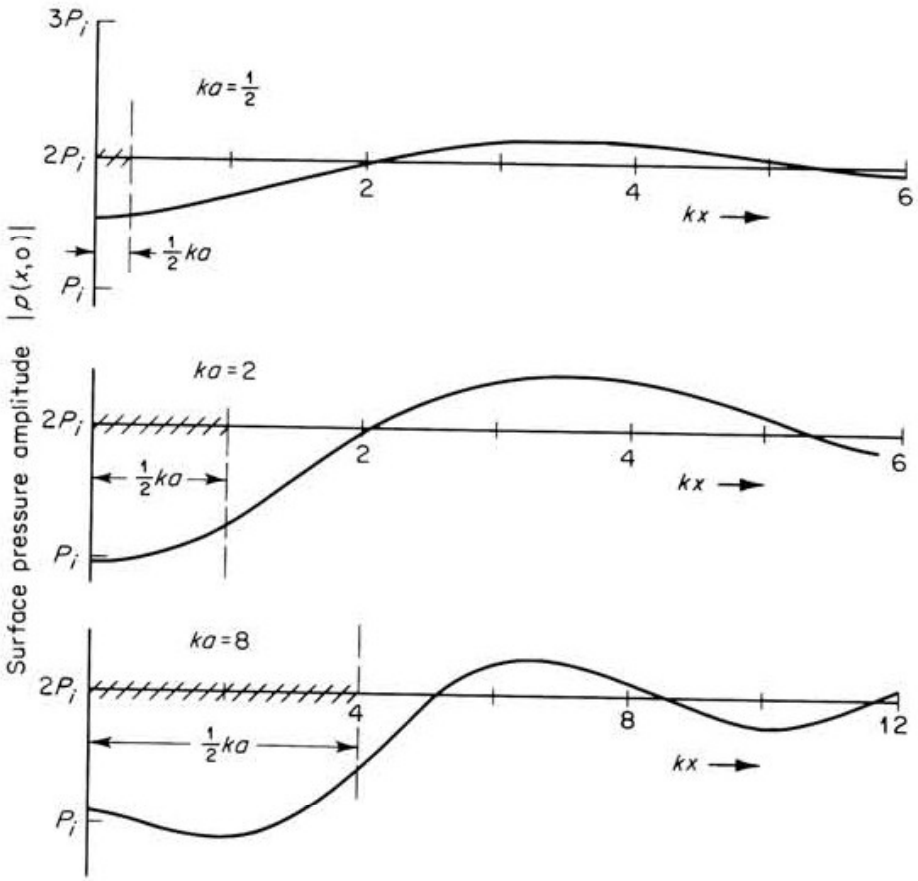


FIGURE 8.16
Pressure amplitude on wall having strip of admittance $\beta = 1$ of width a, otherwise rigid, produced by normally incident plane wave of wavelength $2\pi/k$ and amplitude P_i, as function of distance x from center of strip, for different values of k. Vertical dashed line indicates edge of strip.

for the scattered wave by setting the same "best" function into Eq. (8.4.20). The best value of the variational expression is, of course, $F_{\theta_i}(k \sin \theta_i)$, the scattered amplitude at the angle of reflection $\theta_s = \theta_i$.

As an indication of the adequacy of this solution, we plot in Fig. 8.16 the amplitude $p(x,0)$ of the surface pressure from Eq. (8.4.25) as function of x, for $\theta_i = 0$, for $\beta = 1$, and for several different values of k. We see that, for $|x| < \frac{1}{2}a$, the pressure amplitude is not far from being constant, and thus that the curves are not far from those of the exact solution. For $|\beta| < 1$ the fit would be even better.

We note that when ka is very small, the pressure on the soft strip is not

much different from the $2P_i$ which would be present if the wall were all rigid; the longer wavelength cannot accommodate itself to the narrow strip; so the dip in pressure is shallow and extends well beyond the edge of the strip. As k is increased, the pressure at the center of the strip approaches the value P_i which it would have if the strip were infinitely wide (for $\beta = 1$ there is no reflected wave from a normally incident wave; the only pressure there is the incident pressure P_i). For $ka \gg 1$ the pressure amplitude approaches a step function, going from P_i for $|x| < \frac{1}{2}a$ to $2P_i$ for $|x| > \frac{1}{2}a$, with a diffraction pattern noticeable at the strip edge.

Problems

1 Write out the long-wavelength expressions for the angle distribution of the pressure wave scattered from a rigid cylinder and a rigid sphere from Eqs. (8.1.1) and (8.2.2). What are the ratios between the forward-, sideward-, and backward- scattered intensity? In the case of the sphere, what are the separate contributions from monopole and dipole scattering?

2 When the scattering sphere of radius a is immovable and incompressible, the surface integral of Eq. (7.1.17) can be used, and the integral equation for the incident plus scattered wave takes the form

$$p_\omega(\mathbf{r}) = p_i(\mathbf{r}) + a^2 \iint \left[p_\omega(\mathbf{r}_0) \frac{\partial}{\partial r_0} g_\omega(\mathbf{r} \mid \mathbf{r}_0) \right]_{r_0=a} d\Omega_0$$

where $d\Omega_0$ is the element of solid angle in the $\mathbf{r}_0$ coordinates. Show that the asymptotic form of the scattered wave is

$$p_s(\mathbf{r}) \to -\frac{ika^2}{4\pi r} e^{ikr} \iint [p_\omega(\mathbf{r}_0)]_{r_0=a} e^{-ika\cos\Psi} \cos\Psi \, d\Omega_0$$

where Ψ is the angle between $\mathbf{r}$ and $\mathbf{r}_0$. Show that the Born approximation to this asymptotic form, if the incident wave is the plane wave $A \exp(i\mathbf{k}_i \cdot \mathbf{r})$, is

$$p_s(\mathbf{r}) \simeq -\frac{ia^2 A}{4\pi r} e^{ikr} \iint \exp(-i\boldsymbol{\mu} \cdot \mathbf{a}_0) [(\boldsymbol{\mu} + \mathbf{k}_i) \cdot \mathbf{a}_0] \, d\Omega_0$$

$$= \frac{aA}{2r} e^{ikr} (\mu a) j_1(\mu a) \qquad \boldsymbol{\mu} = \mathbf{k}_s - \mathbf{k}_i \qquad \mu = 2k \sin\frac{\vartheta}{2}$$

where $\mathbf{a}_0$ is the unit vector in the direction of the element of solid angle $d\Omega_0$ (*Hint*: use the direction of $\boldsymbol{\mu}$ as the axis for the angles of $d\Omega_0$). Show that this does not agree, even at long wavelengths, with the exact solution of Eqs. (8.2.19), for $\kappa_e = 0$ and $\rho_e \to \infty$. Why is this?

3 In a heavy rain the mean radius of the raindrops is 2 mm and there is, on the average, one drop per 1,000 cu cm. Use Eqs. (8.2.22) to calculate the fraction of energy removed from a plane wave, per meter, at 100 and at 1,600 cps, assuming that $\gamma_\kappa = -1$ and $\gamma_\rho = \frac{3}{2}$. Include both absorption and scattering cross sections. Carry out the same calculations for a mist in which the mean radius of the droplets is 0.1 mm but the same amount of water per cubic centimeter is present as in the rain.

4 The material inside an infinite cylinder of radius a, with axis along the z axis, has density ρ_e and compressibility κ_e. It is surrounded by a medium of density ρ and compressibility κ. An incident plane wave of sound

$$p_i = \exp(ik_z z + ik_i x - i\omega t) = \exp(ik_z z + ik_i r\cos\phi - i\omega t)$$

where $k_z^2 + k_i^2 = \rho\kappa\omega^2$, is incident on the cylinder, producing a scattered wave. Show that the pressure amplitude inside and outside the cylinder can be expressed in terms of the cylindrical coordinates z, r, ϕ by the series

$$p_\omega = \begin{cases} e^{ik_z z}\sum \epsilon_m i^m B_m \cos(m\phi) J_m(k_e r) & r < a \\ e^{ik_z z}\sum \epsilon_m i^m \cos(m\phi)\,[J_m(k_i r) + D_m H_m^{(1)}(k_i r)] & a < r \end{cases}$$

where $k_e^2 = (\rho_e\kappa_e/\rho\kappa)k_i^2$. Show that requirements of continuity of p and u_r across the cylindrical surface require that

$$D_m = \frac{J_m(k_e a)J_m'(k_i a) - \alpha J_m'(k_e a)J_m(k_i a)}{\alpha J_m'(k_e a)H_m^{(1)}(k_i a) - J_m(k_e a)H_m^{(1)\prime}(k_i a)} \qquad \alpha^2 = \frac{\kappa_e\rho}{\kappa\rho_e}$$

where the primes indicate differentiation with respect to the argument. Show that the asymptotic form of the scattered wave is

$$p_s \to \sqrt{\frac{2}{\pi i k r}}\, e^{ik_z z + ik_i r}\sum \epsilon_m D_m \cos(m\phi)$$

5 Using the results of Prob. 4, plus the series expansions of J_m and N_m, show that the long-wavelength form for the wave scattered from the cylinder, to second order in $k_i a$, is

$$p_s \to \sqrt{\frac{2}{\pi i k_i r}}\, e^{ik_z z + ik_i r}\frac{i\pi k_i^2 a^2}{4}\left(\frac{\kappa_e - \kappa}{\kappa} + \frac{2\rho_e - 2\rho}{\rho_e + \rho}\cos\phi\right)$$

6 Use the Born approximation of Eq. (8.1.18) and the two-dimensional Green's function $g_\omega(\mathbf{r} \mid \mathbf{r}_0) = (i/4)H_0^{(1)}(k\,|\mathbf{r} - \mathbf{r}_0|)$ to calculate the scattered wave of Prob. 4. If γ_κ and γ_ρ are functions of the cylindrical coordinate r only, show that

$$p_s \simeq \tfrac{1}{2}\pi i\sqrt{\frac{2}{\pi i k_i r}}\, e^{ik_z z + ik_i r} k^2 \int_0^a [\gamma_\kappa(r) + \gamma_\rho(r)\cos\phi] J_0(\mu r) r\, dr$$

where $\mu = 2k_i \sin(\vartheta/2)$. When γ_κ and γ_ρ are constant inside $r = a$ and zero outside, show that the integral is approximately equal to $(a^2/2)(\gamma_\kappa + \gamma_\rho\cos\phi)$. Compare this result with that of Prob. 5. What does it indicate regarding the range of validity of the Born approximation?

7 The cylinder of Prob. 4 contains material of large viscosity and thermal conduction, but the surrounding medium has values μ, K, and C_P, which cannot be neglected. Show that, at long wavelengths, if the incident wave has amplitude A and moves normal to the cylindrical axis ($k_i = k = \omega/c$), the scattered wave is, approximately,

$$p_s \to A\sqrt{\frac{i\pi}{8kr}}\, e^{ikr} k^2 a^2 \left\{\frac{\kappa_e - \kappa}{\kappa} - 2(1-i)(\gamma - 1)\frac{d_h}{a} + \frac{2\rho_e - 2\rho}{\rho_e + \rho}\left[1 - (1+i)\frac{2\rho_e}{\rho_e + \rho}\frac{d_v}{a}\right]\cos\phi\right\}$$

Compute the energy lost per unit length of cylinder.

8 Show that, neglecting the difference between γ_ρ and $(3\rho_e - 3\rho)/(2\rho_e + \rho)$, the results of Eqs. (8.2.22) can be obtained from the Born approximation if we assume that the quantity in braces in the first integral of Eq. (8.1.13) is

$$k^2\gamma_\kappa(\mathbf{r}_0)p_i(\mathbf{r}_0) - \operatorname{div}_0[\gamma_\rho(\mathbf{r}_0)\,\nabla_0 p_i] + (i-1)(\gamma-1)\,d_h \operatorname{div}[p_i(0)\mathbf{a}_{r_0}\,\delta(r_0-a)] + \tfrac{1}{2}(i+1)\gamma_\rho d_v \operatorname{div}_0[\mathbf{a}_{\theta_0}(\mathbf{a}_{\theta_0}\cdot\nabla_0 p_i)\,\delta(r_0-a)]$$

where $r_0 = 0$ is the center of the sphere, γ_κ and γ_ρ are as defined in Eq. (8.1.11), and γ is the ratio of specific heats, where δ is the Dirac delta function. Vector $\mathbf{a}_{r_0}$ is the unit vector in the direction of $\mathbf{r}_0$, and $\mathbf{a}_{\theta_0}$ is the unit vector perpendicular to $\mathbf{a}_{r_0}$ in the $r_0 z$ plane, and thus $\mathbf{a}_{\theta_0}(\mathbf{a}_{\theta_0}\cdot\nabla_0 p_i)$ is the component of the gradient of p_i perpendicular to $\mathbf{r}_0$. Show that these terms correspond to forces acting on the surface of the sphere. Discuss the relationship between these forces and the physics of the heat conduction and viscous flow.

9 Suppose the sphere of radius a, centered at the origin, contains material of the same density ρ as the medium in the rest of space, but has compressibility $\kappa_e = \kappa(1+\gamma_\kappa)$ differing from the κ for the medium outside. Show that the integral equation for p_ω, for an incident plane wave,

$$p_\omega(\mathbf{r}) = e^{i\mathbf{k}_i\cdot\mathbf{r}} + \iiint k^2\,\gamma_\kappa(\mathbf{r}_0)p_\omega(\mathbf{r}_0)g_\omega(\mathbf{r}\mid\mathbf{r}_0)\,dv_0$$

can be converted into the variational expression

$$4\pi\Phi(\mathbf{k}_s) = k^2\iiint\gamma_\kappa(\mathbf{r})p(\mathbf{r})e^{-i\mathbf{k}_s\cdot\mathbf{r}}\,dv + k^2\iiint\gamma_\kappa(\mathbf{r})p^a(\mathbf{r})e^{i\mathbf{k}_i\cdot\mathbf{r}}\,dv - k^2\iiint\gamma_\kappa(\mathbf{r})p^a(\mathbf{r})p(\mathbf{r})\,dv + k^4\iiint\gamma_\kappa(\mathbf{r})p^a(\mathbf{r})\,dv\iiint g_\omega(\mathbf{r}\mid\mathbf{r}_0)\gamma_\kappa(\mathbf{r}_0)p(r_0)\,dv_0$$

where p^a is the adjoint function, the solution of the integral equation, with k_i changed to $-k_s$. Show that, as the shape of p inside $r = a$ is varied, the stationary value of Φ comes when p is the solution of the integral equation, and that when the chosen shape of p differs somewhat from the correct solution p_ω, the resulting value of Φ differs from the correct Φ_s to second order. Use $p = Ae^{i\mathbf{k}_i\cdot\mathbf{r}}$ and $p^a = Ae^{-i\mathbf{k}_s\cdot\mathbf{r}}$ as trial functions and show that the best values of A and Φ are

$$A \simeq \left\{1 - k^2\frac{\iiint\gamma_\kappa e^{-i\mathbf{k}_s\cdot\mathbf{r}}\,dv\iiint g_\omega\gamma_\kappa e^{i\mathbf{k}_i\cdot\mathbf{r}_0}\,dv_0}{\iiint\gamma_\kappa(\mathbf{r})\exp[i(\mathbf{k}_i-\mathbf{k}_s)\cdot\mathbf{r}]\,dv}\right\}$$

$$\Phi_s \simeq \frac{k^2A}{4\pi}\iiint\gamma_\kappa(\mathbf{r})\exp[i(\mathbf{k}_i-\mathbf{k}_s)\cdot\mathbf{r}]\,dv$$

10 Suppose γ_κ in Prob. 9 is constant throughout the sphere. Show that the integrals in the expression for A and Φ are

$$\iiint\gamma_\kappa e^{-i\mathbf{k}_s\cdot\mathbf{r}}\,dv\iiint g_\omega\gamma_\kappa e^{i\mathbf{k}_i\cdot\mathbf{r}_0}\,dv_0 = \frac{8\pi}{15}\gamma_\kappa{}^2a^5\left[1 + \tfrac{5}{6}ika\,\tfrac{1}{21} - k^2a^2\,(13-\cos\vartheta)\cdots\right]$$

$$\iiint\gamma_\kappa\exp[i(\mathbf{k}_i-\mathbf{k}_s)\cdot\mathbf{r}]\,dv = \frac{4\pi}{3}\gamma_\kappa a^3\left[1 - \tfrac{1}{10}k^2a^2 + \tfrac{1}{280}k^4a^4\cdots\right]$$

Calculate the angle-distribution factor Φ and compare with the Born approximation and with the exact solution for the same case.

11 Show that the backscattered sound of frequency $\omega/2\pi$ from a patch of variable acoustic admittance β, in an otherwise rigid wall, is, approximately,

$$p_{\omega b} \to \frac{ik}{2\pi r} e^{ikr} \int B(x_0) \exp(2ikx_0 \sin\theta)\, dx_0$$

where the angle of incidence is θ and the angle of scattering is $\vartheta = -\theta$ for backscattering, the direction of the incident wave being in the xz plane, and where $B(x) = \int \beta(x,y)\, dy$. Show that the component of the pulsed incident-plus-reflected wave

$$p_{pi} = A\delta\left(t + \frac{z}{c}\cos\theta - \frac{x}{c}\sin\theta\right) + A\delta\left(t - \frac{z}{c}\cos\theta - \frac{x}{c}\sin\theta\right)$$

which has frequency $\omega/2\pi$, is

$$p_{\omega i} = \frac{A}{2\pi}[\exp(-ikz\cos\theta + ikx\sin\theta) + \exp(ikz\cos\theta + ikx\sin\theta)]$$

which is the incident wave producing the $p_{\omega b}$ above. Show thus that the backscattered wave produced by the incident pulse is

$$p_{pb} \simeq \frac{A}{4\pi r \sin\theta}\frac{d}{dt} B\left(\frac{ct - r}{2\sin\theta}\right)$$

Explain in simple terms why the variations in space of B have turned into variations in time of p. If the material on the wall is laid out in periodic bands, parallel to the y axis, so that $B \simeq B_0 \sin(2\pi x/l)$ for $-\frac{1}{2}d < x < +\frac{1}{2}d$ $(d \gg l)$, what frequency sound will be backscattered from the pulse-wave?

CHAPTER

9

SOUND WAVES IN DUCTS AND ROOMS

9.1 ACOUSTIC TRANSMISSION LINES

A large number of sound-generating devices are tubular in shape, sound waves of large amplitude being set up inside the tube, and some of this stored-up energy being radiated out into the open. Other tubular devices, such as mufflers, are designed to attenuate the sound passing through them.

When a sound wave is transmitted along the interior of a tube, and when the wavelength is large compared with the transverse dimensions of the tube, the fluid motion is predominantly parallel to the tube axis, and the wave motion is very nearly one-dimensional. The mean fluid velocity through a cross-sectional area a distance x from one end of the tube, at time t, can be written $u(x,t)$, and the mean acoustic pressure there is $p(x,t)$. If the first-order wave equation (6.2.4) is to be valid for this motion, the fluid should be at rest and in thermal equilibrium when no sound is present, and u and p must be small compared with c, the wave velocity, and with P, the equilibrium pressure, respectively. For these waves the tube is analogous to an electric transmission line, and ac circuit theory can be used. Constrictions or openings in the tube can be considered as lumped-circuit elements, and uniform yielding of the tube walls can be considered to be contributing to the line impedance.

Standing waves

A long rigid tube of uniform internal cross section is a useful apparatus with which to measure the acoustic properties of a surface placed at the end of the tube. A vibrating piston, generating sound of frequency $\omega/2\pi$, is placed at the end $x = 0$, and a sample of the surface to be tested closes the other end of the tube, at $x = l$. By measurement of the pressure amplitude of the standing wave within the tube, the acoustic impedance of the surface can be determined. To see what measurements are to be made, we must study the nature of the standing wave set up in the tube.

Suppose two simple-harmonic waves are traveling along the tube, one, $p_+ = A_+e^{ikx-i\omega t}$, going in the positive x direction with frequency $\omega/2\pi$ and

wavelength $\lambda = 2\pi/k = 2\pi c/\omega$, and the other, $p_- = A_- e^{-ikx-i\omega t}$, with the same frequency and wavelength, but going in the negative x direction. The actual acoustic pressure p at any x and t is of course given by the sum $p_+ + p_-$, as long as the amplitudes are small compared with P. Using Eqs. (6.2.3), we find that the fluid velocity at x, t is

$$u(x,t) = \frac{1}{i\omega p}\frac{\partial p}{\partial x} = \frac{1}{\rho c}[p_+(x,t) - p_-(x,t)] \tag{9.1.1}$$

where

$$p(x,t) = p_+(x,t) + p_-(x,t)$$

As long as the tube walls are completely rigid and no energy is absorbed as the waves progress, the wave velocity $c = \omega/k = \sqrt{1/\rho\kappa}$ is real and equal to the wave velocity in the open (i.e., in the same fluid, of infinite extent, with no tube walls present). Also, the amplitudes $|p_+|$ and $|p_-|$ are independent of x and t. On the other hand (as we shall see), if the tube walls are not perfectly rigid, or if the viscous and thermal-conduction effects are non-negligible, the wave number k will have a positive imaginary part, corresponding to wave attenuation. Usually, this part is small compared with the real part of k, small enough so that the relationship $\mathrm{Re}\, k = 2\pi/\lambda$, valid when k is real, is still a good approximation. Thus we can write

$$k = \frac{2\pi}{\lambda} + i\pi\gamma \tag{9.1.2}$$

The acoustic quantities may be conveniently related by means of the ratio (p/u) at point x for a simple-harmonic wave of frequency $kc/2\pi$, which can be called the impedance z at x for that frequency. The value z_0 at $x = 0$ determines the relation between the piston velocity and the pressure at the piston surface; the value z_l must equal the acoustic impedance of the material closing the end of the tube. These impedances are most compactly expressed in terms of the hyperbolic tangent function of a complex quantity $\pi(\alpha - i\beta)$, where α and β turn out to be linear functions of x (note that this β is *not* the specific acoustic admittance of Chap. 6). The relationship between α and β and the real and imaginary parts of the hyperbolic tangent are shown graphically in Plates I and II.

With these goals in mind, we write out the expressions for the pressure and velocity, in a plane wave of frequency $kc/2\pi$, as

$$\begin{aligned}
p &= A_+ e^{ikx} + A_- e^{-ikx} = A\cosh(ikx + \Phi_0) = A\cosh(ikd - \Phi_l) \\
u &= \frac{A}{\rho c}\sinh(ikx + \Phi_0) = -\frac{A}{\rho c}\sinh(ikd - \Phi_l) \\
A_+ &= \tfrac{1}{2}Ae^{\Phi_0} \qquad A_- = \tfrac{1}{2}Ae^{-\Phi_0} \qquad d = l - x \qquad \Phi_l = \Phi_0 + ikl \\
\Phi_0 &= \pi\alpha_0 - i\pi(\beta_0 + \tfrac{1}{2}) \qquad \Phi_l = \pi\alpha_l - i\pi(\beta_l + \tfrac{1}{2}) \\
ik &= -\pi\gamma + i\pi\frac{2}{\lambda} \qquad \alpha_0 = \alpha_l + \gamma l \qquad \beta_0 = \beta_l + \frac{2l}{\lambda}
\end{aligned} \tag{9.1.3}$$

where the value of A is determined by the velocity amplitude of the piston at $x = 0$, and the values of α_0 and β_0 are determined by the acoustic reaction of the material closing the duct at $x = l$. This reaction is measured by the phase angle Φ_l; the ratio between reflected- and incident-wave amplitudes at $x = l$ is $\exp(-2 \operatorname{Re} \Phi_s) = e^{-2\pi\alpha_l}$, and the phase change on reflection is $-2 \operatorname{Im} \Phi_s = \pi(2\beta_s + 1)$.

If the reaction of the end material can be expressed in terms of an impedance $z_l = (p/u)_l = \rho c \zeta_l = \rho c(\theta - i\chi)$ [Eq. (6.3.4)], the equation determining α_l and β_l is

$$\zeta_l = \coth \Phi_l = \coth \pi(\alpha_l - i\beta_l - \tfrac{1}{2}i) = \tanh \pi(\alpha_l - i\beta_l) \qquad (9.1.4)$$

since $\coth x = \tanh(x - \frac{1}{2}\pi i)$. If the specific acoustic impedance ζ_l is known, α_l and β_l can be computed graphically from Plates I and II, and then the impedance of the fluid in the tube on the piston

$$\zeta_0 = \coth \Phi_0 = \tanh \pi(\alpha_0 - i\beta_0) = \tanh \pi\left[(\alpha_l + \gamma l) - i\left(\beta_l + \frac{2l}{\lambda}\right)\right] \qquad (9.1.5)$$

can also be computed from the same charts. A typical example is shown in Fig. 9.1.

Measurement of impedance

On the other hand, if the impedance $\rho c \zeta_l$ is not known, it can be measured by measuring the pressure amplitude in the tube as a function of x. The mean-square pressure a distance d from the material at $x = l$ is

$$|A|^2 |\cosh(ikd - \Phi_l)|^2 = |A|^2 \left|\cosh \pi\left[(\alpha_l + \gamma d) - i\left(\beta_l + \frac{2d}{\lambda} + \tfrac{1}{2}\right)\right]\right|^2$$

$$= |A|^2\left[\cosh^2 \pi(\alpha_l + \gamma d) - \cos^2 \pi\left(\beta_l + \frac{2d}{\lambda}\right)\right] \qquad (9.1.6)$$

As with any standing wave, this has a sequence of minima, a half-wavelength apart, separated by maxima, halfway between. The minima come at a distance $d_{\min}$ from the $x = l$ end, where

$$\beta_l + \frac{2d_{\min}}{\lambda} = n \qquad \text{(an integer)} \qquad \text{or} \qquad d_{\min}(n) = -\lambda(n - \beta_l)$$

with the rms pressure there

$$p_{\min}(n) = |A| \sinh \pi[\alpha_l + \tfrac{1}{2}\gamma\lambda(n - \beta_l)]$$

The maxima come at $d_{\max}(n + \frac{1}{2}) = \frac{1}{2}\lambda(n + \frac{1}{2} - \beta_l)$, where n again is an integer; the rms pressure there is

$$p_{\max}(n + \tfrac{1}{2}) = |A| \cosh \pi[\alpha_l + \tfrac{1}{2}\gamma\lambda(n + \tfrac{1}{2} - \beta_l)]$$

The larger the argument of the sinh, the less sharp is the pressure minimum and the less is the difference between maxima and minima. If there is no friction (i.e., if α_l and γ are both zero), the pressure minimum is zero, and the standing wave is "perfect." Usually, γ is small; if the material

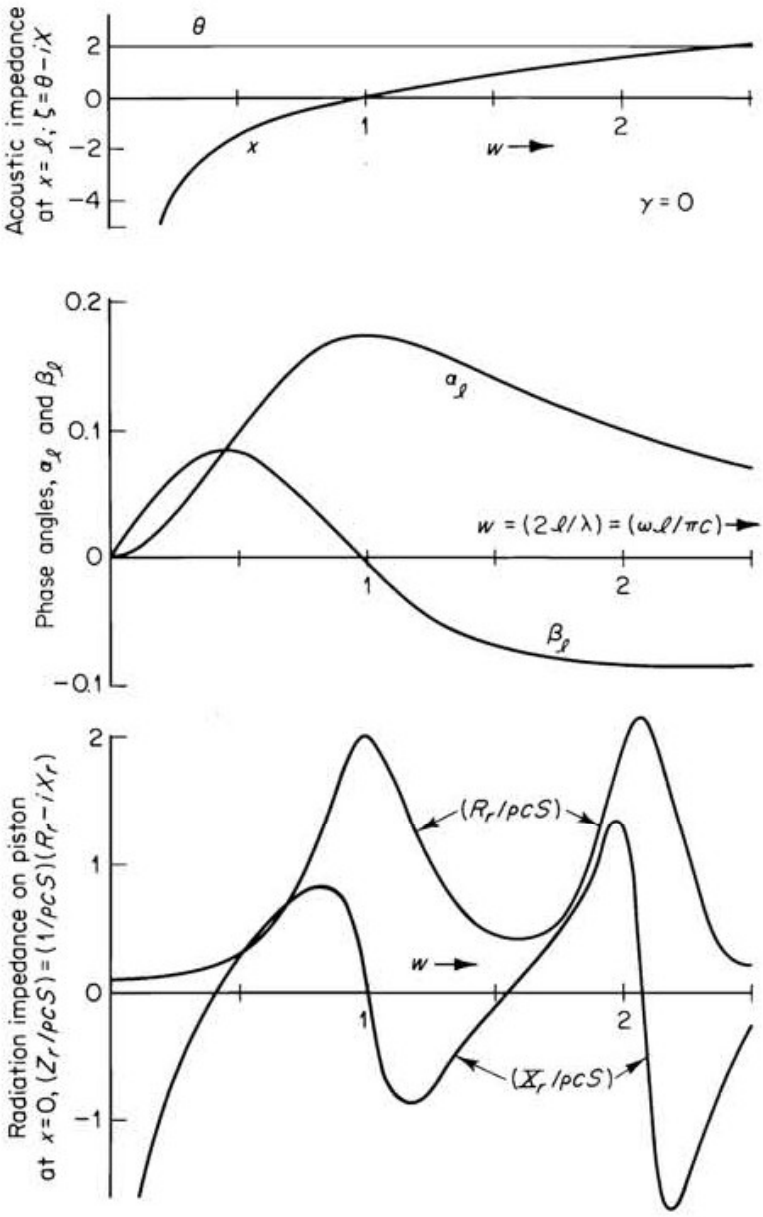


FIGURE 9.1
Specific acoustic impedance ζ of material at $x = l$ end of tube, phase angle Φ_l of standing wave there, and corresponding radiation impedance Z_r on piston at $x = 0$.

at $x = l$ is fairly rigid, α_l also is small, and the pressure minima are quite pronounced. On the other hand, if the impedance at $x = l$ is equal to the characteristic impedance ρc of the medium, then $\zeta = 1$ and $\alpha_l \to \infty$, in which case $|p_{\min}| \to |p_{\max}|$; no wave is reflected, and there is no interference; so there can be no minima.

To measure ζ_l, we first determine the spacing between pressure minima and the distance between the nearest minimum, $n = 1$, and the termination, $x = l$. The spacing is equal to $\frac{1}{2}\lambda$, and $\beta_l = 1 - [2d_{\min}(1)/\lambda]$. The value of γ is determined by measuring the rms pressure at two successive minima, say, for n and $n + 1$, and at the intermediate maximum. The difference between the pressure amplitudes at the two minima is

$$2\,|A|\cosh \pi[\alpha_l - \tfrac{1}{2}\gamma\lambda(n + \tfrac{1}{2} - \beta_l)] \sinh \frac{\gamma\lambda}{4}$$

and the ratio between this and the amplitude at the maximum,

$$\frac{|p_{\min}(n)| - |p_{\min}(n+1)|}{|p_{\max}(n + \frac{1}{2})|} = 2 \sinh \frac{\gamma\lambda}{4} \to \frac{\gamma\lambda}{2} \qquad \gamma\lambda \ll 1 \qquad (9.1.7)$$

serves to determine the attenuation factor γ.

To determine α_l, we compute the ratio of the mean value of $|p_{\min}|$ at the successive minima to the intermediate $|p_{\max}|$.

$$\frac{|p_{\min}(n)| + |p_{\min}(n+1)|}{2\,|p_{\max}(n + \frac{1}{2})|} = \cosh \frac{\gamma\lambda}{4} \tanh \pi[\alpha_l - \gamma d_{\max}(n + \tfrac{1}{2})] \qquad (9.1.8)$$

Knowing γ, λ, and $d_{\max}(n + \frac{1}{2})$, this equation allows one to obtain the value of α_l. Then, from Plate I or II, we can compute $\rho c\zeta_l$, the impedance of the material at $x = l$ and $\rho cS\zeta_0$, the acoustic load of the air in the tube on the driving piston.

Open tube end

When the end of the tube at $x = l$ is open to free space, the conditions of flow and the distribution of pressure across the opening are not uniform, even when the wavelength is much longer than the tube diameter. In this long-wavelength limit, however, the only wave which can propagate inside the tube is the plane wave, the fundamental mode, which is the situation under discussion in this section. When this is the situation, it is possible to ignore the nonuniformity of velocity across a tube cross section and to assume that the air in the open end, at $x = l$, acts like a piston, radiating sound out into the open, as well as reflecting some back toward the driving piston at $x = 0$. At very long wavelengths little is radiated out of the open end, a strong standing wave is built up inside the tube, and the simple approximation we are discussing is close to the actual behavior. But as the driving frequency is increased, more and more energy leaks out of the open end, and the simple model loses validity.

For a circular tube of length l and inside radius a, with end $x = 0$ provided with a driving piston and the end $x = l$ flush with a rigid plane wall (i.e., the open end is provided with a large, rigid flange), the air in the open end may be considered, for long wavelengths, to be a piston of zero mass, radiating some energy into the open and returning some back down the tube.

To this approximation we can talk about an acoustic impedance of the open end, the ratio of the mean pressure at $x = l$ to the mean axial velocity there. The reactive part of this impedance would produce reflection back to the driving piston at $x = 0$; the resistive part would represent energy lost from the tube by being radiated out of the open end. Reference to Eq. (7.4.31) indicates that this open-end impedance, for a flanged open end, would be the function $\theta_0 - i\chi_0$ (plotted in Fig. 7.9 and shown in Table IX) multiplied by ρc.

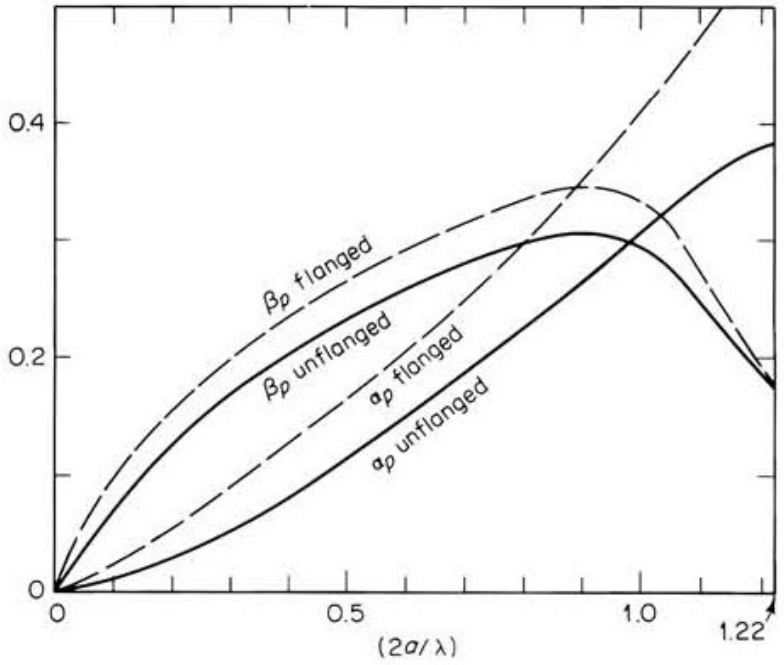


FIGURE 9.2
Impedance parameters $\Phi_p/\pi = \beta_p + i\alpha_p$ for open end of circular tube. Curves marked *unflanged* are for open end in infinite space; curves marked *flanged* are for opening in plane wall, radiation confined to one side of wall.

Therefore the standing-wave parameters α_l and β_l for the wave inside the tube can be determined. We define the quantities $\alpha_p = \alpha_l$ and $\beta_p = \beta_l$ such that

$$\theta_0 - i\chi_0 = \tanh \pi(\alpha_p - i\beta_p) \qquad \text{(see Table IX)}$$

The radiation load on the piston at $x = 0$ is then easily computed from Eq. (9.1.8).

$$Z_r = R_r - iX_r = \rho c S \tanh \pi \left[\alpha_p + \gamma l - i\left(\beta_p + \frac{2l}{\lambda}\right)\right] \qquad (9.1.9)$$

where $S = \pi a^2$ is the cross-sectional area of the tube. R_r and X_r can thus be calculated by using Plates I or II. The parameters α_p and β_p for a tube with flanged open end are plotted as the dashed lines marked *flanged*, as functions of $2a/\lambda = a\omega/\pi c$, in Fig. 9.2. We see that, for $\lambda > 10a$, the

majority of the energy stays inside the tube (the ratio of reflected to incident intensity is $e^{-4\pi\alpha}$, and for $\alpha < 0.05$, this ratio is greater than 0.5, indicating that a minority of the energy coming to the open end, from the piston, escapes from the tube). We also see that the reactive effect of the open end is considerable (this reactive effect is measured by the phase change $e^{2\pi i\beta_p}$ of the pressure wave on reflection, and β_p is larger than 0.1 unless $\lambda > 20a$).

In many cases the tube is not flanged, but radiates into free space (as with an open organ pipe, for example), in which case the impedance functions θ_0 and χ_0 given in the dashed curves of Fig. 9.2 are not appropriate. The equivalent impedance of an unflanged circular tube can be computed exactly for $\lambda > 2a$ [see Levine and Schwinger, *Phys. Rev.*, **73:** 383 (1948)]. It requires the solution of a Wiener-Hopf integral equation, a subject beyond the scope of this book. The results may be translated into values of α_p and β_p, and are included in Fig. 9.2 as the solid lines marked *unflanged.* We note that, because the escaping sound must spread out over the whole solid angle 4π, instead of the 2π in front of the flange in the previous case, the *unflanged* curves indicate a smaller reactive effect and less energy radiated than for the flanged tube at the same frequency (a larger solid angle corresponds to a poorer impedance match between inside and outside). The general trend of the curves is the same, however. The calculations for the *unflanged* case are invalid for $2a/\lambda$ larger than 1.22, above which a higher-mode symmetric wave can be transmitted inside the tube, as will be shown in Sec. 9.2.

Having values of α_p and β_p, at least for the longer wavelengths, we now can use Eq. (9.1.9) to compute the radiation impedance on the driving piston at $x = 0$. A single example of the results is displayed in Fig. 9.3, for an unflanged tube twice as long as its diameter. The lower curve gives the real part, and the upper curve the imaginary part, of the hyperbolic tangent. The resonances are clearly indicated, particularly at the lower frequencies. If the boundary condition at $x = l$ had been that p is zero there (as is sometimes assumed in calculating resonance frequencies for open tubes), α_p, β_p, and R_r would have been zero, and X_r would have been $\rho cS \tan(2\pi l/\lambda)$. The resonances would have come at $2l/\lambda = \frac{1}{2}, \frac{3}{2}, \ldots$. Figure 9.3 shows that the actual resonances are for somewhat smaller values, for $2l/\lambda = 0.43, 1.33, 2.25, 3.21$. As the frequency is increased, more and more energy is lost through the open end (α_p increases); so the resonance peaks get broader and less high until, for $2l/\lambda > 4.88$, the plane-wave approximation loses all validity. Obviously, a much narrower tube, in relation to its length, would have many more sharp resonances, coming at values of $2l/\lambda$ much closer to half-integer values, at least for the lower resonances.

If the tube is used as a musical instrument, the "driving piston" is either a vibrating reed or vibrating jet of air, which generates sound of all frequencies. In this case the energy radiated will be more or less proportional to the radiation resistance R_r at the piston. This radiated energy is concentrated

in narrow frequency bands, corresponding to the peaks in the curve of R_r. For a long narrow tube, these peaks come for frequencies such that $2l/\lambda \simeq n + \frac{1}{2}$, the usual formula for resonance in an open-ended tube. For the higher harmonics, however, when n begins to be as large as l/a, the peaks drop off in height and narrowness, and the resonances differ more and more from the simple-harmonic ratio $2n + 1$ to the fundamental.

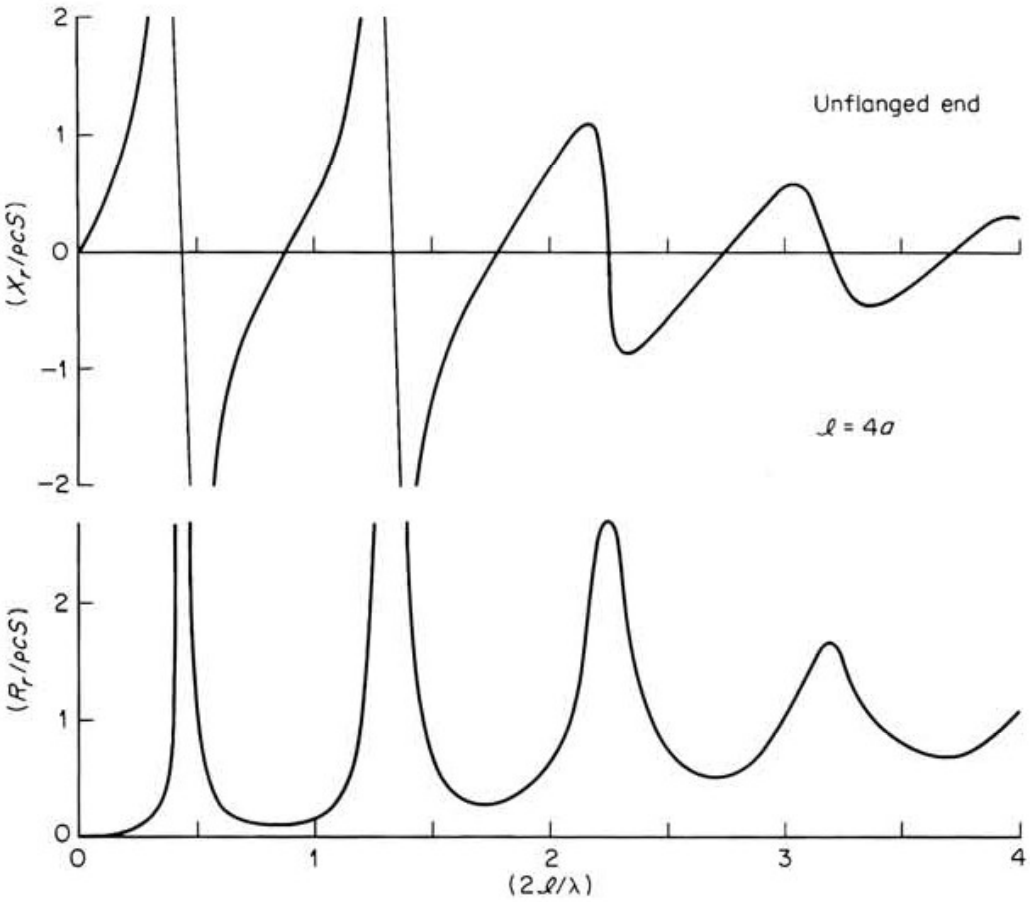


FIGURE 9.3
Radiation resistance R and reactance X of a piston driving air in a circular tube of radius a and length l, the other end open to free space, as functions of $kl/\pi = 2l/\lambda$.

Analogous impedance

When the wavelength of the sound wave in the tube is much greater than the cross-sectional dimensions of the tube, the wave motion is quite analogous to the flow of electric current in a transmission line. If the tube has cross-sectional area S, the total flux of fluid, $U = Su$, is the analogue of the electric current I, and the sound pressure p is the analogue of the voltage E. The inductance L_l per unit length of transmission line is defined, in circuit theory, by saying that the magnetic energy per unit length of line is $\frac{1}{2}L_l I^2$. The analogous inductance L_a, per unit length of the pipe, is likewise defined by saying that the kinetic energy of the fluid, per unit length of pipe, is $\frac{1}{2}L_a U^2$,

so that

$$L_a = \frac{2}{U^2}\,\mathrm{KE} = \frac{2}{U^2}\,\tfrac{1}{2}S\rho u^2 = \frac{\rho}{S} \tag{9.1.10}$$

from Eq. (6.1.7), since the volume of a unit length of pipe is S.

Similarly, we can define the analogous capacitance C_a per unit length of pipe by saying that the potential energy per unit length is $\frac{1}{2}C_a p^2$. Again from Eq. (6.1.7),

$$C_a = \frac{2}{p^2}\,\mathrm{PE} = \frac{2}{p^2}\,\tfrac{1}{2}S\kappa p^2 = S\kappa = \frac{S}{\rho c^2} \tag{9.1.11}$$

Thus the analogous characteristic impedance of the acoustic transmission line and the velocity of wave motion along it are

$$\sqrt{\frac{L_a}{C_a}} = \frac{\rho c}{S} \qquad \sqrt{\frac{1}{L_a C_a}} = c$$

and the power transmitted along the wave is $pU = (\rho c/S)U^2 = S(\rho c u^2)$, where $\rho c u^2$ is the intensity of the sound wave.

This is all that needs to be said if the tube walls are perfectly rigid, if we are willing to neglect energy losses at the tube walls, and if the tube cross section is independent of x. But if we desire to include the effects of heat conduction and viscosity at the tube walls, we must also include an analogous resistance R_a per unit length of tube. By analogy the resistance would be defined by stating that the power loss per unit length is $R_a|U|^2$. According to Eqs. (6.4.37) and (6.4.38), for a wave moving tangentially to the surface ($k_t = \omega/c = k$), the power loss per unit area of surface is $[kd_v + (\gamma - 1)kd_h](|p|^2/2\rho c)$, where d_v and d_h are defined in Eqs. (6.4.31). If D is the perimeter of the duct's internal cross section, and since $|p| \simeq \rho c\,|u| = (\rho c/S)\,|U|$ on the average, we can write the equation for the analogous resistance per unit length of duct of uniform cross-sectional area S and perimeter D as

$$R_a = \frac{\rho c D}{2S^2}\,[kd_v + (\gamma - 1)kd_h] \tag{9.1.12}$$

This resistance is proportional to the square root of the driving frequency; for ducts of cross-sectional area larger than 1 sq cm and for frequencies of a few kilocycles or less, it can ordinarily be neglected.

Ducts with yielding walls

The equation of motion given in Eqs. (6.2.3) for free space may be written for a plane wave in a duct in terms of acoustic pressure and flux $U = Su$, in accord with the electric-circuit analogy,

$$L_a \frac{\partial U}{\partial t} + R_a U = -\frac{\partial p}{\partial x} \tag{9.1.13}$$

where, as we have just said, we can often neglect the R_a term. If the duct walls yield somewhat to the internal pressure, the equation of continuity, relating the time rate of change of pressure to the gradient of U, must be modified.

The term $-(\partial U/\partial x)$ represents a rate of influx of gas into a unit length of duct, and this corresponds to a change of density, and thus of pressure there. If the duct walls are rigid, this influx equals the compressibility $\kappa = 1/\rho c^2$ of the gas times the time rate of change of pressure. But if the duct walls yield, so that an increase of pressure produces a fractional change of cross-sectional area, this dilutes somewhat the increased compression of the gas, as though the two effects acted in parallel. Thus the equation of continuity would be written

$$-\frac{\partial U}{\partial x} = S\left(\kappa + \frac{1}{K_w}\right)\frac{\partial p}{\partial t}$$

where K_w, the *wall stiffness constant*, is the ratio between the pressure p and the fractional change in cross-sectional area of the duct, produced by p.

The pressure p is not static, however, and we also should take into account the inertia of the duct walls. In a stiffness-controlled system [Eqs. (2.3.4)] the impedance is $K/-i\omega$, where $\omega/2\pi$ is the frequency of the wave. If mass is to be considered, the impedance is $-i\omega M + (K/-i\omega) = Z$. Therefore the equation of continuity for a duct with yielding walls is

$$-\frac{\partial U}{\partial x} = S\left(\kappa + \frac{1}{-i\omega Z_w}\right)\frac{\partial p}{\partial t} = S\left[\frac{1}{\rho c^2} + \frac{1}{M_w(\omega_0^2 - \omega^2)}\right]\frac{\partial p}{\partial t}$$

where $\omega_0^2 = K_w/M_w$, $\omega_0/2\pi$ being the resonance frequency of transverse expansion oscillation of the duct walls, unencumbered by the fluid inside. Thus the second of Eqs. (6.2.3) becomes

$$-\frac{\partial U}{\partial x} = S\kappa\frac{\omega_1^2 - \omega^2}{\omega_0^2 - \omega^2}\frac{\partial p}{\partial t} \to S\kappa\frac{\partial p}{\partial t} \qquad \text{as} \qquad K_w \to \infty \qquad (9.1.14)$$

where $\omega_1^2 = \omega_0^2 + (\rho c^2/M_w)$, $\omega_1/2\pi$ being the resonance frequency of the walls when stiffened by the air inside it. It should be noted that this analysis assumes that the duct walls are *locally reacting*, in the sense of page 260; that no expansive wave motion is produced along the duct by the wave motion inside (see Prob. 1 of Chap. 10 for waves in the duct walls).

In an electric transmission line the corresponding equation is $-(\partial I/\partial x) = C(\partial V/\partial t)$, where C is the capacitance per unit length of the line. Therefore, for a tube with locally yielding walls, Eq. (9.1.11) for the analogous capacitance per unit length of duct becomes

$$C_a = \frac{S}{\rho c^2}\frac{\omega_1^2 - \omega^2}{\omega_0^2 - \omega^2} \qquad (9.1.15)$$

The wave velocity in the duct is then

$$c_\varphi = \frac{1}{\sqrt{L_a C_a}} = c\left(\frac{\omega_0^2 - \omega^2}{\omega_1^2 - \omega^2}\right)^{\frac{1}{2}} \qquad c^2 = \frac{1}{\rho\kappa} \tag{9.1.16}$$

as long as the wavelength is long compared with the tube perimeter D. The effect of the wall motion is to make this velocity a function of frequency. If the walls are "soft," so that ω_0 and ω_1 are in the range of frequencies for which the transmission-line analogy holds (i.e., for which $\omega_0 D/c$ and $\omega_1 D/c$ are much smaller than unity), the wave velocity inside the tube differs greatly from the speed c of sound in the open.

As ω is increased from zero, the wave velocity first diminishes, becoming zero when $\omega = \omega_0$, when the wave energy is entirely diverted to exciting tube oscillations. For $\omega_0 < \omega < \omega_1$, the wave velocity is imaginary, indicating that acoustic motion is so strongly attenuated that no true wave motion can exist (this is identical with the anomalous dispersion and absorption in optical media). Finally, when ω is larger than ω_1, the wave velocity is again real, but larger than c. It decreases as ω increases further, approaching c as $\omega \to \infty$. Of course, when ω becomes larger than c/d, the wavelength of the sound is no longer much greater than the tube diameter, and our simple one-dimensional theory is no longer valid.

Thus the wave velocity in the tube is a function of the frequency of the wave. Optical media, in which the light velocity is a function of frequency, exhibit *dispersion*, so that a medium in which the wave velocity is frequency-dependent is called a *dispersive medium*. A pipe with yielding walls is a dispersive medium for longitudinal acoustic waves. Waves of arbitrary shape will not maintain their shape as they travel along the interior of the tube.

Phase and group velocity

With dispersive waves, when c is a function of ω, we must distinguish between a number of different wave velocities. First there is the *phase velocity* c_φ, the velocity with which the phase angle $\omega[t - (x/c_\varphi)]$ of a simple-harmonic wave of frequency $\omega/2\pi$ progresses along the tube. This is the wave velocity of the wave of Eq. (9.1.16).

Then there is the *group velocity*, the velocity of progress of the "center of gravity" of a group of waves that differ somewhat in frequency. For example, we might combine a sequence of simple-harmonic waves, each of the form $\exp[i(\omega/c_\varphi)(x - c_\varphi t)]$, with pressure amplitudes which are maximum for $\omega = \omega_a$ and fall off on either side, as given by the "error-function" formula, $(A/\delta\sqrt{2\pi})\exp[-(\omega - \omega_a)^2/2\delta^2]$, so that the acoustic pressure is

$$p = \frac{A}{\delta\sqrt{2\pi}} \int_{-\infty}^{\infty} \exp\left[-i\omega t + ix\frac{\omega}{c_\varphi(\omega)} - \left(\frac{1}{2\delta^2}\right)(\omega - \omega_a)^2\right] d\omega \tag{9.1.17}$$

Here $\omega_a/2\pi$ is the mean frequency of the group, and $\delta/2\pi$ is the mean deviation in frequency of any one component of the wave from this average. If the phase velocity c_φ were independent of ω, this group of waves would have the form

$$p = A \exp\left[-i\omega_a\left(t - \frac{x}{c_\varphi}\right) - \tfrac{1}{2}\delta^2\left(t - \frac{x}{c_\varphi}\right)^2\right]$$

which is a pulse extending, roughly, from $x = c_\varphi t - (c_\varphi/\delta)$ to $c_\varphi t + (c_\varphi/\delta)$ in space, traveling with velocity c_φ and oscillating with frequency $\omega_a/2\pi$ as it travels along.

But if c is a function of ω, we must take this into account in performing the integration. We can, for example, expand the quantity

$$\frac{\omega}{c_\varphi(\omega)} = \frac{\omega_a}{c_a} + (\omega - \omega_a)\frac{1}{c_g} + \cdots$$

where

$$c_a = c_\varphi(\omega_a) \qquad \frac{1}{c_g} = \left[\frac{d}{d\omega}\frac{\omega}{c_\varphi(\omega)}\right]_{\omega=\omega_a} \tag{9.1.18}$$

in a Taylor's series about the average value ω_a. If δ, the "spread" in frequency of the group, is small compared with ω_a, we can usually neglect all the terms higher than the first order in this expansion, and the exponent of the integrand of Eq. (9.1.17) becomes

$$-i\omega_a\left(t - \frac{x}{c_a}\right) - i(\omega - \omega_a)\left(t - \frac{x}{c_g}\right) - \frac{1}{2\delta^2}(\omega - \omega_a)^2$$

The integration can then be carried out, giving

$$p = A \exp\left[-i\omega_a\left(t - \frac{x}{c_a}\right) - \tfrac{1}{2}\delta^2\left(t - \frac{x}{c_g}\right)^2\right] \tag{9.1.19}$$

This represents a pulse of spatial length c_g/δ and of frequency $\omega_a/2\pi$. The velocity of the surfaces of constant phase angle in this group wave is $c_a = c_\varphi(\omega_a)$, the phase velocity of the component of average frequency. But the velocity of the wave peak, the point where the various components are all in phase, is not c_a, but $c_g = 1/[d(\omega/c_\varphi)/d\omega]_{\omega_a}$, which is the group velocity of any group of waves of frequency centered around ω_a. If c_φ is independent of ω, $c_g = c_a$, but if c_φ does vary with ω,

$$c_g = c_a\left[1 - \frac{\omega_a}{c_a}\left(\frac{\partial c_\varphi}{\partial \omega}\right)_{\omega_a}\right]^{-1}$$

which is smaller than c_a if $dc/d\omega$ is negative (as it is for acoustic waves in a yielding tube).

Finally, there is the *signal velocity*, which is the velocity of the *front* of a group of waves, the speed at which one end of the tube first learns that a signal has been started from the other end. Since a wave, to have a beginning, must be a combination of waves of different frequencies, it is obvious that the signal velocity (if there be one) is some sort of average value of c_φ. But if there are waves with phase velocity of any value, no matter how large (as there are with waves in a nonrigid tube), it is not obvious that a wavefront can be maintained. In fact, it would seem probable that the components of high phase velocity would inevitably draw ahead of the rest and that eventually there would be no sharp wavefront.

This is the case with the diffusion of heat, for example. If the temperature at the end of a rod is suddenly increased at time $t = 0$, the temperature at a distance x along the rod begins *immediately* to rise, slowly at first but continuously, so that at no time after $t = 0$ can we say that the "heat front" has suddenly arrived. There is no wavefront, and thus no signal velocity for heat flow (in fact, there is no true wave motion for it). One can ask whether there can be such a thing as a sharp wavefront (and hence a signal velocity) in a dispersive medium, such as a pipe with yielding walls.

It turns out that the crucial test is not whether the phase velocity goes to infinity for some intermediate value of ω, but whether c has a finite limiting value as $\omega \to \infty$. By extension of Eqs. (1.3.16) and (2.3.6), we see that the pressure at point x at time t in a one-dimensional dispersive wave, for which the pressure is $p_0(t)$ at $x = 0$, is

$$p(x,t) = \int_{-\infty}^{\infty} P(\omega) \exp\left(i\frac{\omega}{c_\varphi}x - i\omega t\right) d\omega$$

where

$$P(\omega) = \frac{1}{2\pi}\int_{-\infty}^{\infty} p_0(t)\, e^{i\omega t}\, dt \qquad (9.1.20)$$

and c_φ is some function of ω. Now, if $p_0(t)$ is zero for $t < 0$, then all the poles and other singularities of $P(\omega)$ will be *on or below the real axis* of the variable ω, and the contour of integration of ω will be just above its real axis. Also, the singularities and zeros of $c_\varphi(\omega)$ are on or below the real axis of ω [Eq. (9.1.16)], so that the contour of integration for ω lies above all the singularities of the integrand. Thus, according to Eqs. (1.2.15), the acoustic pressure $p(x,t)$ is zero for $t - [x/c(\infty)] < 0$, and so, if $c_\varphi(\omega)$ approaches a finite value, $c_\varphi(\infty)$, as $\omega \to \infty$, nothing will occur at point x until time $t = x/c_\varphi(\infty)$; the wave will have a true wavefront which travels with the signal velocity $c_\varphi(\infty)$.

The velocity of simple-harmonic "waves" of heat is proportional to $\sqrt{\omega}$; thus $c_\varphi(\omega) \to \infty$ as $\omega \to \infty$, and heat conduction has no wavefront, as we pointed out earlier. On the other hand, for waves in a pipe, if we assume that Eq. (6.4.21) holds over the whole range of ω, then $c_\varphi(\infty)$ is just equal to c, the velocity of sound waves in free space; thus the signal velocity of waves in a tube exists and equals c.

Lumped-circuit elements

Sudden changes of duct cross section produce sudden changes of pressure, and in the long-wavelength approximation, their effects are equivalent to the lumped-circuit impedances, capacitances, and resistances familiar in electric circuits. For example, a constriction in a duct gives rise to a concentration of flow through the constriction, with consequent increase in kinetic-energy density. If the net increase is concentrated in a region small compared with the wavelength, the total increase can be represented by a lumped inductance. If the constriction also produces an increase in viscous-energy loss, this addition can be represented as a lumped resistance.

The various types of acoustical circuit elements are shown in Fig. 9.4, together with their electrical analogues. The closed volume V_D at D behaves like a capacitance, since additional volume of fluid, introduced into D, increases the pressure there. The potential energy of this compression is approximately $\frac{1}{2}V_D\kappa p^2$; so the analogous capacitance corresponding to D is [see also Eq. (9.1.11)]

$$C_D \simeq \frac{V_D}{\rho c^2} \tag{9.1.21}$$

To calculate the analogous impedance and resistance of a constriction like the openings at C or B of Fig. 9.4, we compute the extra kinetic energy and viscous-energy loss, produced by steady flow through the opening. The simplest case is that of a circular opening of radius b in a thin but rigid plate. If the area πb^2 is considerably smaller than the area S of the duct cross section, we can consider the flow pattern through the hole to be unaffected by the duct walls and calculate the flow through a circular hole in an infinite plate.

As shown in Fig. 9.5, the lines of flow are hyperbolas, η = constant, with foci the traces of the sharp edge of the hole on the rx plane. The surfaces of constant velocity potential, ξ = constant, are oblate spheroids, with elliptical sections in the rz plane, having the same foci. Thus ξ, η, and

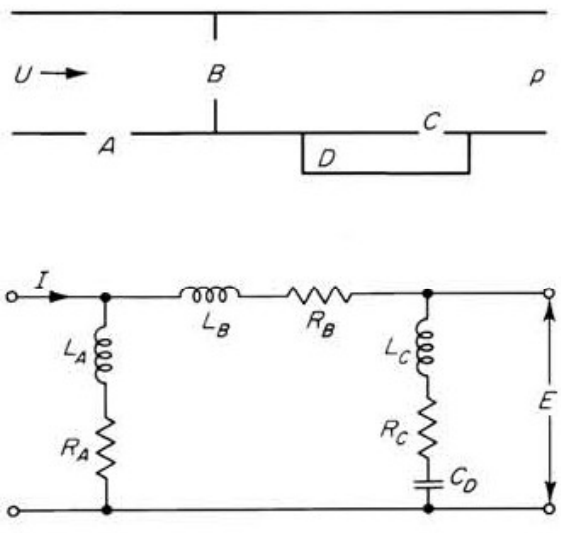


FIGURE 9.4
Illustration of electric-circuit elements analogous to an acoustical transmission line with openings, constrictions, and shunt volumes.

ϕ, the angle around the x axis, the appropriate set of coordinates to describe the motion, are related to x, y, and z by the equations

$$x = b\xi\eta$$
$$y = b\sqrt{(\xi^2 + 1)(1 - \eta^2)}\cos\phi$$
$$z = b\sqrt{(\xi^2 + 1)(1 - \eta^2)}\sin\phi$$

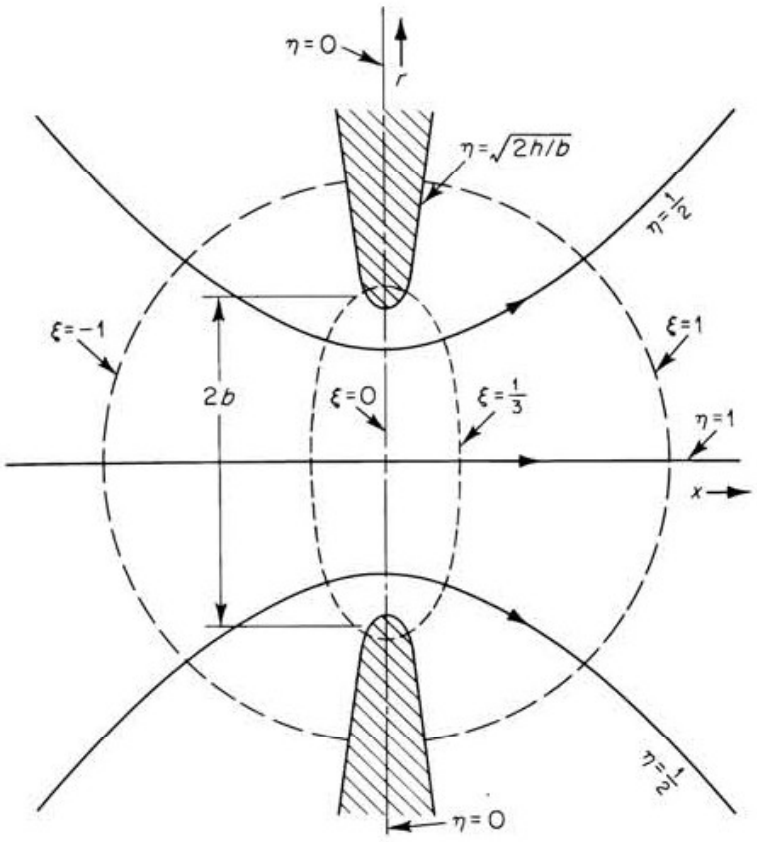


FIGURE 9.5
Lines of flow, η = const, and velocity-potential surfaces, ξ = const, for steady flow through a circular orifice.

It can be shown that the magnitude u of the fluid velocity at the point x, y, z or ξ, η, ϕ is $(U/2\pi b^2)[(1 + \xi^2)(\xi^2 + \eta^2)]^{-\frac{1}{2}}$, going to zero at infinite distances from the hole ($\xi \to \infty$) and going to infinity at the edge of the hole ($\xi \to \eta \to 0$) if the plate is infinitely thin. Factor U is the total rate of flow through the opening, and thus is the value of the analogue to the current, as already used. The volume element in the ξ, η, ϕ coordinates is

$$b^3(\xi^2 + \eta^2)\, d\xi\, d\eta\, d\phi$$

So the total kinetic energy of the fluid is

$$\tfrac{1}{2}\rho\left(\frac{U}{2\pi b^2}\right)^2 \int_0^{2\pi} d\phi \int_0^1 d\eta \int_{-\infty}^{\infty} \frac{b^3(\xi^2 + \eta^2)\, d\xi}{(\xi^2 + 1)(\xi^2 + \eta^2)} = \frac{\rho U^2}{2\pi b} \int_0^{\infty} \frac{d\xi}{1 + \xi^2} = \frac{\rho}{4b} U^2$$

Thus, in accord with Eq. (9.1.10), when πb^2 is much smaller than S, the lumped-circuit inductance of the opening is

$$L_a \simeq \frac{\rho}{2b}$$

If we had chosen a mechanical, instead of electrical, analogue, we should have talked about the air in and near the opening as equivalent to a solid plug of material, moving back and forth through the opening with velocity $u = U/\pi b^2$ and kinetic energy $\frac{1}{2}M_a u^2$. In this case the effective mass would be

$$M_a \simeq \tfrac{1}{2}\pi^2 b^3 \rho = (\pi b^2)^2 L_a$$

which is equivalent to a slug of fluid of density ρ, of cross section equal to $S_0 = \pi b^2$, the area of the opening, and of length $l_0 = \frac{1}{2}\pi b$ equal to one-quarter of the perimeter of the opening. This leads us to a way of writing these formulas, in terms of the area S_0 of the opening and its perimeter D_0.

$$M_a \simeq \tfrac{1}{4}D_0 S_0 \rho \qquad L_a \simeq \frac{\rho D_0}{4S_0} \tag{9.1.22}$$

which we have just shown is valid for circular holes, as long as $S_0 \ll S \ll \lambda^2$. We should expect such formulas to apply reasonably well to square holes or holes of other shape, as long as $(D_0/4)^2$ is of the same order of magnitude as S_0 (i.e., as long as the opening is about as long as it is wide).

To compute the analogous resistance of the circular hole, we use Eq. (6.4.39) to compute the additional power lost because of the increase in velocity near the edge of the opening. Equation (9.1.12) gives the analogous resistance per unit length of duct for the uniform duct. The tangential velocity near the sharp edges of the hole is much larger than that tangential to the duct walls. Thus, though the thermal-conduction loss rate is not increased much, the viscous loss may be quite large near the edge of the hole. In fact, if we assume that the surface of the plate corresponded to the surface $\eta = 0$ (i.e., the plate were of zero thickness), the tangential velocity next to the plate would be $U/2\pi b^2\sqrt{\xi(1 + \xi^2)}$, which goes to infinity at $\xi = 0$, at the infinitely sharp edge of the opening.

This formula for the tangential velocity next to the plate is incorrect for two reasons. First, the plate has a finite thickness, and the edge has a finite radius of curvature, not zero. It would be more accurate to approximate the surface of the plate by the surface $\eta_s = \sqrt{2h/b}$, where $h \ll b$ is the radius of curvature of the edge of the hole, and thus $2h$ is roughly equal to the thickness of the plate near its edge; h is small but not zero. In the second place, the formula of Eq. (6.4.39) has to do with tangential velocity just *outside* the viscous boundary layer; the tangential velocity at the surface of the plate is zero. The thickness $d_h = \sqrt{2\mu/\rho\omega} \simeq 0.21/\sqrt{\nu}$ cm for air at

standard conditions applies only when d_h is smaller than the radius of curvature of the surface. Only when this is true can we assume that the $u_{\tan}$ of Eq. (6.4.39) is the $u_{\tan}$ calculated for the surface when viscosity is neglected, the way Eq. (6.4.39) has been used. Thus the h in the formula $\eta_s = \sqrt{2h/b}$ is either the half-thickness of the plate near the edge of the hole, or else is the thickness d_v of the viscous boundary layer, whichever is *larger*.

Using Eq. (6.4.39), the power lost by flow through a circular hole of radius b is the integral of $-\rho\omega d_v(u_{\tan})^2$ over the surface $\eta_s = \sqrt{2h/b}$.

$$\tfrac{1}{2}\rho\omega d_v\left(\frac{U}{2\pi b^2}\right)^2\int_0^{2\pi} d\phi \int_{-\infty}^{\infty} \frac{\sqrt{\xi^2 + (2h/b)}}{(\xi^2+1)\left(\xi^2 + \dfrac{2h}{b}\right)}\, b^2\, d\xi \simeq \frac{\rho\omega d_v}{4\pi b^2}\, U^2 \ln\frac{2b}{h}$$

when $h \ll b$. Therefore the analogous resistance of a circular hole of radius $b \ll \sqrt{S/\pi}$ is

$$R_a \simeq \frac{\rho\omega d_v}{4\pi b^2}\ln\frac{2b}{h} = \frac{1}{4S_0}\sqrt{2\rho\omega\mu}\ln\frac{2b}{h} \qquad (9.1.23)$$

where $h \ll b$ is either the half-thickness of the plate near the hole edge (i.e., is the mean radius of curvature of the edge) or else is the viscous-boundary-layer thickness d_v, whichever is larger. (When b becomes the same size as d_v, the boundary layers merge in the hole, and the exact solutions of Sec. 6.4 must be used; fortunately, such a minute hole is of no great practical interest.) The resistance R_a is in series with the lumped-circuit inductance L_a of Eq. (9.1.22) for the hole, as shown in Fig. 9.4. At moderate and large intensities, turbulence around the edges modifies R; see Eq. (11.3.36).

Two-dimensional flow

To determine the lumped-circuit impedance and resistance of a constricted opening which is considerably longer than it is wide, we resort to a technique which can be used whenever the problem is a two-dimensional one. If the duct is rectangular in cross section, with two walls parallel to the xy plane, everywhere a distance d apart, the distance between the other two walls varying with x, then the fluid motion in the duct will be parallel to the xy plane, and p and u will be functions of x and y only (except for the time dependence). We then can use the complex notation (Fig. 1.1) to assist us. Both velocity and pressure can be expressed in terms of the velocity potential Ψ of Eq. (6.2.13) (for convenience here we shall use minus the potential, $\psi = -\Psi$).

When the wavelength is long compared with the duct width, the function $\psi(x,y)$ will approximate a solution of the Laplace equation, $(\partial^2\psi/\partial x^2) + (\partial^2\psi/\partial y^2) \simeq 0$. In this case ψ will turn out to be the real part of a function

of the complex variable $z = x + iy$:

$$F(z) = \psi(x,y) + i\theta(x,y) \qquad z = x + iy \qquad z^* = x - iy$$

$$F^* = \psi - i\theta \qquad \frac{\partial}{\partial x} = \frac{\partial}{\partial z} + \frac{\partial}{\partial z^*} \qquad \frac{\partial}{\partial y} = i\frac{\partial}{\partial z} - i\frac{\partial}{\partial z^*}$$

and the velocity potential ψ and the *flow function* θ, so defined, will be related by the Cauchy relations

$$\frac{\partial \psi}{\partial x} = \frac{\partial \theta}{\partial y} \qquad \frac{\partial \psi}{\partial y} = -\frac{\partial \theta}{\partial x}$$

We can then use the geometric representation of a complex quantity, pictured in Fig. 1.1, to define the vector velocity of the fluid, the real part, $\partial\psi/\partial x$, being the x component, and the imaginary part, $\partial\psi/\partial y$, being the y component, so that

$$\frac{\partial \psi}{\partial x} + i\frac{\partial \psi}{\partial y} = \frac{1}{2}\frac{\partial}{\partial x}(\psi - i\theta) + \frac{1}{2}i\frac{\partial}{\partial y}(\psi - i\theta) = \frac{1}{2}\frac{\partial}{\partial x}F^* + \frac{1}{2}i\frac{\partial}{\partial y}F^*$$

$$= \frac{1}{2}\frac{\partial}{\partial z}F^* + \frac{1}{2}\frac{\partial}{\partial z^*}F^* - \frac{1}{2}\frac{\partial}{\partial z}F^* + \frac{1}{2}\frac{\partial}{\partial z^*}F^* = \frac{\partial F^*}{\partial z^*}$$

Since F is a function of z alone (not z^*), F^* will be a function of z^* alone, and $\partial F^*/\partial z^*$ will be the complex conjugate of the complex quantity dF/dz. Thus the complex quantity representing the magnitude and direction of the fluid flow at the point $x + iy$ within the duct is given by the complex conjugate of the derivative dF/dz, where the real part of $F(z) = \psi + i\theta$ is the negative velocity potential.

$$u_x = \mathrm{Re}\,\frac{dF}{dz} \qquad u_y = -\mathrm{Im}\,\frac{dF}{dz} \tag{9.1.24}$$

$$p \simeq i\rho\omega\,\mathrm{Re}\,F \qquad |u|^2 = \left|\frac{dF}{dz}\right|^2$$

Inductance and resistance of a slit

If the traces of the duct walls perpendicular to the xy plane consist of portions of straight lines, we can use the Schwartz-Christoffel transformation to find F as a function of z (actually, we find z as a function of F, but this is only moderately embarrassing). As an example of the method, we consider the duct of Fig. 9.6, having depth d perpendicular to the xy plane and having constant width a in the y direction, except for a diaphragm at $x = 0$ with an open slit of width b symmetrically located.

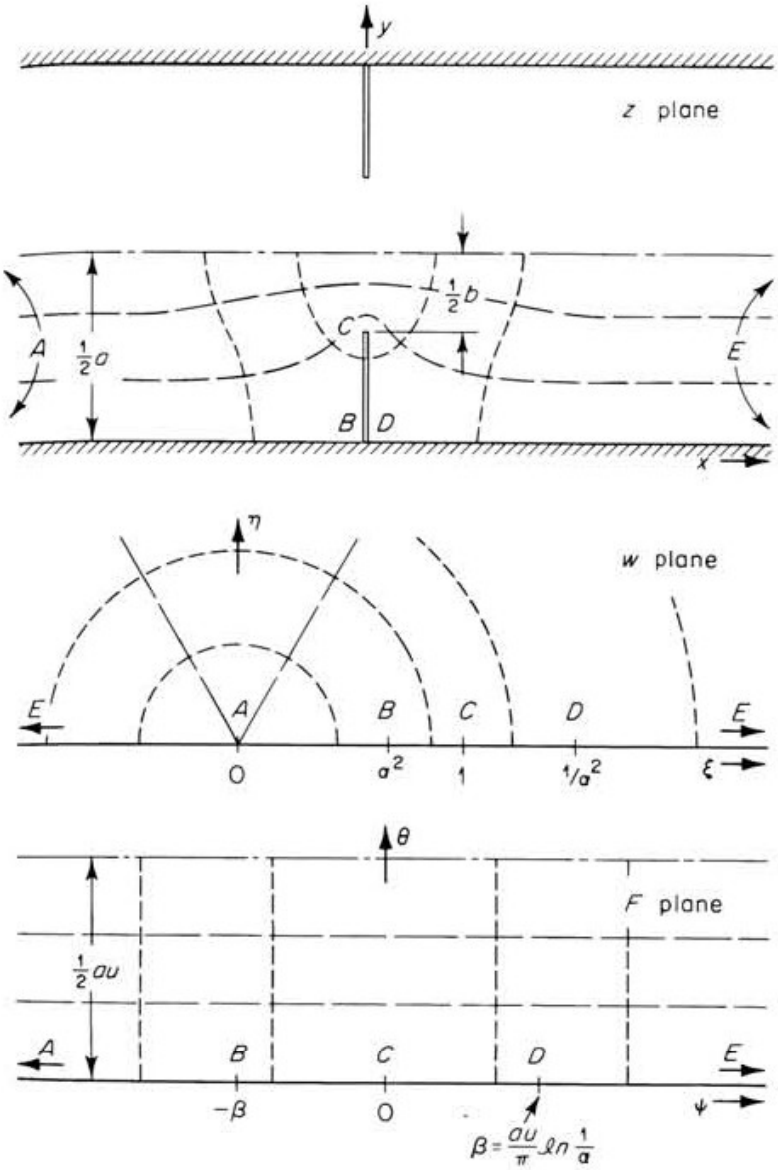


FIGURE 9.6
Conformal transformations from the z plane of the duct to the velocity-potential F plane, via the w plane, for half a rectangular duct with slit of width b. Dashed lines are streamlines, $\theta = \text{const}$; dotted lines, velocity-potential contours, $\psi = \text{const}$.

To find the steady-state flow, we first transform the interior of the half-duct, between the lines $y = 0$ and $y = -\frac{1}{2}a$ to the upper half of the $w = \xi + i\eta$ plane, by the Schwartz-Christoffel transformation

$$\frac{dz}{dw} = \frac{a}{2\pi w} \frac{w - 1}{\sqrt{(w - \alpha^2)(w - 1/\alpha^2)}}$$

$$z = \frac{a}{\pi} \ln \frac{\sqrt{w - \alpha^2} + \sqrt{w - (1/\alpha)^2}}{\sqrt{(1/\alpha)^2 - (1/w)} + \sqrt{\alpha^2 - (1/w)}} \to \begin{cases} \dfrac{a}{2\pi} \ln \dfrac{4w}{Q} & w \to \infty \\ \dfrac{a}{2\pi} \ln \dfrac{wQ}{4} & w \to 0 \end{cases} \tag{9.1.25}$$

where $Q = (1/\alpha)^2 + \alpha^2 + 2 = [(1/\alpha) + \alpha]^2$, and where, in order that point C $(w = 1)$ correspond to $z = (i/2)(a - b)$, the quantity α must equal $\tan(\pi b/4a)$.

The transformation from the w to the F plane is simple.

$$w = e^{2\pi F/au} \qquad F = \frac{au}{2\pi} \ln w$$

if the fluid velocity at $x = \pm\infty$ is u, so that the total flux is $uad = U$. Thus at point E ($x \to \infty$ or $w \to \infty$ or $\psi \to \infty$), the fluid velocity, in magnitude and direction, is the limiting value of the complex conjugate of

$$\frac{dF}{dz} = \frac{dF}{dw}\frac{dw}{dz} = \frac{au}{2\pi w}\frac{2\pi w}{a(w-1)}\sqrt{(w-\alpha^2)\left[w - \left(\frac{1}{\alpha}\right)^2\right]} \to u \qquad w \to \infty$$

The limiting value is real, indicating that the vector velocity is parallel to the x axis, and has magnitude u, as it should.

To calculate the lumped-circuit inductance of the slit at $x = 0$, we need to calculate the total kinetic energy of the fluid in the duct between $x = -l$ and $x = +l$, where $l \gg a$. This, minus the quantity $\frac{1}{2}\rho u^2(2lad)$ (which would be the kinetic energy if there were no constriction), must equal $\frac{1}{2}L_a U^2$, where L_a is the analogous inductance and $U = uad$. To compute the corresponding resistance we must integrate $|u|^2$ along the surface of the plate, from points B to C to D (or from B to C times 2). From Eq. (6.4.39), the analogous resistance R_a of the slit is $\rho\omega d_v/U^2$ times the integral of $|dF/dz|^2$ from B to C.

To transform the integral from the z to the F plane, we use the relation $dx\,dy = |dz/dF|^2\,d\psi\,d\theta$. For the inductance we integrate over half the duct and multiply by 2.

$$L_a = \frac{4}{U^2}\left(\tfrac{1}{2}\rho d\int_{-l}^{l} dx \int_0^{a/2} dy \left|\frac{dF}{dz}\right|^2 - \tfrac{1}{2}\rho l a d u^2\right)$$

$$= \frac{2\rho d}{(uad)^2}\left(\int_{\psi_-}^{\psi_+} d\psi \int_0^{\frac{1}{2}au} d\theta - lau^2\right) = \frac{\rho}{aud}\left[(\psi_+ - \psi_-) - 2lu\right]$$

where ψ_+ is the value of ψ at $x = +l$, and ψ_- is its value at $-l$. Since $w_+ = e^{2\pi\psi_+/au}$ and $w_- = e^{2\pi\psi_-/au}$, we can use the second line of Eqs. (9.1.25) to relate ψ_+ and ψ_- to $\pm l$.

$$l \simeq \frac{\psi_+}{u} - \frac{a}{\pi}\ln\left(\frac{\alpha}{2} + \frac{1}{2\alpha}\right) \qquad -l \simeq \frac{\psi_-}{u} + \frac{a}{\pi}\ln\left(\frac{\alpha}{2} + \frac{1}{2\alpha}\right)$$

Thus, finally, the lumped-circuit inductance of the slit, of width b, in a duct

of cross section a by d, is

$$L_a = \frac{2\rho}{\pi d} \ln\left(\tfrac{1}{2}\alpha + \tfrac{1}{2}\alpha^{-1}\right) = \frac{2\rho}{\pi d} \ln\left(\tfrac{1}{2}\tan\frac{\pi b}{4a} + \tfrac{1}{2}\cot\frac{\pi b}{4a}\right)$$

$$\rightarrow \begin{cases} \dfrac{2\rho}{\pi d}\ln\dfrac{2a}{\pi b} & b \ll a \\ \dfrac{\pi\rho}{4d}\left(\dfrac{a-b}{a}\right)^2 & a - b \ll a \end{cases} \tag{9.1.26}$$

Since the Schwartz-Christoffel transformation includes the duct sides, this formula is valid for all values of b in the range $0 \leqslant b \leqslant a$, as long as λ is much larger than a. If the slit is wide, the obstruction being but a pair of fins sticking out from the walls, the inductive effect is small, being proportional to the square of the relative extension $(a - b)/a$. For a relatively narrow slit, the analogous inductance goes to infinity logarithmically as slit width goes to zero, in contrast to that of the circular hole, which is inversely proportional to the radius of the hole when this radius is small compared with a.

The effective mass of the high-speed air in the slit is

$$M_a = (bd)^2 L_a = \frac{2}{\pi}\rho b^2 d \ln\left(\tfrac{1}{2}\tan\frac{\pi b}{4a} + \tfrac{1}{2}\cot\frac{\pi b}{4a}\right)$$

When $b \ll a$, this is equivalent to the mass of a slug of air of cross section equal to that of the slit bd and of length $(2b/\pi)\ln(2a/\pi b)$, which is longer and longer, compared with its width b, as b goes to zero.

According to Eqs. (6.4.39) and (9.1.23), the additional power lost because of the constriction, $R_a U^2$, should be $2d$ times the integral of $\frac{1}{2}\rho\omega d_v (u_{\tan})^2\, dz$ over the surface, in the z plane, from B to C to D. The magnitude of u^2 equals $|dF/dz|^2 = |dF/dw|^2\,|dw/dz|^2$, and if we transform to the w plane, $dz = |dz/dw|\, dw$. Therefore

$$R_a = \frac{2\rho\omega d_v}{a^2\, du^2}\int_{\alpha^2}^{1}\left|\frac{dF}{dw}\right|^2\left|\frac{dw}{dz}\right| dw = \frac{\rho\omega d_v}{\pi a d}\int_{\alpha^2}^{1}\left|\frac{(w-\alpha^2)[(1/\alpha)^2 - w]}{w^2(1-w)^2}\right|^{\frac{1}{2}} dw$$

If we assume that the fins forming the constriction have zero thickness, the path of integration will be along the real axis in the w plane, and the integral will diverge. But if we assume that the fins have small but finite thickness, with maximum radius of curvature h at their edges, the integration will be along the line $\eta_s = \{(4\pi h/a)[(1/\alpha) - \alpha]\}^{\frac{1}{2}}$ above the axis in the $w = \xi + i\eta$ plane. The result, if h is small compared with a, is the same as if we integrate

along the ξ axis from α to $1 - \eta_s$:

$$R_a \simeq \frac{\rho\omega d_v}{2\pi a d}\left(\frac{1}{\alpha} - \alpha\right) \ln\left\{\frac{a}{\pi h}\frac{(1/\alpha) - \alpha}{[(1/\alpha) + \alpha]^2}\right\}$$
$$\rightarrow \begin{cases} \dfrac{2\rho\omega d_v}{\pi^2 b d} \ln\dfrac{b}{4h} & 4h \ll b \ll a \\ \dfrac{\rho\omega d_v (a-b)}{2a^2 d} \ln\dfrac{a-b}{4h} & a - b \ll a \end{cases} \tag{9.1.27}$$

where $\alpha = \tan(\pi b/4a)$, and $d_v = \sqrt{2\mu/\rho\omega}$, as before. Also as before, with Eq. (9.1.23), h is either the half-thickness of the plate near the slit edge, or else it is d_v, the viscous-boundary-layer thickness, whichever is larger. When the slit width b becomes as small as d_v, the formula no longer holds. Turbulence also modifies these results, as shown in Eq. (11.3.36).

Change of duct width

The same analysis can be applied to the case of a rectangular duct of depth d and width b for $x < 0$ and a for $x > 0$, as shown in Fig. 9.7. The details will be left for a problem; the results are given here. The lumped-circuit inductance and resistance corresponding to the sudden increase in cross section are

$$L_a = \frac{\rho}{\pi d}\left[\frac{(a-b)^2}{2ab} \ln\frac{a+b}{a-b} + \ln\frac{(a+b)^2}{4ab}\right]$$
$$\rightarrow \begin{cases} \dfrac{\rho}{\pi d}\left(1 + \ln\dfrac{a}{4b}\right) & d_v \ll b \ll a \\ \dfrac{\rho}{\pi d}\left(\dfrac{a-b}{2a}\right)^2\left(1 + \ln\dfrac{2a}{a-b}\right) & b \rightarrow a \end{cases}$$
$$R_a = \frac{\rho\omega d_v}{2ad}\frac{a-b}{b}\left(1 + \frac{a^2 - b^2}{\pi a b} \ln\frac{a+b}{a-b}\right) \tag{9.1.28}$$
$$\rightarrow \begin{cases} \dfrac{\rho\omega d_v}{2bd}\dfrac{2+\pi}{\pi} & d_v \ll b \ll a \\ \dfrac{\rho\omega d_v}{2ad}\dfrac{a-b}{b} & b \rightarrow a \end{cases}$$

Both L_a and R_a vanish when $a = b$ (i.e., when there is no change in width). When b is much smaller than a, both L_a and R_a are fairly large since the excess velocity at shoulder C becomes large. The resistance increases as the inverse of b, whereas the inductance increases only as the logarithm of $a/4b$. Since the angle at c is only 90° (instead of the 180° at the edge of the plates of Figs. 9.5 and 9.6), the integral of $(u_{\tan})^2$ does not diverge, and we need not introduce the minimal radius of curvature h.

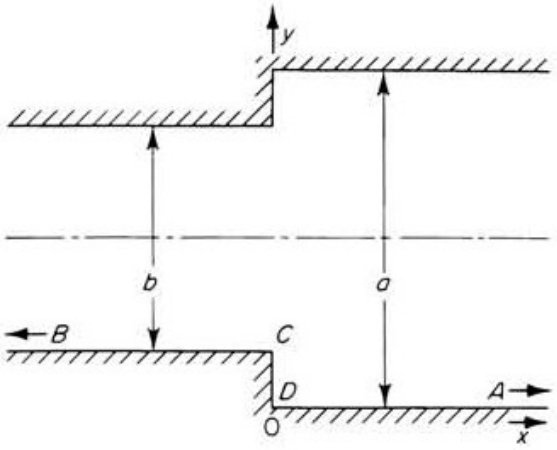


FIGURE 9.7
Section of a rectangular duct with sudden change of width in the y direction.

Acoustical circuits

Returning to Fig. 9.4, the effective impedance of opening A, which allows energy to escape from the duct, would be a combination of the local mass and viscous loads, represented by Eqs. (9.1.22) and (9.1.23), and the radiation impedance of the opening, represented by the functions $\theta_0 - i\chi_0$ used in Eq. (9.1.9) and plotted in Fig. 7.9 (or else the impedance corresponding to the α_p, β_p marked "unflanged" in Fig. 9.1). Since reactance χ_0 corresponds to the mass load outside the hole, the reactance of Eq. (9.1.22) should be divided by 2, to represent only the concentration of flow inside the duct, near the hole. Therefore the analogous impedance of opening A of Fig. 9.4 is

$$\begin{aligned} Z_A &= R_A - i\omega L_A \qquad L_A \simeq \frac{\rho}{S_A}\left[\tfrac{1}{8}D_A + \frac{\lambda}{2\pi}\chi_0\left(2k\sqrt{\frac{S_A}{\pi}}\right)\right] \\ R_A &\simeq \frac{\rho c}{S_A}\left[\tfrac{1}{8}kd_v \ln\left(\frac{4S_A}{\pi h_A{}^2}\right) + \theta_0\left(2k\sqrt{\frac{S_A}{\pi}}\right)\right] \end{aligned} \tag{9.1.29}$$

where $k = \omega/c = 2\pi/\lambda$; S_A and D_A are the area and perimeter, respectively, of the opening A; h_A is the half-thickness of the duct wall; and θ_0, χ_0 are the functions shown in Table IX, with argument $w = 2k\sqrt{S_A/\pi}$.

The impedance of opening B is, of course, $R_B - i\omega L_B$, where

$$L_B \simeq \frac{\rho D_B}{4S_B} \qquad R_B \simeq \frac{\rho c k d_v}{8S_B} \ln \frac{4S_B}{\pi h_B{}^2}$$

unless B is a slit, extending from one side of the duct to the other, in which case Eqs. (9.1.26) and (9.1.27) can be used, with d and b equaling the length and width, respectively, of the slit, and a equaling the cross-sectional area of the duct S divided by d (that is, $S = ad$). All these formulas are valid only as long as the wavelength of the sound is considerably longer than the square root of the cross-sectional area of the duct, S.

The opening C and volume D of Fig. 9.4 constitute a resonating acoustical system, called a *Helmholtz resonator*. The analogous elements C_D,

R_C, and L_C are given in Eqs. (9.1.21), (9.1.22), and (9.1.23). The resonance frequency is $\omega_0/2\pi$, where

$$\omega_0 = \frac{1}{\sqrt{L_C C_D}} \simeq 2c\sqrt{\frac{S_C}{D_C V_D}} \tag{9.1.30}$$

The Q of the resonator [Eq. (2.2.4)] is

$$Q = \sqrt{\frac{\omega L_C}{R_C}} \simeq \left[\frac{2D_C}{d_v \ln (4S_C/\pi h_C^2)}\right]^{\frac{1}{2}}$$

This defines the rate of damping of free oscillations of the resonator and the width of the resonance peak. If opening C looks out into open space instead of the duct interior, the inductance and resistance of the analogous circuit will be given by Eqs. (9.1.29), since radiation resistance must be added. The resonance frequency is then the solution of the implicit equation

$$\omega_0 \simeq 2c\sqrt{\frac{S_C}{D_C V_D}}\left[\tfrac{1}{2} + \frac{8}{D_C}\sqrt{\frac{S_C}{\pi}}\frac{1}{w_0}\chi_0(w_0)\right]^{-\frac{1}{2}} \qquad w_0 = 2\frac{\omega_0}{c}\sqrt{\frac{S_C}{\pi}}$$

and the Q of the resonator will be

$$Q \simeq \left[\frac{\chi_0(w_0) + w_0(D_C/16)\sqrt{\pi/S_C}}{\theta_0(w_0) + w_0(d_v/16)\sqrt{\pi/S_C}\ln (4S_C/\pi h_C^2)}\right]^{\frac{1}{2}}$$

which is smaller than the Q of Eq. (9.1.30), since it is reduced by the added radiation resistance.

Periodic structures

The acoustical elements can, finally, be arranged sequentially to form a filter network. For example, a duct with equally spaced constrictions, as shown in Fig. 9.8, is equivalent to a network of series inductances and shunt capacitances, making a low-pass filter. The equations of motion for flow through the nth constriction are

$$p_n - p_{n+1} = (R_a - i\omega L_a)U_n = Z_a U_n$$

for low frequencies, where R_a and L_a are given by Eqs. (9.1.22) and (9.1.23),

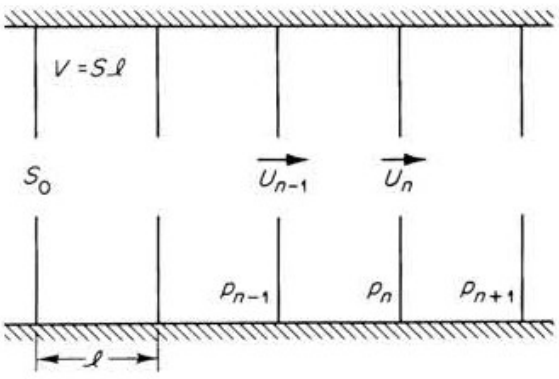


FIGURE 9.8
Acoustical low-pass filter circuit.

or else (9.1.26) and (9.1.27), if the opening is a slit. The equation of continuity, relating the compressibility times the pressure change in the $(n+1)$st enclosure to the net influx to this volume, is

$$U_n - U_{n+1} = \kappa V \frac{\partial p_{n+1}}{\partial t} = -i\omega C_a p_{n+1}$$

where C_a is given in Eq. (9.1.21).

Expressing U_{n+1} and p_{n+1} in terms of U_n and p_n, we have

$$\begin{aligned} p_{n+1} &= p_n - Z_a U_n \\ U_{n+1} &= i\omega C_a p_n + (1 - i\omega C_a Z_a) U_n \end{aligned} \tag{9.1.31}$$

For wave motion propagated in the positive n direction, p_{n+1} and U_{n+1} must both be a constant factor times p_n and U_n, respectively. If we write this factor $e^{i\Phi}$, the real part of Φ will be the phase change from element to element in a simple-harmonic wave, and the imaginary part will measure the attenuation of the wave. Solving Eq. (9.1.31), with $p_{n+1} = e^{i\Phi} p_n$ and $U_{n+1} = e^{i\Phi} U_n$, we find that

$$e^{i\Phi} = 1 - \tfrac{1}{2} i\omega C_a Z_a \pm \sqrt{-i\omega C_a Z_a - \tfrac{1}{4}(\omega C_a Z_a)^2}$$

or

$$\cos\Phi = 1 - \tfrac{1}{2} i\omega C_a Z_a = 1 - \frac{1}{2}\left(\frac{\omega}{\omega_0}\right)^2 - \frac{1}{2} i \left(\frac{\omega}{\omega_0 Q^2}\right) \tag{9.1.32}$$

where

$$\omega_0^2 = \frac{1}{L_a C_a}, \qquad \text{and} \qquad Q^2 = \frac{\omega_0 L_a}{R_a} = \left(\frac{1}{R_a}\right)\sqrt{\frac{L_a}{C_a}}.$$

The real and imaginary parts of Φ can be determined graphically from Plate III.

For frequencies considerably below the resonance frequency $\omega_0/2\pi$, the relation

$$\Phi \simeq \frac{\omega}{\omega_0} + \frac{1}{2} i \frac{1}{Q^2} \simeq \frac{l\omega}{2c}\sqrt{\frac{SD_0}{S_0 l}} + i\frac{d_v \omega}{16c}\sqrt{\frac{S_0 D_0}{Sl}} \tag{9.1.33}$$

is valid. It provides a basis for calculating the wave velocity and attenuation in the filter sequence. Since the pressure in the nth enclosure, roughly, a distance $x = nl$ from the beginning, is $P_0 e^{in\Phi}$, the pressure a distance x from the beginning is

$$P_0 e^{ix\Phi/l} \simeq P_0 \exp\left[i\omega\left(\frac{x}{2c}\sqrt{\frac{SD_0}{S_0 l}} - t\right) - \frac{x}{l}\frac{kd_v}{16}\sqrt{\frac{S_0 D_0}{Sl}}\right]$$

$$\text{for } \omega \ll \omega_0 \qquad Q \gg 1 \tag{9.1.34}$$

where S = cross-sectional area of duct
l = distance between successive constrictions
S_0 = area of constricted opening
D_0 = perimeter of opening

Thus we see that the effective phase velocity c_φ of the wave along the network, and the damping constant γ, the inverse of the distance within which the amplitude decreases by a factor e^{-1}, are

$$c_\varphi \simeq c\sqrt{\frac{4S_0 l}{SD_0}} \qquad \text{and} \qquad \gamma \simeq \frac{kd_v}{16}\sqrt{\frac{S_0 D_0}{Sl}}$$

As the driving frequency is increased to $\omega_0/2\pi$ and greater, these formulas are no longer valid, and one must solve Eq. (9.1.32) graphically or numerically. A sudden change comes at the frequency ω_0/π, particularly when $Q \gg 1$. For at driving frequencies greater than ω_0/π, the real part of $\cos \Phi$ is less than -1, and the imaginary part of Φ, which had been small for $\omega < 2\omega_0$, now increases rapidly with frequency.

$$\Phi \simeq \pi + i \cosh^{-1}\left[\frac{1}{2}\left(\frac{\omega}{\omega_0}\right)^2 - 1\right] \qquad \omega > 2\omega_0 \qquad Q^2 \gg 1 \qquad (9.1.35)$$

Each enclosure oscillates out of phase with its neighbors, and the wave is rapidly damped out with increasing n. Above this cutoff frequency ω_0/π, true wave motion is impossible.

Other sequential acoustical circuits can be devised, to act as high-pass or bandpass filters. The details will be left to the problems.

9.2 HIGHER MODES IN DUCTS

It is possible to consider a sound wave in a pipe as a one-dimensional wave, somewhat like a wave in a string, only when the wavelength of the sound transmitted is much longer than the transverse dimensions of the pipe. This limiting case was dealt with in detail in the preceding section; it is now time to take up the higher-frequency waves, where this simplification is not valid. In addition to the fundamental wave, traveling in the axial direction and having wavefronts which are uniform across the duct cross section, there are waves which reflect back and forth from the duct walls as they travel along, for which the pressure distribution is not uniform across the duct.

These higher modes of wave transmission have phase velocities which are greater than the velocity $c = \sqrt{1/\kappa\rho}$ of sound in free space. As the frequency is decreased, the phase velocity of each higher mode increases, to become infinite at some cutoff frequency, characteristic of the mode considered. Below the cutoff, true transmission cannot take place for this mode; the wave attenuates rapidly. Thus, at low frequencies, only the plane wave, the fundamental mode, is transmitted. At higher frequencies some of the higher modes also are propagated, and these additional waves must be included in our calculations.

Internal reflections and higher modes

Thus we can consider a wave inside the duct as a combination of plane-wave components, incident on and reflecting from the duct walls. When the wavelength $\lambda = 2\pi c/\omega$ in free space is small enough, in addition to the plane wave traveling in the direction of the tube axis, there will be other waves, which reflect from side to side as they travel along. They cannot strike the sides at any angle; the incidence must be such as to avoid destructive interference between successively reflected waves.

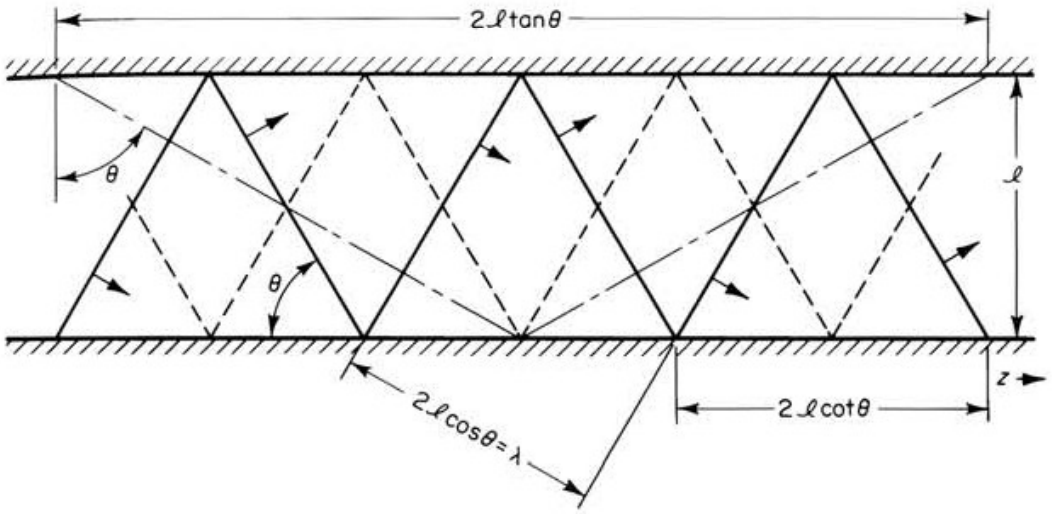


FIGURE 9.9
Reflected-wave components making up the first higher mode propagating between two parallel plates. Solid lines represent pressure maxima of the component wave; dotted lines, pressure minima. Arrows, representing direction of propagation of the components, are normal to the wavefronts.

To illustrate these points we first consider a two-dimensional model, that of wave motion between plane parallel plates, as shown in Fig. 9.9. Reference to Eq. (6.3.5) indicates that if the duct surfaces are rigid, the phase of the incident and reflected waves must be equal at the plate surface, maximum coinciding with maximum and minimum with minimum. If the alternate reinforcements are a single wavelength apart, so that $2l \cos\theta = \lambda$, as shown, the wave is the first transverse mode; if they are m wavelengths apart, so that $2l \cos\theta = m\lambda$, the wave is the mth transverse mode. The wave for $\theta = \frac{1}{2}\pi$ $(m = 0)$ is, of course, the fundamental mode. Thus the distance between successive maxima on the sides of the duct is

$$\frac{2l}{m} \cot\theta = \frac{\lambda}{\sqrt{1 - (m\lambda/2l)^2}}$$

and since $\omega/2\pi = c/\lambda$ of them must pass a given point in a second, the speed

of the mth mode down the duct is

$$\text{Phase velocity } c_\varphi = \frac{c}{\sin\theta_m} = \frac{c}{\sqrt{1-(m\lambda/2l)^2}}$$
$$\text{Angle of incidence} = \theta_m = \cos^{-1}\frac{m\lambda}{2l} = \cos^{-1}\frac{\pi mc}{\omega l} \tag{9.2.1}$$

The maximum λ for the mth mode, corresponding to $\theta_m = 0°$, is $\lambda_m = 2l/m$. At the frequency $\omega_m/2\pi = mc/2l$, corresponding to this maximum λ, the phase velocity of the mth mode is infinite; below this mth *cutoff frequency* the mth mode cannot propagate along the tube. Finally, by noting where pressure maxima cross pressure minima of the reflected waves, we can convince ourselves that the mth mode has m nodal surfaces (where p is zero) parallel to the duct axis.

This same geometrical analysis can also provide an approximate answer when the acoustic admittance of the walls is not zero. For example, in the case of the parallel plates of Fig. 9.9, if the lower plate has specific acoustic admittance β_1 and the upper one has admittance β_2 (with $\beta = \xi - i\sigma$ in both cases), then Eq. (6.3.5) indicates that at each reflection the wave is changed in amplitude and phase by the factor

$$C_{sm} = \frac{1-(\beta_s/\cos\theta_m)}{1+(\beta_s/\cos\theta_m)} \simeq \exp\frac{-2\xi_s + 2i\sigma_s}{\sqrt{m\lambda/2}} \qquad \text{if} \qquad m\lambda \gg 4l\,|\beta_s| \tag{9.2.2}$$

the subscript s being 1 for reflection from the lower plate, and 2 for reflection from the upper plate. For $m\lambda \gg |4l/\beta_s|$, the formula for θ_m in Eqs. (9.2.1) is still valid. Thus, at each reflection, the amplitude of the wave is reduced by a factor roughly equal to $\exp(-2\xi_s/\cos\theta_m)$, and the phase of the wave is advanced by $2\sigma_s/\cos\theta_m$ radians, so that incident maxima do not exactly coincide with reflected maxima at the sides of the duct.

Since in two reflections, one from each side, the acoustic ray has progressed a distance $2l\tan\theta_m$ down the duct, the attenuation of the wave per unit distance is given by the factor

$$\exp\left(-\frac{2\xi_1+2\xi_2}{\cos\theta_m}\frac{1}{2l\tan\theta_m}\right) = \exp\left(-\frac{\xi_1+\xi_2}{l\sin\theta_m}\right) \tag{9.2.3}$$

and the phase of the wave is advanced by $(\sigma_1+\sigma_2)/l\sin\theta_m$ radians per unit length, because of the reflections. However, even if the wall susceptances σ_1 and σ_2 were zero, the phase would be advanced in a unit length by an amount equal to the angular velocity $\omega = 2\pi c/\lambda$ divided by the phase velocity c_φ of Eqs. (9.2.1). Thus the total change of phase per unit length along the duct is, roughly, $(2\pi/\lambda)\sin\theta_m + [(\sigma_1+\sigma_2)/l\sin\theta_m]$, and the

dependence of the pressure on the distance z along the duct is via the factor

$$\exp\left\{\left[\frac{2\pi i}{\lambda}\sqrt{1-\left(\frac{m\lambda}{2l}\right)^2}+i\frac{\sigma_1+\sigma_2}{\sqrt{l^2-\frac{1}{4}m^2\lambda^2}}-\frac{\xi_1+\xi_2}{\sqrt{l^2-\frac{1}{4}m^2\lambda^2}}\right]z\right\} \quad (9.2.4)$$

when $|\beta| \ll m\lambda/4l$. Compare these results with the exact solution, Eqs. (9.2.14) and (9.2.16).

An approximate answer is all we can expect from this mixture of wave and geometrical acoustics. Furthermore, the effect of reflections, when the duct walls are not planes, is not easily computed this way. On both counts it is desirable to work out the exact solution for a wave traveling along the inside of a uniform duct.

General formulas for transmission

We set the z axis parallel to the axis of the duct. The interior cross section, parallel to the xy plane, is some area S, bounded by a perimeter D, the intersection of the cross-sectional plane and the inner duct surface. The wave equation for simple-harmonic waves

$$\left(\frac{\partial^2}{\partial x^2}+\frac{\partial^2}{\partial y^2}+\frac{\partial^2}{\partial z^2}\right)p+\left(\frac{\omega}{c}\right)^2 p=0 \quad (9.2.5)$$

thus allows the z factor to be separated off, $p=\Psi(x,y)e^{ik_z z}$, where we have, as usual, omitted the time-dependent factor $e^{-i\omega t}$. The equation for the transverse factor Ψ is then

$$\left(\frac{\partial^2}{\partial x^2}+\frac{\partial^2}{\partial y^2}\right)\Psi+\varkappa^2\Psi=0 \qquad \left(\frac{\omega}{c}\right)^2=k^2=k_z{}^2+\varkappa^2 \quad (9.2.6)$$

Note that the $\varkappa$ of this section is *not* the compressibility κ.

This equation for Ψ is the same as Eq. (5.2.3) for the vibrations of a membrane, except that now it is for a factor of the pressure, instead of transverse displacement. As with the earlier problem, the solutions which fit the appropriate boundary conditions occur only for a discrete set of values of the constant $\varkappa$, these values being called characteristic values (or eigenvalues), and the corresponding solutions Ψ being called characteristic functions (or eigenfunctions). Since the boundary conditions in the present case differ from that for the membrane, the functions and values differ in the two cases, but many of the general properties are the same.

For the membrane within rigid boundaries, the displacement has to be zero along the perimeter. For a duct with rigid walls, the fluid velocity normal to the surface wall must be zero. Since the vector velocity is related to the pressure according to the equation

$$u=\frac{1}{i\rho ck}\operatorname{grad} p \qquad \omega=ck$$

the boundary condition for rigid walls is that the component of grad Ψ, normal to the perimeter (which we can write $\partial\Psi/\partial n$), be zero at every point on the perimeter.

On the other hand, if the duct walls are locally reactive to the pressure, so that we can ascribe to the surface an acoustic impedance $z = p/u_n$ or a specific acoustic admittance $\beta = \xi - i\sigma = \rho c/z$, then the boundary condition, to be satisfied everywhere on the perimeter, is

$$\frac{\partial\Psi}{\partial n} = ik\beta\Psi \qquad k = \frac{\omega}{c} \tag{9.2.7}$$

where the normal is directed into the wall, away from the interior of the duct. The discrete set of eigenvalues of $\varkappa$ for which this boundary condition is satisfied may, for simplicity, be distinguished from each other by the index number n (though we shall see later that it is often more convenient to use a pair of index numbers). The characteristic function satisfying boundary condition (9.2.7), corresponding to $\varkappa_n$, will be denoted $\Psi_n(x,y)$.

If the impedance of the duct surface is purely reactive, so that β is pure-imaginary, the eigenvalues $\varkappa_n$ will all be real numbers. If, however, β has a real part, then $\varkappa_n$ will have a negative-imaginary part (as will be demonstrated later), and thus the wavenumber $k_z \equiv k_n = [(\omega/c)^2 - \varkappa_n^2]^{\frac{1}{2}}$ for this mode will have a positive-imaginary part. The corresponding characteristic functions Ψ_n have the same general orthogonality properties as indicated in Eqs. (5.2.16) and (5.2.26). These general properties can be summarized as follows:

$$p_\omega = \sum_n A_n\Psi_n(x,y)e^{ik_nz - i\omega t}$$

$$\left(\frac{\partial^2}{\partial x^2} + \frac{\partial^2}{\partial y^2}\right)\Psi_n \equiv \nabla_2^2\Psi_n = -\varkappa_n^2\Psi_n$$

Ψ_n satisfies Eq. (9.2.7) along the perimeter D,

$$k_n \equiv \frac{2\pi}{\lambda_n} + i\pi\gamma_n = \sqrt{\left(\frac{\omega}{c}\right)^2 - \varkappa_n^2} \tag{9.2.8}$$

$$\iint_S \Psi_n\Psi_m\,dx\,dy = \begin{cases} 0 & m \neq n \\ S\Lambda_n & m = n \end{cases}$$

where the subscript 2 is used to specify that the Laplace operator ∇_2^2 is for the two-dimensional area of cross section. The complex dimensionless factor Λ_n is the mean value of Ψ_n^2 averaged over the duct cross section S. Note that if the duct surface is *not* locally reactive, the β of Eq. (9.2.7) will depend on m and the set of functions Ψ_m will *not* be mutually orthogonal.

The separation of k_n into its real and imaginary parts shows that the wavelength along the duct axis of the nth mode is λ_n, and thus that its phase velocity is $c_n = \omega\lambda_n/2\pi$, and that the pressure amplitude attenuates by a factor of e^{-1} in a distance $1/\pi\gamma_n$. Since $|\varkappa_n|$ increases as n increases, we note that λ_n tends to decrease as n increases. Therefore, for any specified frequency, there is a value of n for which $\text{Re}\,\varkappa_n^2 < (\omega/c)^2 < \text{Re}\,\varkappa_{n+1}^2$. At this frequency the imaginary part of k_n, for all values of n greater than this, is much larger than the imaginary parts for smaller n's, indicating that all these higher modes are strongly attenuated. To put it another way, each mode has a *cutoff frequency* c/λ_n; for driving frequencies above this the mode propagates along the duct with (usually) quite small attenuation, but for driving frequencies less than this the attenuation is very large, so large that the mode cannot be said to propagate as a wave.

When the duct walls are rigid ($\beta = 0$), the lowest eigenvalue $\varkappa_0$ is zero, for which $\Psi_0 = 1$, so that $\Lambda_0 = 1$. This is the fundamental mode; when $\beta = 0$, its phase velocity is c, the velocity of sound in free space; it propagates as a plane wave. For frequencies below the cutoff frequency of the lowest higher mode (i.e., when $\omega < 2\pi c/\lambda_1$), only this fundamental mode is propagated without attenuation (if $\beta = 0$); all higher modes are strongly attenuated. (This is the justification of the assumptions made in Sec. 9.1.) As ω is increased, when it becomes larger than $2\pi c/\lambda_1$, the first higher mode also propagates with zero attenuation (if $\beta = 0$), though at a phase velocity higher than c. And so on; as the frequency is increased, successively higher modes can be transmitted along the duct, and the phase velocity of each decreases, coming closer to the constant value c of the fundamental mode. Compare this with the discussion of Eqs. (9.2.1); the quantity $\varkappa_n$ replaces the quantity $\pi m/l$ of the simple model, and for $\beta = 0$, the effective angle of incidence θ_n of the simple model is equivalent to $\cos^{-1}(\varkappa_n c/\omega)$ of the exact solution.

This same behavior is also true when the specific admittance β is not zero but is pure-imaginary, except that here the phase velocity of even the fundamental mode differs from c; all modes exhibit dispersion, as discussed on page 477. If the specific conductance ξ of the duct walls is not zero, all modes are attenuated at all frequencies, and thus the distinction between no attenuation above the cutoff frequency and no transmission below it becomes less clear-cut. As long as ξ is small compared with unity, however, it still is true that above its cutoff frequency the attenuation of the nth mode is slight; below it the mode is sharply attenuated.

We should also mention that, unless the tube is very narrow, the surface effects of thermal conduction and viscosity may be expressed in terms of the equivalent surface admittance

$$\beta_s \simeq (1 - i)\left[(\gamma - 1)kd_h + \left(\frac{k_t}{k}\right)^2 kd_v\right]$$

of Eq. (6.4.36) (see also page 292), which may be added to the admittance of the surface itself to obtain the β of Eq. (9.2.7). We shall show later, for various duct shapes, how to compute the value of the ratio (k_t/k) for each mode. Calculation of the effects in a very narrow circular tube will be given at the end of this section.

Dispersion of the higher modes

Thus we see that wave propagation, for all modes except the fundamental mode in a duct with rigid walls (and neglecting thermal and viscous effects), is dispersive in the sense of the discussion of page 477. For a duct with rigid walls, the phase velocity of the nth mode is

$$c_\varphi = \frac{\omega}{k_n} = \frac{c}{\sqrt{1 - (c\varkappa_n/\omega)^2}}$$

where c is the velocity of sound in free space. Below the cutoff frequency $c\varkappa_n/2\pi$, the phase velocity is imaginary, indicating no propagation. Just above the cutoff frequency the phase velocity is very large and real, and as $\omega \to \infty$, c_φ approaches c from above. The group velocity, for a group of waves centering at frequency $\omega_a/2\pi$, is, according to Eq. (9.1.18),

$$c_g = \left(\frac{\partial k_n}{\partial \omega}\right)^{-1} = c\sqrt{1 - \left(\frac{c\varkappa_n}{\omega_a}\right)^2} = \frac{c^2}{c_\varphi}$$

which is less than c for the frequencies above the cutoff.

The signal velocity $c_\varphi(\infty)$ is c, in spite of the fact that the phase velocity is greater than c for all frequencies for which the wave transmits. For example, by use of Eq. (9.1.20) and an extended table of Fourier transforms, we can show that a delta-function pulse, for the nth mode, started at $z = 0$ at $t = 0$, becomes the wave

$$p = \frac{1}{2\pi}\Psi_n(x,y)\int_{-\infty}^{\infty} \exp\left[i\frac{z}{c}\sqrt{\omega^2 - (\varkappa_n c)^2} - i\omega t\right] d\omega$$

$$= \Psi_n(x,y)\left\{\delta\left(t - \frac{z}{c}\right) - u\left(t - \frac{z}{c}\right)\varkappa_n z\frac{J_1[\varkappa_n c\sqrt{t^2 - (z/c)^2}]}{\sqrt{t^2 - (z/c)^2}}\right\}$$

a time t later (where u is the unit step function). The pulse, represented by the $\delta(t - z/c)$ term, travels with the free-space velocity c; trailing behind it is a "wake," represented by the second term. Although the dispersive propagation spreads out the wave behind the pulse, nothing reaches the observer at z until time z/c, when the pulse arrives.

For ducts with nonrigid walls even the fundamental mode is dispersive, and the expressions for phase and group velocities are more complicated than the ones just discussed; but as long as the duct walls have stiffness and mass, the signal velocity $c_\varphi(\infty)$ is equal to the free-space value c.

Generation of sound in a duct

Sound can be generated by placing a vibrating piston at one end of the duct. Suppose the duct extends from $z = 0$ to $z = \infty$, and suppose the driving surface at $z = 0$ has velocity in the z direction, at point x, y on its surface, equal to $U(x,y)e^{-i\omega t}$. As with Eq. (5.2.17), we use the properties of the eigenfunctions given in Eqs. (9.2.8) to work out the series expansions for the wave in the duct.

$$u_z = \frac{1}{i\rho\omega}\frac{\partial p}{\partial z} = \sum_n U_n \Psi_n e^{ik_n z - i\omega t} \qquad U_n = \frac{1}{S\Lambda_n}\iint_S U(x,y)\Psi_n \, dx\, dy$$
$$p = \rho c \sum_n \frac{\omega}{ck_n} U_n \Psi_n e^{ik_n z - i\omega t} = \rho c \sum_n \left[1 - \left(\frac{c\varkappa_n}{\omega}\right)^2\right]^{-\frac{1}{2}} U_n \Psi_n e^{ik_n z - i\omega t} \tag{9.2.9}$$

All modes are present (unless U_n is identically zero) close to the driving surface, but those modes having cutoff frequencies greater than $\omega/2\pi$ die out rapidly, leaving only the lower modes to transmit energy any appreciable distance along the tube. The wave cannot transmit all the details of the piston motion, as represented by the function $U(x,y)$; fine detail of dimensions smaller than $\lambda = 2\pi c/\omega$ is lost in transmission.

If the duct wall is rigid and we neglect thermal and viscous losses at the walls, the lowest characteristic function is $\Psi_0 = 1$, and $\varkappa_0$ is zero, as mentioned earlier. Thus, by the last of Eqs. (9.2.8), the integrals $\iint \Psi_n \, dx\, dy$, for all $n > 0$, are zero. In this case, if the driving surface at $z = 0$ is a perfect piston, with velocity U independent of x and y, U_0 will equal U, all U_n for $n > 0$ will be zero, and the propagated wave

$$u_z = Ue^{i(\omega/c)z - i\omega t} \qquad p = \rho c U e^{i(\omega/c)z - i\omega t}$$

will be the plane wave discussed in Sec. 9.1, with constant ratio between pressure and velocity. If the driving surface is not a perfect piston, however, some of the higher modes will be excited, and the ratio between p and u_z at the driving surface will not be exactly ρc. In fact, for those modes for which $\varkappa_n > k$, k_n will be positive-imaginary and the radical in the sum for p will be imaginary.

$$\rho c\left[1 - \left(\frac{c\varkappa_n}{\omega}\right)^2\right]^{-\frac{1}{2}} = \frac{\rho\omega}{k_n} = -i\omega\rho\left[\varkappa_n^2 - \left(\frac{\omega}{c}\right)^2\right]^{-\frac{1}{2}}$$

and the corresponding radiation impedance at the driving surface will contain a mass-reactance term.

If the duct walls are not perfectly rigid, or if thermal and viscous effects at the surface are not neglected, some of the higher modes will be excited, even if the driving surface is a perfect piston. For in this case Ψ_0 will be a function of x and y, and therefore the integrals $\iint \Psi_n \, dx\, dy$ $(n > 0)$ will not be zero, and the radiation impedance will have reactive terms even for a perfect piston. This effect will be accentuated if the driving frequency happens to be just below some cutoff frequency, so that the factor $[\varkappa_n^2 - (\omega/c)^2]^{-\frac{1}{2}}$ is large for that n.

The Green's function

If the sound generator is a simple source, at point x_0, y_0, z_0 within a duct which extends from $z = -\infty$ to $z = +\infty$, the resulting wave can be computed from the Green's function for an infinite duct, the solution of the equation

$$\left[\frac{\partial^2}{\partial x^2} + \frac{\partial^2}{\partial y^2} + \frac{\partial^2}{\partial z^2} + \left(\frac{\omega}{c}\right)^2\right] g_\omega(x,y,z \mid x_0,y_0,z_0) = -\delta(x - x_0)\,\delta(y - y_0)\,\delta(z - z_0)$$

which satisfies the boundary conditions of Eq. (9.2.7). It can be expressed in terms of a series of the eigenfunctions Ψ_n.

$$g_\omega = \sum_n F_n(z)\Psi_n(x,y)$$

Insertion in the differential equation, multiplication by Ψ_n, and integration of both sides over S results in a set of equations

$$\left(\frac{d^2}{dz^2} + k_n^2\right)F_n = -\frac{\Psi_n(x_0,y_0)}{S\Lambda_n}\,\delta(z - z_0) \qquad k_n^2 = \left(\frac{\omega}{c}\right)^2 - \varkappa_n^2$$

Reference to the derivation of Eq. (4.4.11) from Eq. (4.4.9) shows that

$$F_n = \frac{i\Psi_n(x_0,y_0)}{2k_nS\Lambda_n}\exp\left(ik_n\,|z - z_0|\right)$$

where, when $\operatorname{Re}\varkappa_n^2 > (\omega/c)^2$, k_n must equal i (not $-i$) times the radical $[\varkappa_n^2 - (\omega/c)^2]^{\frac{1}{2}}$ in order that the higher modes attenuate, rather than augment, with increasing values of $|z - z_0|$.

Thus the Green's function for the infinite duct is

$$g_\omega(x,y,z \mid x_0,y_0,z_0) = \frac{i}{2S}\sum_n \frac{\Psi_n(x,y)\Psi_n(x_0,y_0)}{\Lambda_n k_n}\exp\left(ik_n\,|z - z_0|\right) \qquad (9.2.10)$$

As mentioned before, if we can assume that the duct walls are rigid, $\varkappa_0 = 0$ and $\Psi_0 = 1$, the eigenvalues $\varkappa_n$ are real, nonnegative quantities, and the Ψ_n's are real, satisfying the condition $\partial\Psi/\partial n = 0$ along the perimeter of S. In this case we can separate the attenuated upper modes (for which $n > N$, where $\varkappa_N < \omega/c < \varkappa_{N+1}$) from the propagated upper modes for $n \leqslant N$.

$$g_\omega = \frac{ic}{2\omega S}e^{i(\omega/c)|z-z_0|} + \frac{i}{2S}\sum_{n=1}^{N}\frac{\Psi_n(x,y)\Psi_n(x_0,y_0)}{\Lambda_n k_n}e^{ik_n|z-z_0|} + \frac{1}{2S}\sum_{n=N+1}^{\infty}\frac{\Psi_n(x,y)\Psi_n(x_0,y_0)}{\Lambda_n K_n}e^{-K_n|z-z_0|} \qquad (9.2.11)$$

$$k_n = \sqrt{\left(\frac{\omega}{c}\right)^2 - \varkappa_n^2} \qquad K_n = \sqrt{\varkappa_n^2 - \left(\frac{\omega}{c}\right)^2}$$

This series looks very different from the simple expression $(1/4\pi R)e^{ikR}$ of Eq. (7.1.6) for the Green's function in free space. Indeed it is; the

reflections from the duct walls have so modified the wave that the radiated energy is channeled outward only along the $\pm z$ axis, instead of going out in all directions. Of course, if the source point is a large number of wavelengths away from the nearest portion of the duct wall, the interior of the duct will look almost like free space to the source. In this limiting case, when N is very large, k_n will be real for a large number of terms in the series. Physical intuition thus tells us that, for x, y, z close to $x_0, y_0, z_0\,(R < \lambda)$, the series of Eq. (9.2.10) approaches $(1/4\pi R)e^{ikR}$ when the driving frequency is larger than the cutoff frequencies of a large number of modes of the duct. This can be proved mathematically, though the manipulations required are too lengthy to go into here.

Impedance of a simple source

When the wavelength is roughly the same size as the transverse dimensions of the duct, the radiated pressure wave is appreciably different from the free-space Green's function, even in the region close to the source point. In this case the presence of the duct walls appreciably modifies the reaction of the medium back on the simple source, even more than the presence of a nearby plane surface [Eq. (7.4.14)]. To show this more specifically, we suppose the sound generator to be a simple source, of strength S_ω (not to be confused with S, the cross-sectional area of the duct) and of driving frequency $\omega/2\pi$, of the sort discussed in Sec. 7.1. The pressure wave inside a duct with rigid walls and outside the sphere of radius $R = a[R^2 = (x - x_0)^2 + (y - y_0)^2 + (z - z_0)^2]$ is $-i\omega\rho S_\omega g_\omega(\mathbf{r}_0 + \mathbf{R} \mid \mathbf{r}_0)$. For wavelengths of the same size as the duct dimensions, or longer, ω/c is smaller than $\varkappa_n$ for all but the first N modes, with N small, and all but a few of the terms in series (9.2.11) are nearly equal to

$$\frac{1}{2S\varkappa_n\Lambda_n}\Psi_n(x,y)\Psi_n(x_0,y_0)e^{-\varkappa_n|z-z_0|} \qquad n > N$$

It is possible to show that, close to the source point,

$$\frac{1}{4\pi R} \to -\frac{|z - z_0|}{2S} + \frac{1}{2S}\sum_{n=1}^{\infty}\frac{\Psi_n(x,y)\Psi_n(x_0,y_0)}{\Lambda_n\varkappa_n}e^{-\varkappa_n|z-z_0|} \qquad \text{as } R \to 0$$

For the longer wavelengths (N small), therefore, the terms in series (9.1.11, for $n > N$ are approximately equal to the corresponding terms in the series for $1/4\pi R$, for R small.

Adding and subtracting this comparison series, we finally obtain an approximate formula for g_ω, valid for the longer wavelengths.

$$g_\omega \simeq \left[\frac{1}{4\pi R} + \frac{i}{2Sk}e^{ik|z-z_0|} + \frac{|z - z_0|}{2S} + \sum_{n=1}^{N}\frac{\Psi_n(x,y)\Psi_n(x_0,y_0)}{2S\Lambda_n}\left(\frac{ie^{ik_n|z-z_0|}}{k_n} - \frac{e^{-\varkappa_n|z-z_0|}}{\varkappa_n}\right)\right]e^{-i\omega t}$$

The mean pressure $-i\omega\rho g_\omega$ on the small sphere of radius a of the source is, approximately,

$$P_s \simeq \frac{\rho\omega}{2S}\left\{\frac{-iS}{4\pi a} + \frac{1}{k} + \sum_{n=1}^{N}\frac{[\Psi_n(x_0,y_0)]^2}{\Lambda_n}\left(\frac{1}{k_n} + \frac{i}{\varkappa_n}\right)\right\} S_\omega e^{-i\omega t}$$

The fluid flux at the surface of the sphere is, by definition,

$$S_\omega(1 - ika)e^{ika - i\omega t} \simeq S_\omega e^{-i\omega t}$$

Therefore the limiting forms for the mechanical force, velocity, and impedance of a simple source in a duct are

$$F_s \simeq \left\{-i\rho\omega a\left[1 - \frac{2\pi a}{S}\sum_{n=1}^{N}\frac{\Psi_n^2(x_0,y_0)}{\Lambda_n\varkappa_n}\right] + \rho c\,\frac{2\pi a^2}{S}\left[1 + \sum_{n=1}^{N}\frac{k\Psi_n^2(x_0,y_0)}{\Lambda_n k_n}\right]\right\} S_\omega e^{-i\omega}$$

$$U_s \simeq \frac{S_\omega}{4\pi a^2}\,e^{-i\omega t} \qquad (9.2.12)$$

$$Z_s \simeq -i\omega(4\pi\rho a^3)\left[1 - \frac{2\pi a}{S}\sum_{n=1}^{N}\frac{\Psi_n^2(x_0,y_0)}{\Lambda_n\varkappa_n}\right] + \rho c\,\frac{8\pi^2 a^4}{S}\left[1 + \sum_{n=1}^{N}\frac{k}{k_n}\,\frac{\Psi_n^2(x_0,y_0)}{\Lambda_n}\right]$$

for $ka \ll 1$ and for N small.

This is an interesting formula, particularly in comparison with Eqs. (7.1.11), the analogue for a simple source in free space. The first term in the reactive part is the same as the reactive part in Eqs. (7.1.11); the presence of the duct walls reduces the mass load on the source by a small amount, proportional to the ratio between the radius a of the source and the mean dimension $\sqrt{S}$ of the duct cross section, the exact value depending on the placement of the source.

In contrast, the resistive term in Eqs. (9.2.12) is larger than the resistance for a source in free space by the large factor $(1/ka)^2$. The radiation resistance does not go to zero as $(ka)^2$ for ka small as it does for waves spreading out radially in three dimensions; it approaches a constant value, independent of ka, as it does for plane waves moving in one direction. The first term, corresponding to the fundamental (plane-wave) mode, is equal to the radiation resistance on a plane piston of area $8\pi^2a^4/S$ (much smaller than S) radiating plane waves normal to its surface. The additional terms, one for each higher mode which propagates at the driving frequency, have a more complicated frequency dependence. When the driving frequency is just larger than the cutoff frequency of a particular mode (say, the nth one), its radiation resistance is larger than that of the fundamental mode [unless the source is at a node of the nth mode, i.e., unless $\Psi_n^2(x_0,y_0)$ is zero].

As the frequency is increased, the radiation resistance increases stepwise, each new step corresponding to a new mode becoming propagational, being introduced by a narrow peak of cross-duct resonance for that mode. The steps get closer and closer together, and the peaks get narrower and narrower and, if we average out the narrow peaks, the curve approaches the value $\rho c(4\pi a^2)k^2a^2$, which is the radiation resistance of the source in free space.

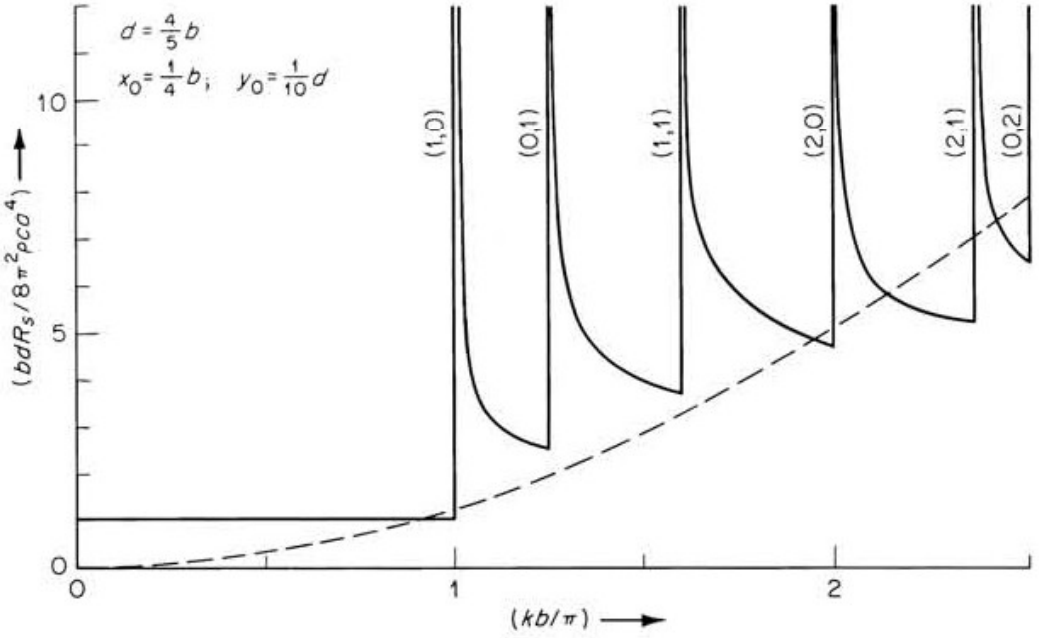


FIGURE 9.10
Radiation resistance R_s of a simple source of radius a at point x_0, y_0, 0 in a rectangular duct of sides b, d. Numbers by each peak indicate the m, n of the mode resonating. Dashed curve is radiation resistance for same source in free space.

Figure 9.10 is a plot of the real part R_s of the Z_s of Eqs. (9.2.12) for a rectangular duct of width b and depth d, with the source at x_0, y_0 as noted. The stepwise character of the curve is apparent. The dashed curve is the corresponding free-space resistance.

The impedance of a simple dipole in a duct differs even more from its counterpart in free space, as described in Eqs. (7.1.12). For example, if the dipole is oriented transverse to the duct axis, there is no radiation below the first cutoff frequency; at low frequencies the radiation impedance is purely reactive. However, the general formulas do not merit writing down here.

Rectangular ducts

To make further progress we must deal with specific forms of duct cross section. The simplest case is the rectangular duct, of breadth b in the x direction and depth d in the y direction. If the duct walls are rigid, we

choose the z axis to run along one corner of the duct, so that the boundary conditions are

$$\frac{\partial p}{\partial x} = 0 \qquad \text{at } x = 0,\ x = b \qquad \frac{\partial p}{\partial y} = 0 \qquad \text{at } y = 0,\ y = d$$

The characteristic functions and values for the transverse factors of the various modes are then

$$\Psi_{mn} = \cos\frac{\pi m x}{b}\cos\frac{\pi n y}{d} \qquad \Lambda_{mn} = \frac{1}{\epsilon_m \epsilon_n} \qquad \epsilon_m = \begin{cases} 1 & m = 0 \\ 2 & m > 0 \end{cases}$$
$$\varkappa_{mn} = \sqrt{\left(\frac{\pi m}{b}\right)^2 + \left(\frac{\pi n}{d}\right)^2} \qquad k_{mn}^2 = \left(\frac{\omega}{c}\right)^2 - \varkappa_{mn}^2 \tag{9.2.13}$$

Contrast these functions with those of Eqs. (5.2.15) for the displacement of a rectangular membrane, which must go to zero at the boundary. The fundamental mode is, of course, the $m = n = 0$ case. In the change from the two-index notation used here to the one-index notation used earlier, the particular sequence of (m,n) pairs, which will form a monotonically increasing sequence of $\varkappa_{mn}$'s, is one which depends on the value of b/d. The cutoff frequency for the (m,n)th mode is $c\varkappa_{mn}/2\pi$.

Incidentally, these results should be compared with the simple reflection model of Fig. 9.9. Since the earlier model considers reflections from one pair of planes, we should compare with the modes for $n = 0$. The phase velocity $c_\varphi = \omega/k_{mo}$ is equal to $c/\sqrt{1 - (\pi mc/\omega b)^2}$, from Eq. (9.2.13), which checks with Eq. (9.2.1) exactly. Therefore, in general, the angle of incidence on the sidewalls of the (m,n)th mode is $\cos^{-1}\sqrt{(\pi mc/\omega b)^2 + (\pi nc/\omega d)^2}$. The number of nodal surfaces (where p is zero) parallel to the x walls is m; the number parallel to the y walls is n.

If the duct walls are not rigid, but have uniform specific acoustic admittance, β_x for the two walls perpendicular to the x axis and β_y for the two y walls, then it is somewhat more convenient to run the z axis along the central line of the pipe, so that the boundary condition is

$$\frac{\partial p}{\partial x} = \pm ik\beta_x p \qquad \text{at } x = \pm\tfrac{1}{2}b \qquad \frac{\partial p}{\partial y} = \pm ik\beta_y p \qquad \text{at } y = \pm\tfrac{1}{2}d$$

In this case we must distinguish between even and odd symmetry in each direction. We set

$$\Psi_{mn} = Cs_m\left(q_m, \frac{x}{b}\right) Cs_n\left(q_n, \frac{y}{d}\right)$$

where

$$Cs_m(q_m,u) = \begin{cases} \cos(\pi q_m u) & \text{when } n = 0, 2, 4, \ldots \\ \sin(\pi q_m u) & \text{when } n = 1, 3, 5, \ldots \end{cases}$$

The boundary conditions for the x factor are met, for the even functions, by adjusting q_m so that

$$\mp \frac{\pi q_m}{b} \sin \frac{\pi q_m}{2} = \pm ik\beta_x \cos \frac{\pi q_m}{2}$$

or

$$\tfrac{1}{2}\pi q_{xm} \tan (\tfrac{1}{2}\pi q_{xm}) = -\tfrac{1}{2}i\beta_x kb \qquad \text{for } m \text{ an even integer}$$

Those for the odd functions require that q_m satisfy

$$\frac{\pi q_m}{b} \cos \frac{\pi q_m}{2} = ik\beta_x \sin \frac{\pi q_m}{2}$$

or

$$\tfrac{1}{2}\pi q_{xm} \cot (\tfrac{1}{2}\pi q_{xm}) = \tfrac{1}{2}i\beta_x kb \qquad \text{for } m \text{ an odd integer}$$

Two similar equations relate q_{yn} to β_y.

In many cases of practical interest, the wall admittance is small enough so that $\beta kb = (2\pi b/\lambda)\beta$ is considerably smaller than unity for both the x and the y walls. When this is true we can use first approximations to the solutions. For the x walls,

$m = 0$:

$$i\pi q_{x0} \equiv i\pi(\mu_{x0} - i\nu_{x0}) \simeq \sqrt{2i\beta_x kb}$$

or

$$\mu_{x0} \simeq \frac{1}{\pi} \operatorname{Im} [\sqrt{(\sigma_x + i\xi_x)2kb}] \qquad \nu_{x0} \simeq \frac{1}{\pi} \operatorname{Re} [\sqrt{(\sigma_x + i\xi_x)2kb}]$$

$m > 0$: (9.2.14)

$$iq_{xm} \equiv i\mu_{xm} + \nu_{xm} \simeq im + 2\beta_x \frac{kb}{\pi^2 m}$$

or

$$\mu_{xm} \simeq m - \frac{2\sigma_x kb}{\pi^2 m} \qquad \nu_{xm} \simeq \frac{2\xi kb}{\pi^2 m}$$

and the x factor in the characteristic function, with its normalizing factor, is

m even:

$$N_{xm} = \frac{1}{b}\int_{-b/2}^{b/2} \cos^2 \left(\frac{\pi q_{xm} x}{b}\right) dx \simeq \begin{cases} 1 + \tfrac{1}{6}(\sigma_x + i\xi_x)kb & m = 0 \\ \tfrac{1}{2} - (\sigma_x + i\xi_x)\dfrac{kb}{\pi^2 m^2} & m > 0 \end{cases}$$

$$Cs_m\left(q_{xm}, \frac{x}{b}\right) \simeq \cos \frac{\pi \mu_{xm} x}{b} + i \frac{\pi \nu_{xm} x}{b} \sin \frac{\pi \mu_{xm} x}{b}$$

m odd: (9.2.15)

$$N_{xm} = \frac{1}{b}\int_{-b/2}^{b/2} \sin^2 \left(\frac{\pi}{b} q_{xm} x\right) dx \simeq \tfrac{1}{2} + (\sigma_x + i\xi_x)\frac{kb}{\pi^2 m^2}$$

$$Cs_m\left(q_{xm}, \frac{x}{b}\right) \simeq \sin \left(\frac{\pi \mu_{xm} x}{b}\right) - i \frac{\pi \nu_{xm} x}{b} \cos \frac{\pi \mu_{xm} x}{b}$$

as long as $\beta_x kb \ll 1$. We note that, since the wall conductance must be positive, ν_{xm} is positive for all values of m.

The y factors are constructed similarly, with d instead of b in the equations, and with different values of β if it should happen that the y walls differ in admittance from the x walls. Thus the characteristic functions, their normalizing factors, and their propagation constants may be written

$$\Psi_{mn} = Cs_m\left(q_{xm}, \frac{x}{b}\right) Cs_n\left(q_{yn}, \frac{y}{d}\right) \qquad \Lambda_{mn} = N_{xm}N_{yn}$$

$$\varkappa_{mn}^2 = \left(\frac{\pi q_{xm}}{b}\right)^2 + \left(\frac{\pi q_{yn}}{d}\right)^2 \simeq \left(\frac{\pi m}{b}\right)^2 + \left(\frac{\pi n}{d}\right)^2 - \frac{2i\epsilon_m\beta_x k}{b} - \frac{2i\epsilon_n\beta_y k}{d} \tag{9.2.16}$$

$$k_{mn} \simeq k_{mn}^0 + \frac{k}{k_{mn}^0}\left(\frac{\epsilon_m\sigma_x}{b} + \frac{\epsilon_n\sigma_y}{d}\right) + i\frac{k}{k_{mn}^0}\left(\frac{\epsilon_m\xi_x}{b} + \frac{\epsilon_n\xi_y}{d}\right)$$

where $(k_{mn}^0)^2 = k^2 - (\pi m/b)^2 - (\pi n/d)^2$; the approximate formulas are for $kb\beta$ small; and as always, $\epsilon_m = 1$ when $m = 0$, $\epsilon_m = 2$ when $m > 0$.

It is interesting to note that for a two-walled duct the transmission factor would be

$$k_m \simeq k\sqrt{1 - \left(\frac{\pi m}{kb}\right)^2} + \frac{\epsilon_m(\sigma + i\xi)}{\sqrt{b^2 - (\pi m/k)^2}}$$

and therefore, to this approximation, the factor $e^{ik_m z}$ corresponds to the factor of Eq. (9.2.4), obtained from the geometrical model for the higher modes ($m > 0$, $\epsilon_m = 2$) when $\beta_1 = \beta_2 = \beta$. The reflection model, however, gave an indeterminate answer for the fundamental mode, whereas the present, more detailed analysis shows that the fundamental mode is affected just half as much ($\epsilon_0 = 1$) as are the higher modes, to this approximation.

Thus, when $|\beta|$ is small compared with the ratio between the wavelength $\lambda = 2\pi/k$ and the perimeter $2(b + d)$ of the duct, the attenuation factor $\operatorname{Im} k_{mn}$ equals the weighted mean $(\epsilon_m\xi_x/b) + (\epsilon_n\xi_y/d)$ of the specific conductances of the walls, divided by the sine of the angle of incidence, $\sin\theta_{mn} = [1 - (\pi m/kb)^2 - (\pi n/kd)^2]^{\frac{1}{2}}$. The numerator is the same (to this approximation) for all modes except those which travel parallel to a pair of walls (i.e., for which m and/or n are zero). For the fundamental ($m = n = 0$), the numerator would be $(\xi_x/b) + (\xi_y/d)$; for waves tangential to the x walls ($m = 0$, $n > 0$), it would be $(\xi_x/b) + (2\xi_y/d)$; and so on. This is, of course, true only for those waves which propagate at the frequency $\omega/2\pi$; for those modes having cutoff frequencies higher than this, k_{mn}^0 is imaginary, and no true propagation is possible.

When the duct is fitted with a piston at $z = 0$ which drives the air in the region $z > 0$, with a uniform velocity amplitude $U(x,y) = U_0$, the formulas of Eqs. (9.2.9) hold. In this case the approximate formulas for the

amplitude factors U_{mn} of the transmitted wave turn out to be (if $\beta_x = \beta_y = \beta$)

$$U_{00} \simeq U_0[1 - \tfrac{1}{12}(\sigma + i\xi)k(b+d)] \qquad U_{mn} = 0 \text{ if } m \text{ and/or } n \text{ is odd}$$

$$U_{0,2n} \simeq U_0(-1)^{n-1}(\sigma + i\xi)\frac{kd}{\pi^2 n^2}$$

$$U_{2m,0} \simeq U_0(-1)^{m-1}(\sigma + i\xi)\frac{kb}{\pi^2 m^2} \tag{9.2.17}$$

$$U_{2m,2n} \simeq U_0(-1)^{n+m}(\sigma + i\xi)^2\frac{k^2bd}{(\pi^2 mn)^2} \qquad m, n > 0$$

Thus, even though the piston is perfectly rigid, so that only the fundamental mode would be radiated if the duct walls were rigid, when the walls are nonrigid, the higher modes are also excited to some extent. And when the driving frequency happens to be just greater than some cutoff frequency, so that some k_{mn} is very small, Eqs. (9.2.9) indicate that this mode will have a large amplitude and a phase velocity markedly different from the other components of the pressure wave. Measurements made in such a tube, if interpreted on the assumption that only the fundamental mode is present, will appear to produce erroneous results, since both the phase velocity and attenuation constants of these higher modes may differ, by fairly large factors, from those of the fundamental.

Finally, we can see, by reference to page 519 and to Eq. (6.4.36), that the thermal and viscous effects can be approximated by ascribing to the duct walls an additional specific acoustic admittance β_h and, for the (m,n)th mode, admittances β_{vxm} and β_{vyn} for the x and y walls, respectively, where

$$\beta_h \simeq (1-i)(\gamma - 1)kd_h \qquad \beta_{vxm} \simeq (1-i)\left[1 - \left(\frac{\pi m}{kb}\right)^2\right]kd_v$$

$$\beta_{vyn} \simeq (1-i)\left[1 - \left(\frac{\pi n}{kd}\right)^2\right]kd_v \tag{9.2.18}$$

Large wall admittances

When $|\beta|\, kb$ is not a small quantity, the tangent-cotangent equations for q_m must be solved numerically. A graphical method is illustrated by Plate IV. We set $q_m = -2ig$, so that $g = \frac{1}{2}\nu_m + \frac{1}{2}i\mu_m$, and we set

$$\frac{\beta kb}{2\pi} = \frac{\rho c}{|z|}\frac{b}{\lambda}e^{i\varphi} = he^{i\varphi}$$

so that

$$h = \frac{\rho c}{|z|}\frac{b}{\lambda} = \frac{|\beta|\, kb}{2\pi}$$

where $z = R - iX = |z|\, e^{-i\varphi}$ is the acoustic impedance of the duct walls,

$|z|$ its magnitude, and φ its phase. Then the equations giving g in terms of h and φ are

$$g \tanh(\pi g) = ihe^{i\varphi} \quad \text{for } m \text{ even} \qquad g \coth(\pi g) = ihe^{i\varphi} \quad \text{for } m \text{ odd}$$

The conformal transformation between $\nu + i\mu$ and $he^{i\varphi}$ is plotted for these two cases in Plate IV. Knowing $|z|$ and φ, b and λ, we can determine h and φ, and the corresponding values of μ and ν can be picked off the chart, for both the x and the y walls. Then the transverse function for that mode is

$$\Psi_{mn}(x,y) = Cs_m\left(\mu_{xm} - i\nu_{xm}, \frac{x}{b}\right) Cs_n\left(\mu_{yn} - i\nu_{yn}, \frac{y}{d}\right)$$

and its propagation factor k_{mn} is given by

$$k_{mn}^2 = \left(\frac{\omega}{c}\right)^2 - \left(\frac{\pi\mu_{xm}}{b}\right)^2 + \left(\frac{\pi\nu_{xm}}{b}\right)^2 - \left(\frac{\pi\mu_{yn}}{d}\right)^2 + \left(\frac{\pi\nu_{yn}}{d}\right)^2 + 2i\frac{\pi\mu_{xm}}{b}\frac{\pi\nu_{xm}}{b} + 2i\frac{\pi\mu_{yn}}{d}\frac{\pi\nu_{yn}}{d} \quad (9.2.19)$$

The values of μ and ν for m (or n) $= 0$ lie in the region marked "first even mode" in the chart to the right; those for $m = 1$ are in the region marked "first odd mode" in the chart to the left; and so on. These values can then be used in Eqs. (9.2.15) and (9.2.16) in place of the approximate formula given there.

Conversely, if the real and imaginary parts of k_{mn}^2 can be measured (for a single mode), the values of μ_x, ν_x, μ_y, and ν_y may be computed (if $b = d$, $q_x = q_y$ for $m = n$, for example), and the charts can be used to determine h, and therefrom the wall admittance β. For the reasons given in the discussion of Eqs. (9.2.17), it is usually difficult to isolate a single mode, even the fundamental, so that this procedure for measuring wall impedance has not been very successful.

When three sides of the duct are rigid, the fourth side (say, the side at $x = b$) having admittance β, the same charts can be used to compute μ_x and ν_x. We set the z axis along a corner of the duct, away from the soft wall. Then

$$\Psi_{mn} = \cos\frac{\pi q_{xm} x}{b}\cos\frac{\pi n y}{b}$$

so that Eq. (9.2.7) is automatically satisfied for the two y walls and for the rigid x wall and becomes $(\pi q)\tan(\pi q) = -i\beta kb$ for the soft wall. Setting

$$q_{xm} = -ig \qquad \text{and} \qquad h = |\beta|\frac{kb}{\pi} = \frac{\rho c}{|z|}\frac{2b}{\lambda}$$

produces the equation

$$g \tanh(\pi g) = ihe^{i\varphi}$$

which is plotted on the right-hand side of Plate IV. Thus, introducing the extra factor 2 in the calculation of h and multiplying the values read from the chart by $\frac{1}{2}$ to obtain μ_{xm} and ν_{xm} enables one to use the same chart to work out this case. The corresponding propagation constant can be obtained from

$$k_{mn}^2 = \left(\frac{\omega}{c}\right)^2 - \left(\frac{\pi n}{d}\right)^2 - \left(\frac{\pi \mu_{xm}}{b}\right)^2 + \left(\frac{\pi \nu_{xm}}{b}\right)^2 + 2i\,\frac{\pi \mu_{xm}}{b}\,\frac{\pi \nu_{xm}}{b} \qquad (9.2.20)$$

It is obvious that the behavior of the sound waves, even of the principal wave, is quite complicated when the admittance ratio of the walls is not small compared with unity. If one adds to this the fact that many porous acoustic materials have impedances that vary considerably with change in frequency, it becomes apparent that very few sweeping generalities can be made concerning the behavior of sound in ducts with highly absorbent walls. An examination of Plate IV shows that, for negative phase angles (stiffness reactance) and for large values of h (small values of impedance and/or high frequencies), the value of ν can become quite large, and therefore even the principal wave can be highly damped. Further examination shows that in these cases the principal wave is far from a uniform plane wave, the negative reactance of the walls having in some way pulled most of the energy of the wave away from the center of the duct to the periphery, where it is more quickly absorbed as it travels along. A positive phase angle (mass reactance) has the opposite effect. The change of acoustic behavior with frequency is greatest when h and ϑ are close to one of the "branch points" of the equation for g, shown as circles on the dashed lines separating the modes.

Figure 9.11 gives a typical example for a fairly "soft" duct wall (with acoustic impedance similar to a number of sound-absorbent materials). The real and imaginary parts of $k_{mn} = (2\pi/\lambda_{mn}) + i\pi\gamma_{mn}$ [Eq. (9.2.8)] have physical significance for the transmission properties of the (m,n)th mode. As discussed on page 497, the reciprocal of the real part is proportional to the phase velocity of this mode, $c_{mn} = c(k/k_{mn})$, and the imaginary part is the attenuation factor $\pi\gamma_{mn}$ per unit length of duct. Since a reduction of $|p|$ by a factor of e^{-1} corresponds to a power reduction of 8.686 db, the power attenuation of the mode in decibels per unit length is $8.686\pi\gamma_{mn} = 27.3\gamma_{mn}$. The lower sets of curves of Fig. 9.11 show how the phase velocity of the (1,1) mode rises for frequencies just above its cutoff. They also show the very large attenuation of this mode, even for frequencies well above the cutoff, for duct walls as soft as this.

Ducts of circular cross section

When the duct cross section is a circle of radius b, the transverse, eigenfunctions and values are

$$\Psi_{mn}^{\sigma} = \begin{matrix}\cos\\ \sin\end{matrix}(m\phi) J_m\left(\frac{\pi q_{mn} r}{b}\right) \qquad \varkappa_{mn} = \frac{\pi q_{mn}}{b} \qquad (9.2.21)$$

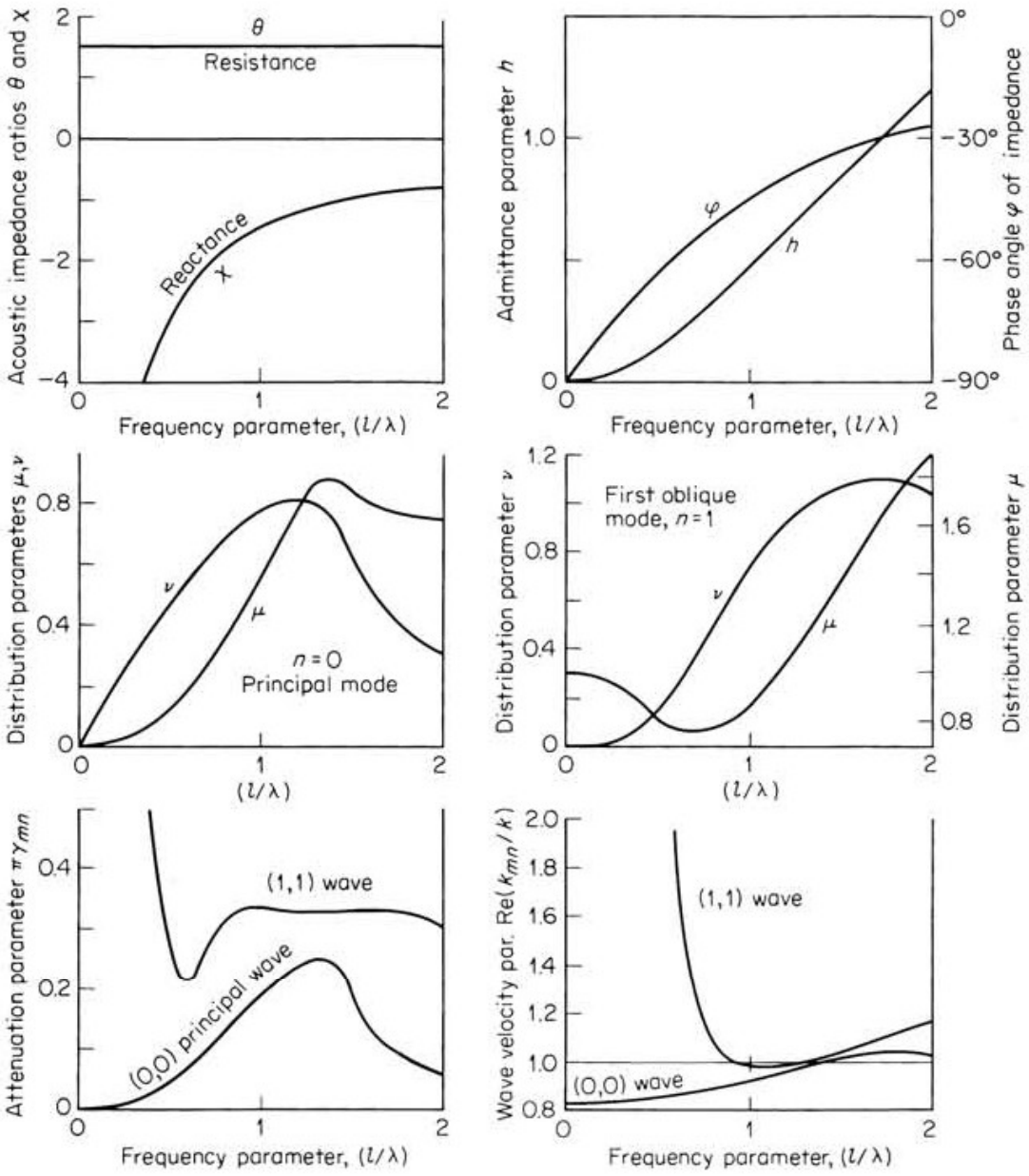


FIGURE 9.11
Transmission of sound along a square duct of width l covered with acoustic material of acoustic impedance $\rho c(\theta - i\chi)$, for principal (0,0)-mode and a higher (1,1)-mode wave. Quantities proportional to attenuation per unit length and phase velocity are plotted against frequency. Sudden rise of γ'_{mn} and k_{mn} for (1,1)-mode illustrates the fact that higher modes cannot be transmitted at low frequencies.

where $\sigma = +1$ for the cosine ϕ factor and -1 for the sine factor, and r, ϕ are polar coordinates about the central axis of the tube. The properties of the Bessel functions are given in Eqs. (5.2.20) and (5.2.21). The boundary condition (9.2.7) is that

$$\pi q_{mn} J'_m(\pi q_{mn}) \equiv \pi q_{mn} J_{m-1}(\pi q_{mn}) - m J_m(\pi q_{mn})$$
$$= i\beta k b J_m(\pi q_{mn})$$

J'_m being the derivative of J_m with respect to its argument. For each integral value of m there is a discrete set of values of q which satisfies this equation; the smallest will be labeled q_{m0}, the next q_{m1}, and so on. When all Ψ_{mn}'s satisfy this condition, their normalizing constants are

$$\int_0^{2\pi} d\phi \int_0^b \Psi_{mn}{}^{\sigma} \Psi_{lk}{}^{\tau} r\, dr = \begin{cases} 0 & \sigma \neq \tau \text{ or } l \neq m \text{ or } k \neq n \\ \pi b^2 \Lambda_{mn} & \sigma = \tau \text{ and } l = m \text{ and } k = n \end{cases} \tag{9.2.22}$$

where

$$\Lambda_{mn} = \frac{1}{\epsilon_m}\left[1 - \frac{m^2 + (\beta kb)^2}{(\pi q_{mn})^2}\right] J_m{}^2(\pi q_{mn})$$

and $\epsilon_m = 1$ when $m = 0$, $= 2$ when $m > 0$. The (m,n)th wave has m plane nodal surfaces, extending radially out from the axis, and n cylindrical nodes concentric with the axis.

For a rigid duct the boundary condition is $J'_m(\pi q) = 0$ or $\pi q J_{m-1}(\pi q) = m J_m(\pi q)$. Solutions of this equation will be called $q = \alpha_{mn}$, to distinguish them from the roots β_{mn} of Eqs. (5.2.23), solutions of $J_m(\pi\beta) = 0$ for the circular membrane. A few values and corresponding values of $J_m(\pi\alpha)$ are

$$\begin{aligned} &\alpha_{00} = 0.0000 \quad \alpha_{01} = 1.2197 \quad \alpha_{02} = 2.2331 \quad \cdots \\ &\alpha_{10} = 0.5861 \quad \alpha_{11} = 1.6970 \quad \alpha_{12} = 2.7140 \quad \cdots \\ &\alpha_{20} = 0.9722 \quad \alpha_{21} = 2.1346 \quad \alpha_{22} = 3.1734 \quad \cdots \\ &\alpha_{mn} \to n + \tfrac{1}{2}m - \tfrac{3}{4} \qquad m < n \gg 1 \end{aligned} \tag{9.2.23}$$

$$\begin{aligned} &J_0(\pi\alpha_{00}) = 1.0000 \quad J_0(\pi\alpha_{01}) = -0.4028 \quad J_0(\pi\alpha_{02}) = 0.3001 \\ &J_1(\pi\alpha_{10}) = 0.5819 \quad J_1(\pi\alpha_{11}) = -0.3461 \quad J_1(\pi\alpha_{12}) = 0.2733 \\ &J_2(\pi\alpha_{20}) = 0.4865 \quad J_2(\pi\alpha_{21}) = -0.3135 \quad J_2(\pi\alpha_{22}) = 0.2547 \end{aligned}$$

$$J_m(\alpha_{mn}) \simeq \sqrt{\frac{2}{\pi^2 \alpha_{mn}}} \qquad m < n \gg 1$$

As expected, the fundamental (0,0) mode for the rigid tube has a zero characteristic value and thus is a plane wave, propagating at the free-space velocity c. The cutoff frequency for the (m,n)th mode is $\alpha_{mn}c/2b$. Thus the first modes to become propagational are (1,0), then (2,0) (each being a pair of modes, one for $\sigma = +1$, the other for $\sigma = -1$), and only after these is the second symmetric mode (0,1) propagated, as the frequency is increased.

Various properties of cylindrical tubes will be worked out in later sections, but we can now use the formulas just developed to illustrate some of the statements made regarding the radiation reaction on a simple source in a duct. If the source, a sphere of radius $a \ll b$, has its center at the point $\phi = 0$, $r = r_0$, $z = 0$, then the frequency-dependent factor in Eqs. (9.2.12) for the radiation resistance, the bracketed factor in the real part of Z_s, becomes

$$\sum_{n,m}^{\pi\alpha<kb} \frac{\epsilon_m [J_m(\pi\alpha_{mn} r_0/b)/J_m(\pi\alpha_{mn})]^2}{[1 - (m/\pi\alpha_{mn})^2]\sqrt{1 - (\pi\alpha_{mn}/kb)^2}}$$

where we have absorbed the unity term (for $m = n = 0$) into the sum, which is over all pairs of values of m and n for which $\alpha_{mn} < kb/\pi$. The graph for this sum is quite similar to that shown in Fig. 9.10, with the successive peaks coming at $kb = \pi\alpha_{mn}$. As before, the radiation resistance jumps discontinuously as the driving frequency reaches the cutoff frequency of another mode. Of course, if the tube were not perfectly rigid (or if we took thermal and viscous surface losses into account), the peaks would be rounded off and finite in height, becoming smaller and closer together as ω is increased, until the curve roughly equals the smooth curve for $\frac{1}{2}(kb)^2$, the corresponding radiation-resistance term for an isolated source. The differences, at lower frequencies, illustrate how much the reaction on the simple source is affected by the walls of the tube which surround it.

When the wall admittance is not zero but is small compared with $\lambda/2\pi b$, one can develop approximate formulas, similar to Eqs. (9.2.14) to (9.2.16), by using the equations

$$J'_m(\pi\alpha_{mn}) = 0 \qquad \text{and} \qquad J''_m(\pi\alpha_{mn}) = -[1 - (m/\pi\alpha_{mn})^2]J_m(\pi\alpha_{mn})$$

To the first approximation, in the small quantity $|\beta|\, kb$, we have

$$i\pi q_{00} \simeq \sqrt{2(i\beta kb)} \qquad k_{00} \simeq k + \frac{1}{2b}(\sigma + i\xi)$$

$$\pi q_{mn} \simeq \pi\alpha_{mn}\left[1 - \frac{(\sigma + i\xi)kb}{(\pi\alpha_{mn})^2 - m^2}\right] \qquad k_{mn} \simeq k^0_{mn} + \frac{(\sigma + i\xi)k}{k^0_{mn}b[1 - (m/\pi\alpha_{mn})^2]}$$

$$\Psi_{00} \simeq 1 + (\sigma + i\xi)\frac{kr^2}{4b} \qquad \Lambda_{00} \simeq 1 - \tfrac{3}{4}(\sigma + i\xi)kb \tag{9.2.24}$$

$$\Psi_{mn} \simeq \begin{matrix}\cos\\ \sin\end{matrix}(m\phi)\left\{J_m\left(\frac{\pi}{b}\alpha_{mn}r\right) - \frac{(\sigma + i\xi)\pi\alpha_{mn}}{(\pi\alpha_{mn})^2 - m^2}\left[\frac{m}{\pi\alpha_{mn}}J_m\left(\frac{\pi}{b}\alpha_{mn}r\right) - J_{m-1}\left(\frac{\pi}{b}\alpha_{mn}r\right)\right]\right\}$$

$$\Lambda_{mn} \simeq \tfrac{1}{2}\left[1 - \left(\frac{m}{\pi\alpha_{mn}}\right)^2\right]\left\{1 - \frac{2(\sigma + i\xi)kb}{[(\pi\alpha_{mn})^2 - m^2]^2}\right\}J_m{}^2(\pi\alpha_{mn})$$

where $k^0_{mn} = \sqrt{k^2 - (\pi\alpha_{mn}/b)^2}$ or $i\sqrt{(\pi\alpha_{mn}/b)^2 - k^2}$, depending on whether the mode's cutoff frequency is below or above the driving frequency.

The lowest mode of any axial symmetry ($n = 0$ for a given m) exhibits the greatest attenuation, for frequencies above its cutoff frequency, because the factor $1 - (m/\pi\alpha_{mn})^2$ in the denominator for k_{mn} is smallest, for a given m, for $n = 0$ (note that $m > \pi\alpha_{m0}$ for all m). This is in contrast to the case of the rectangular duct, where the lowest modes (m or $n = 0$) have a *lower* attenuation than the rest. In the rectangular duct, of course, the higher-mode waves reflect back and forth from plane-parallel walls, so that there can be a whole set of modes which do not reflect at all from one pair of walls (the ones $m = 0$, $n > 0$ or $m > 0$, $n = 0$). But for the cylindrical duct, the

only wave which does not reflect from the curved walls is the fundamental mode, which has an attenuation constant $\xi/2b$, less than half the value $\xi/b\sqrt{1-(\pi\alpha_{mn}/kb)^2}[1-(m/\pi\alpha_{mn})^2]$ for any other mode (to this approximation).

In the case of the circular pipe the waves have in general two possibilities, when the wavelength is small compared with b: they can reflect more or less normally from the surface and thus focus in to the center, with circular nodal surfaces for its standing waves (this corresponds to n large and m small), or they can move in a spiral path, roughly parallel to the wall, with a preponderance of radial nodes (which would correspond to m large and n small). In the latter case the waves would not avoid reflecting from the wall, as they would in the rectangular duct; their angle of incidence is large, and they tend to "cling" to the curved wall. As a matter of fact, the modes for m large and n small have very small amplitude near the tube axis and differ appreciably from zero only for r nearly equal to b. Thus the majority of these modes' energy is close to the duct wall, where it is quickly absorbed; these "spiral-tangential" waves are *more* strongly attenuated than the others, in contrast to the truly tangential waves in the rectangular duct, which are *less* strongly attenuated than the others.

If $|\beta|\,kb$ is not small, the boundary condition

$$-i\beta kb = m - \pi q\frac{J_{m-1}(\pi q)}{J_m(\pi q)} \qquad J_{-1} = -J_1 \text{ for } m = 0$$

must be solved exactly. If we set $q = -iw$, so that $w = \nu + i\mu$, and set $h = |\beta|\,kb/\pi$, with $\beta = |\beta|\,e^{i\varphi} = \rho c/|z|\,e^{-i\varphi}$ as before, the equation for w in terms of h and φ for the J_m modes is

$$ihe^{i\varphi} = -\frac{m}{\pi} - iw\frac{J_{m-1}(-i\pi w)}{J_m(-i\pi w)} \tag{9.2.25}$$

Plate V plots this conformal transform for $m = 0$ and $m = 1$. There is a general similarity to the corresponding plots of Plate IV for the rectangular duct, though the exact locations of branch points, zeros, etc., differ somewhat.

As an example, to compare with Fig. 9.11, we have calculated the values of ν and μ for the fundamental mode (0,0) in a circular pipe, with walls having a unit specific acoustic resistance and a stiffness reactance inversely proportional to the frequency, as in the case of Fig. 9.11. The real and imaginary parts of the propagation parameter

$$k_{00} = \frac{2\pi}{\lambda_{00}} + i\pi\gamma_{00} = \left[k^2 - \left(\frac{\pi q_{00}}{b}\right)^2\right]^{\frac{1}{2}}$$

can then be computed and are plotted in Fig. 9.12. As mentioned earlier, the real part of k_{00}/k is the ratio of the velocity of sound in free space to the phase velocity of the mode in the tube, and its imaginary part is proportional to the attenuation, and thus to the decibel drop in intensity as the wave travels along the tube. These quantities are plotted in Fig. 9.12, for two

different wall stiffness constants. The impedances in the two examples were chosen to display large attenuations. On the w plane of Plate V the dashed curve goes to the right of the branch point at $\eta = 0.41$, $\mu = 0.94$; the solid curve goes to the left. The solid curves resemble those of Fig. 9.11 for the fundamental mode (note that the left-hand curve of Fig. 9.11 is for $\pi\gamma_{00}$, whereas the upper curves of 9.12 are proportional to $\lambda\gamma_{00}$).

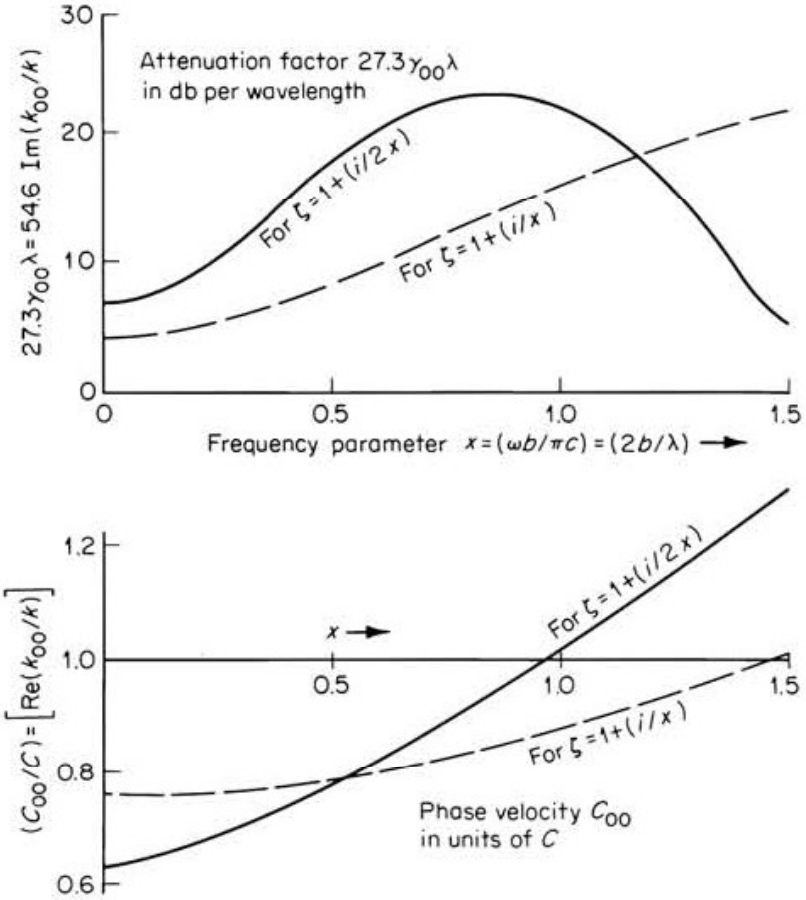


FIGURE 9.12
Attenuation and phase velocity of lowest mode in a circular tube, with walls having specific acoustic impedance $\zeta = Z/\rho c$, as function of frequency, for two different values of stiffness reactance.

Representation of randomly distributed sources

Occasionally, it is of interest to calculate the generation of sound from a region inside the duct, where fluid is being produced (or expanded by radiant heat) in a random manner or where the fluid is in violent turbulence. This problem was discussed in Sec. 7.1 for a turbulent region in free space. The confining effect of the duct walls introduces additional complications, in part because it is less easy to define a random function in a restricted region than in free space. To demonstrate these difficulties and to show how they may be overcome, we consider a region of fluctuating fluid generation inside a rectangular duct with rigid walls.

Our first task is to devise a measure of the variability of some fluctuating function $f(x,y)$ within the finite area $0 < x < b$, $0 < y < d$. In unconfined space this would be given by the autocorrelation function for f, generalizing the definition of Eq. (1.3.13). But if we define

$$\Upsilon_f(\xi,\eta) = \frac{1}{bd}\int_0^b dx \int_0^d f(x,y) f(x+\xi, y+\eta)\, dy \tag{9.2.26}$$

as the correlation function for f, we must somehow decide what values we should use for f when $x + \xi$ exceeds b or $y + \eta$ exceeds d.

We could, of course, say that f is zero outside the limited area, but this leads to computational difficulties. It might seem more "physical" to consider the walls as mirrors and to consider f outside the duct cross section to be the mirror image of the wave inside, somewhat as was done in the case of the string (Fig. 4.7). Another way of saying the same thing is to expand f in terms of the eigenfunctions of the cross section

$$f(x,y) = \sum_{m,n} C_{mn}\Psi_{mn}(x,y) \qquad C_{mn} = \frac{1}{bd\Lambda_{mn}}\int_0^b\int_0^d f\Psi_{mn}\, dx\, dy \tag{9.2.27}$$

and say that f, outside $0 < x < b$, $0 < y < d$, is simply the analytic continuation of the series, over the wider range of the variables. If the walls are rigid, function f will be symmetric about the boundary lines.

If we do this, it is then easy to calculate the expansion of the autocorrelation function in terms of the normal modes of the duct cross section. Inserting series (9.2.27) twice into Eq. (9.2.26), using the formulas

$$\cos[(\pi m/b)(x+\xi)] = \cos(\pi mx/b)\cos(\pi m\xi/b) - \sin(\pi mx/b)\sin(\pi m\xi/b), \text{ etc.}$$

and remembering that the integral of $\cos(\pi mx/b)\sin(\pi mx/b)$ over x from 0 to b is zero, we obtain

$$\Upsilon_f(\xi,\eta) = \sum_{m,n} \Lambda_{mn}|C_{mn}|^2\,\Psi_{mn}(\xi,\eta) \tag{9.2.28}$$

Thus the coefficients in the expansion of the correlation function of f are the squares of the coefficients of the expansion of f itself, a simple extension of the relationship of Eq. (1.3.21). The coefficients C_{mn} can be considered as transforms of function f, with respect to the set of eigenfunctions Ψ_{mn}. Alternatively,

$$|C_{mn}|^2 = \frac{1}{bd\Lambda_{mn}{}^2}\int_0^b d\xi \int_0^d d\eta\; \Upsilon_f(\xi,\eta)\Psi_{mn}(\xi,\eta) \tag{9.2.29}$$

Now suppose the region R_s of the duct from $z = -\frac{1}{2}L$ to $z = \frac{1}{2}L$ is filled with fluctuating production of fluid, at a rate $s(\mathbf{r},t)$ units of volume per

second per unit volume, s being a function which is randomly variable in region R_s, having a mean-square magnitude $\langle s^2 \rangle$ there, a correlation distance in space of w, and a correlation interval in time of $\tau_c = 1/\omega_0$, with $\omega_0/2\pi$ the upper limit of the frequency distribution. Then, from Eqs. (1.3.20), (7.1.33), and (9.1.28), we can write

$$C_{mn}{}^{s}(\omega,K) = \frac{1}{4\pi^2 bd\Lambda_{mn}} \int \cdots \int e^{i\omega t - iKz} \Psi_{mn}(x,y) s(\mathbf{r},t)\, dx\, dy\, dz\, dt$$

$$|C_{mn}{}^{s}(\omega,K)|^2 = \frac{LT}{16\pi^4 \Lambda_{mn}{}^2 bd} \int \cdots \int \Upsilon_s(d,\tau) e^{i\omega\tau - iKd_z} \Psi_{mn}(d_x,d_y)\, d\tau\, dv_d$$

$$\Upsilon_s(d,\tau) = \frac{1}{VT} \int \cdots \int s(\mathbf{r},t) s(\mathbf{r}+\mathbf{d}, t+\tau)\, dt\, dv \qquad (9.2.30)$$

$$= \frac{4\pi^2}{LT} \sum_{mn} \Lambda_{mn} \Psi_{mn}(d_x,d_y) \iint |C_{mn}{}^{s}(\omega,K)|^2 e^{-i\omega\tau + iKd_z}\, d\omega\, dK$$

where the integrations are over the cross section of the duct, over z or d_z from $-\frac{1}{2}L$ to $\frac{1}{2}L$, and over t or τ from $-\frac{1}{2}T$ to $\frac{1}{2}T$, and the final integral over ω and K is from $-\infty$ to $+\infty$.

The component of the pressure wave of frequency $\omega/2\pi$, at point $\mathbf{r} = (x,y,z)$, to the right of region R_s, can be obtained from the Green's function of Eq. (9.2.10) by integrating $-ik\rho c g_\omega$ times the component of $s(\mathbf{r},t)$ having the frequency $\omega/2\pi$.

$$p_\omega(\mathbf{r}) = \frac{k\rho c}{4\pi bd} \sum_{mn}{}' \frac{\Psi_{mn}(x,y) e^{ik_{mn}z}}{\Lambda_{mn} k_{mn}} \int \cdots \int e^{i\omega t - ik_{mn}z_0} \Psi_{mn}(x_0,y_0) s(\mathbf{r}_0,t)\, dv_0\, dt$$

$$= \pi k\rho c \sum_{mn}{}' \frac{C_{mn}{}^{s}(\omega,k_{mn})}{k_{mn}} \Psi_{mn}(x,y) e^{ik_{mn}z} \qquad (9.2.31)$$

Also

$$u_z(\mathbf{r}) = \pi \sum_{mn}{}' C_{mn}{}^{s}(\omega,k_{mn}) \Psi_{mn}(x,y) e^{ik_{mn}z} \qquad \text{for } z \gg \tfrac{1}{2}L$$

is the axial component of fluid velocity for the frequency $\omega/2\pi$. The sums include all those modes for which the eigenvalue $\varkappa_{mn}{}^2 = (\pi m/b)^2 + (\pi n/d)^2$ is less than $k^2 = (\omega/c)^2$, so that $k_{mn}{}^2 = k^2 - \varkappa_{mn}{}^2$ is positive, and the mode propagates (which is the meaning of the prime over the summation sign). The intensity at $\mathbf{r}$ in the unit ω band at ω is then the real part of $(p_\omega u_z^*)$, and the total power radiated to the right from R_s is

$$W_\omega = \int (p_\omega u_z^*)\, dx\, dy = \pi^2 \rho c bd \sum_{mn}{}' \frac{k}{k_{mn}} |C_{mn}{}^{s}(\omega,k_{mn})|^2 \qquad (9.2.32)$$

Now suppose the source distribution has an autocorrelation function which can be approximated by the usual formula

$$\Upsilon_s(\mathbf{d},\tau) = \langle s^2 \rangle \exp\left[-\frac{1}{2}\left(\frac{d}{w}\right)^2 - \tfrac{1}{2}(\omega_0\tau)^2\right] \tag{9.2.33}$$

where $\langle s^2 \rangle$ is the mean-square value of the source function s in region R_s, and w is the correlation length and $1/\omega_0$ the correlation time interval for s. By using Eqs. (9.2.30), if $w \ll L$, b, and d and $(1/\omega_0) \ll T$, we can write out an approximate formula for $|C|^2$ and for the power-spectrum level W_ω.

$$\begin{aligned} |C_{mn}{}^s(\omega,k_{mn})|^2 &\simeq \frac{LTw^3\langle s^2\rangle}{16\pi^2\Lambda_{mn}{}^2bd\omega_0} \exp\left[-\tfrac{1}{2}(kw)^2 - \frac{1}{2}\left(\frac{\omega}{\omega_0}\right)^2\right] \\ W_\omega &\simeq \frac{LTw^3\rho c}{16\omega_0}\langle s^2\rangle \sum_{mn}{}' \frac{\exp\left[-\tfrac{1}{2}(kw)^2 - \tfrac{1}{2}(\omega/\omega_0)^2\right]}{\sqrt{1-(\varkappa_{mn}/k)^2}} \end{aligned} \tag{9.2.34}$$

The total power radiated to the right, for all frequencies, is obtained by using Eq. (2.3.13).

$$\begin{aligned} W = \frac{2\pi}{T}\int_{-\infty}^{\infty} W_\omega\, d\omega &= \frac{\pi^{\frac{3}{2}}Lw^3\rho c}{8[(k_0w)^2+1]}\langle s^2\rangle \sum_{mn}{}' \exp\left[-\tfrac{1}{2}\varkappa_{mn}{}^2\left(w^2 + \frac{1}{k_0{}^2}\right)\right] \\ &\simeq \frac{\sqrt{\pi}}{16}\rho c \frac{V_s w(k_0w)^2}{[(k_0w)^2+1]^2}\langle s^2\rangle \qquad \text{if } w \text{ and } \frac{1}{k_0} \ll \frac{1}{\varkappa_{10}} = \frac{b}{\pi} \end{aligned} \tag{9.2.35}$$

where $k_0 = \omega_0/c$, and $V_s = Lbd$ is the volume of the radiating region R_s. The second formula is valid when the exponential in the sum m, n varies so slowly that we can substitute for the sum an integral over n and m. The quantity $k_0w = 2\pi w/\lambda_0$ is 2π times the ratio between the spatial-correlation length w and the wavelength λ_0 corresponding to the upper limit $\omega_0/2\pi$ of the frequencies present in the random source. The total power radiated is maximum when this quantity is unity.

A similar calculation can be made for the radiation from a turbulent region. Instead of the source function $s(\mathbf{r},t)$, the kinetic-energy function

$$\begin{aligned} T(\mathbf{r},t) = {} & \frac{\partial^2}{\partial x^2}(\rho U_x{}^2) + \frac{\partial^2}{\partial y^2}(\rho U_y{}^2) + \frac{\partial^2}{\partial z^2}(\rho U_z{}^2) \\ & + 2\frac{\partial^2}{\partial x\,\partial y}(\rho U_xU_y) + 2\frac{\partial^2}{\partial x\,\partial z}(\rho U_xU_z) + 2\frac{\partial^2}{\partial y\,\partial z}(\rho U_yU_z) \end{aligned}$$

is the generating term, where U_x, U_y, U_z are the components of the turbulent velocity at $\mathbf{r}$, t. An autocorrelation function Υ_t can be formed from this function, and the expansion coefficients $C_{mn}{}^t$ can be calculated, having relationships to T and Υ_t similar to Eqs. (9.2.30) for $C_{mn}{}^s$. Integration by

parts produces the alternative formula

$$C_{mn}{}^{t}(\omega,K) = \frac{\epsilon_m\epsilon_n}{4\pi^2 bd}\int\cdots\int\rho\Big\{-\Big[U_x{}^2\Big(\frac{m\pi}{b}\Big)^2 + U_y{}^2\Big(\frac{n\pi}{d}\Big)^2 + U_z{}^2K^2\Big]$$
$$\times \cos\frac{m\pi x}{b}\cos\Big(\frac{n\pi y}{d}\Big)$$
$$+ 2U_xU_y\frac{m\pi}{b}\frac{n\pi}{d}\sin\frac{\pi mx}{b}\sin\Big(\frac{\pi ny}{d}\Big)$$
$$+ 2iU_xU_zK\frac{m\pi}{b}\sin\frac{\pi mx}{b}\cos\Big(\frac{\pi ny}{d}\Big)$$
$$+ 2iU_yU_zK\frac{n\pi}{d}\cos\frac{\pi mx}{b}\sin\frac{\pi ny}{d}\Big\}e^{i\omega t-iKz}\,dx\,dy\,dz\,dt$$

The rest of the calculation proceeds as for the function s.

Extension of these formulas to ducts of other shape is made difficult by the complications of relating the expansion coefficients C to an autocorrelation function. For example, for a cylindrical duct of radius a, for which a random function $f(x,y)$ is represented by a series of Bessel functions,

$$f(x,y) = \sum_{mn}[C_{mn}{}^{e}\cos(m\phi) + C_{mn}^{0}\sin(m\phi)]J_m\Big(\frac{\pi\alpha_{mn}r}{a}\Big) \qquad C_{0n}^{0} = 0$$
$$C_{mn}{}^{e} = \frac{1}{\Lambda_{mn}\pi a^2}\int_0^{2\pi}d\phi\int_0^a f(r\cos\phi,\, r\sin\phi)\cos(m\phi)J_m\Big(\frac{\pi\alpha_{mn}r}{a}\Big)r\,dr$$

and similarly for C_{mn}^{0}. If the random behavior of f is isotropic, the autocorrelation function should be independent of ϕ. It can be shown, in that case, that

$$\Upsilon(\delta) \equiv \frac{1}{\pi a^2}\int_0^{2\pi}d\phi\int_0^a f(r\cos\phi,\, r\sin\phi)$$
$$\times f(r\cos\phi + \delta\cos\theta,\, r\sin\phi + \delta\sin\theta)r\,dr$$
$$= \sum_{mn}(\Lambda_{mn}{}^{e}\,|C_{mn}{}^{e}|^2 + \Lambda_{mn}^{0}\,|C_{mn}^{0}|^2)J_m\Big(\frac{\pi\alpha_{mn}\delta}{a}\Big)$$

which is *not* an expansion in terms of the axially symmetric eigenfunctions $J_0(\pi\alpha_{0n}\delta/a)$. Alternatively, one could define a rotational correlation function

$$\Upsilon_r(\theta) \equiv \frac{1}{\pi a^2}\iint f(r\cos\phi,\, r\sin\phi)\,f[r\cos(\phi+\theta),\, r\sin(\phi+\theta)]r\,dr\,d\phi$$
$$= \sum_{mn}(\Lambda_{mn}{}^{e}\,|C_{mn}{}^{e}|^2 + \Lambda_{mn}^{0}\,|C_{mn}^{0}|^2)\cos(m\theta)$$

expressible in terms of the angle functions, but it is not certain what use this function would have. About all we can do is to assume that $|C_{mn}{}^{e}|^2 = |C_{mn}^{0}|^2$ has, roughly, the form given in Eqs. (9.2.34), and continue as before.